ENERGY RESEARCH CENTRE – UNIVERSITY OF CAPE TOWN

A Reliability Evaluation of Solar Power in South Africa's Power System

A Thesis Submitted to the Energy Research Centre
in Partial Fulfilment of the Requirements for the
Degree of

MSc in Sustainable Energy Engineering

In the department of Mechanical Engineering
University of Cape Town
South Africa

by

Nicholas Bailey

ACKNOWLEDGMENTS

The author would like to express his gratitude to his supervisor Adrian Stone and co-supervisor Bruno Mervin for their invaluable guidance and support during the course of this thesis. The ease of access to and ready supply of their knowledge was especially important during the preparation of this work.

The author would also like to acknowledge ARUP, especially the energy team in the Cape Town office, for access to data and lessons on the fundamentals of PV design.

The author would like to take this opportunity to acknowledge the constant encouragement and support from friends and family, especially Kate Sperring.

Financial assistance provided by the National Research Fund in the form of a post graduate bursary is fully acknowledged.

I know the meaning of plagiarism and declare that all the work in the document, save for that which is properly acknowledged, is my own:

_____ Date: 14 February 2014

Nicholas Bailey

ABSTRACT

Global utilisation of renewable energy sources such as solar photovoltaics (PV) in electric power systems is growing rapidly due to government incentives, and negative environmental impacts associated with conventional generators. Many consider solar PV as a promising alternative source of energy due to its apparent environmental, social and economic benefits. This together with government incentives and programmes such as the renewable energy independent power procurement program (REIPPPP) has allowed for investment in PV in South Africa (SA).

Solar irradiation is a variable energy source and thus serious consideration needs to be given to the effect that PV might have on the reliability of the system. As a result traditional methods of evaluating power system reliability cannot be used when utility-scale PV is introduced to the system. Thus probabilistic methods are commonly employed to evaluate reliability.

In this thesis time series data was used to simulate the yield from 27 PV plants, as defined by round 1 and round 2 of the REIPPP process, through a yield model developed for this investigation. The resultant yield data was then input into a dispatch model including conventional generators. Loss-of-load-probability (LOLP) and Monte Carlo Simulation (MCS) were then used to assess the capacity credit (C_r) of PV, or value that PV adds to the system. The C_r was evaluated using the effective load carrying capability (ELCC) method, which describes how much the additional PV capacity contributes to the firm capacity of the system when compared to an equivalent thermal unit. A dispatch model was then created to evaluate the affect that introducing PV has on other aspects of the SA power system, such as CO_2 savings; reliability indices loss-of-load-expected (LOLE) and expected-energy-not-supplied (EENS); fuel consumption; average capacity factors and the associated cost benefits of adding PV generation to the system.

A brief overview of the results shows that:

- PV has an annual C_r of 0.75 for the time window of 12h00-13h00
- C_r values decrease with a decrease in geographic dispersion of PV plants
- C_r values decrease with an increase in technological penetration level of PV
- There is a direct relationship between C_r and average capacity factor of PV capacity connected to the grid

From the results we were able to conclude that PV in SA has substantially higher C_r than has generally been used to characterise PV in the past for the window of daylight all year round. This is particularly true between 10h00 and 16h00, which demonstrates the relatively high reliability of PV over this period. This research aimed to present a novel contribution to the modelling of power systems in SA through the concepts presented and examples evaluated. It is hoped that this will help system planners and utility managers in the decision making process; inform long term policy planning and to aid further research in this area.

TABLE OF CONTENTS

LIST OF TABLES

LIST OF FIGURES:

List of Abbreviations

CDF	Cumulative distribution function
CF	Capacity Factor
C_f	Firm Capacity
CO_2	Carbon Dioxide
C_{pv}	Capacity of additional PV
$C_{PV\ res}$	Resultant PV capacity
C_r	Capacity Credit
c-Si	Crystalline Silicon (as in mono-crystalline silicon PV cells)
CSP	Concentrated solar power
C_{th}	Thermal Capacity
$C_{thermal\ unit}$	Capacity of an additional thermal unit
dC_f	Change in firm capacity
DNI	Direct natural irradiance
DHI	Direct horizontal irradiance
DOE	Department of Energy
EENS	Expected energy not served

Eff	Efficiency
ELCC	Effective load carrying capability
ERC	Energy Research Centre
FC	Firm capacity
FOR	Forced outage rate
GHI	Global horizontal irradiation
GJ	Gigajoule
IPP	Independent power producer
IRP	Integrated resource plan
kW	Kilowatt
kWh	Kilowatt hour
LCC	Load carrying capability
LOEE	Loss of energy expectation
LOL	Loss of load
LOLE	Loss of load expected
LOLP	Loss of load probability
MAE	Mean absolute error
MCS	Monte Carlo Simulation
Mono-Si	Mono-crystalline silicon
MW	Megawatt
PDF	Probability distribution function
poly-Si	Polycrystalline silicon
POR	Planned outage rates
PPA	Power Purchase Agreement
PR	Performance Ratio
PV	Photovoltaic
RE	Renewable energy
REFIT	Renewable energy feed in tariff
REFSO	Renewable energy finance and subsidiary office
REIPPPP	Renewable energy independent power producer procurement programme
RM	Reserve Margin
SA	South Africa
TWh	Terawatt hours

Glossary	
High Demand Period	The period considered to be during the highest loads of the year – defined by Eskom as June, July and August
Low Demand Period	The period considered to be during the lowest loads of the year – defined by Eskom as September, October, November, December, January, February, March, April and May
Winter	June, July, August
Spring	September, October, November
Summer	December, January, February
Autumn	March, April, May
Dispatchable Plants	Plants that can vary their supply on demand
Capacity Credit	The portion of installed capacity that can add to the firm capacity of the system
Firm Capacity	The amount of power that can be guaranteed to be provided at a certain confidence level
LOLP: Loss of load Probability	% probability that load exceeds the available capacity
LOLE: Loss of load Expectation	The expected time duration that the load exceeds the available capacity
LOEE: Loss of Energy Expectancy	The expected energy that will not be delivered when load exceeds capacity
ELCC: Effective Load Carrying Capability	The additional load that can be carried by the system for a given reliability and a given additional capacity of new generating units
Capacity Reserve Margin	The difference between total installed capacity and system peak load expressed as a percentage of peak load
Loss of Largest Unit	The required reserve capacity equal to that of the largest generating unit in the power system
Loss of Largest Unit + Percentage Margin	Similar to above, but with an additional fixed percentage; usually of total installed capacity or peak load
Dry Year	Used in hydro dominated systems to determine effect of poor hydroelectric availability
System Security	The ability of the power system to withstand sudden disturbances
System Adequacy	The existence of sufficient facilities within the system to satisfy the consumer load demand or system operational constraints at all times
Equivalent Firm	Defined as the capacity of a theoretical 100% reliable

Capacity (EFC)	generating unit that will cause the system to have the same LOLP as when the actual unit is added
Effective Load Carrying Capability (ELCC)	Defined as the additional load that can be carried by the system for a given reliability and a given additional capacity of new generating units
Equivalent Conventional Power Plant (ECPP)	Similar to EFC, but using a conventional power plant for comparison with conventional reliability levels, rather than a theoretical power plant.
Guaranteed Capacity	Defined as the least capacity which can be expected to be available with a given probability (not to be confused with LOLP). It considers only capacity of the systems, not the load, with and without an added generator unit
FOR	The probability that a generating unit will be offline at some time in the future

1. INTRODUCTION:

Energy from renewable sources has attracted significant global interest in recent years due to climate change, pollution, extreme environmental impacts and a marked increase in fuel costs for conventional generation methods. This has led to major investment in renewable energy sources worldwide as they allow electricity production without the use of fossil fuels, avoiding production of CO_2 and other greenhouse gasses.

South Africa (SA) has historically had access to a large supply of relatively cheap fuel in the form of coal, with more than 90% of SA's electricity in 2010 coming from the burning of coal (Edkins, et al., 2010). This dominance resulted in a relatively slow start to investment in renewables for SA. Until 2010, the transition to renewable energy (RE) technologies had been viewed as an additional economic cost, but since then RE projects have been seen as an opportunity to create a secure form of sustainable energy production (Edkins, et al., 2010). In particular the cost of power generated by Solar Photovoltaics (PV) has decreased markedly in recent years, making it a particularly attractive and economical renewable energy option (Feldman, et al., 2012).

A series of blackouts in 2008 and a commitment to mitigation of CO_2 emissions led to the development of an electricity supply Plan for South Africa in March 2011. This Plan was finalised in the Integrated Resource Plan (IRP), which provided for 18.7 GW of renewables to be installed by 2030 (DOE, 2011). This Plan demonstrated government's commitment to energy from renewable sources and allowed independent power producers (IPP's) to bid for portions of this installed capacity over a range of RE technologies, particularly small hydro, biogas wind, solar PV and concentrated solar power (CSP). Within this new energy mix the DOE committed to commission 8400 MW of solar PV capacity, 8400 MW of wind capacity and a 1000 MW of CSP capacity (DOE, 2011) through the Renewable Energy Independent Power Producers Procurement Programme (REIPPPP). Investments into RE technologies have now gained significant momentum in South Africa.

In contrast to conventional fossil fuel power production, electricity production from RE in general is sporadic, because of the dependence of the energy source on weather patterns. Unlike conventional thermal generators this makes them a non-dispatchable source of power. Therefore there is a general view that dispatchable power plants, plants that can vary their power output on demand, will be required to "back-up" the variable supply of RE sources. As a result, conventional fossil-fuelled generators might need to run in conjunction with the renewable energy generators adding to the relative cost of energy produced from renewable technologies and possibly negating some of the offset CO_2 emissions.

The question then arises of how much conventional generation capacity will be required to back-up PV generation in SA. If this capacity is the same as installed PV capacity this will mean that PV systems add no particular value to the power system, in terms of cost of capacity.

If however, PV power plants can offset the need for extra conventional generation, they can add to the power system's capacity. Thus it can be said that the PV power system has a **capacity credit** (C_r). In other words, a certain percentage of installed PV capacity can contribute to the firm capacity (FC) of the system.

Historically, the conventional method to determine reliability of a power system is through using the indicator of reserve margin. This refers to an excess of installed capacity over peak demand, which allows for planned outages, such as maintenance, and unplanned outages, such as breakdowns (Bagen, 2005).

This approach cannot be used for PV however; as it does not take the variability of supply into consideration, and as a result would vastly overestimate the contribution of RE if their full capacity is considered in the calculation (Bagen, 2005). As a result, stochastic simulations are now often used to account for this variability and will be used in this dissertation. In particular the Effective Load Carrying Capability (ELCC) C_r metric will be used and this approach will be explored and discussed.

1.1. Aim

The aim of this dissertation then is to quantify the C_r of solar PV in SA, and to explore the effect that geographic dispersion and penetration level has on this value.

This is further defined in the thesis statement below.

1.1.1. Thesis Statement

Grid tied solar PV can add to the firm capacity of South Africa's power system. Hence, a positive C_r for PV can be effectively described using the ELCC metric and is negatively affected by a decrease in geographic dispersion and an increase in PV penetration level.

1.1.2. Research Objectives

The overall research objective of this dissertation is to present the results of simulated studies for assessing the C_r of planned solar PV plants in SA, based on the locations outlined in Round 1 and Round 2 of the REIPPPP process (DOE, 2012)

This overarching objective can be further broken down in smaller objectives. These are:

- To effectively simulate yield from PV plants
- To generate a simple dispatch model depicting SA's power system for different scenarios, that can be used for future research in the public domain
- To calculate the ELCC and C_r of installed solar PV using Monte Carlo Simulation
- To test the effect of geographic dispersion and penetration levels on the C_r of solar PV for the current SA grid and demand profile through scenario analysis
- To show the optimal generation mix including PV to meet demand through a dispatch model
- To use the dispatch model and Monte Carlo Simulation to calculate:

    - CO_2 Produced for the system with and without PV
    - Loss-of-load expectancy and expected energy not supplied reliability indices
    - MWh of energy produced
    - GJ of fuel used
- To draw valid and useful conclusions from the results of the above objectives
- Make recommendations based on these conclusions

1.2. Chapter Overview

This dissertation can be broken down into the follow chapters.

Chapter 1 - introduces the subject of the dissertation before clarifying the goal and objectives of this report.

Chapter 2 - gives a context and background to the research describing PV technology; the growth of utility scale PV and the RE policy context of SA.

Chapter 3 - reviews literature relevant to this research. In particular it examines:

- Simulation of utility scale PV
- Theory of power system reliability
- C_r methodology
- Dispatch modelling
- power systems using variable generators in SA

Chapter 4 - discusses the methodology for simulation of utility scale PV and the data used to achieve this.

Chapter 5 - describes the modelling methodology used to create a dispatch model, calculate C_r for a variety of scenarios and assess CO_2 avoided amongst other outcomes.

Chapter 6 – discusses and analyses the results from the testing process described in chapter 5.

Chapter 7 - draws conclusions based on the findings in chapter 6 and makes recommendations based on these conclusions.

1.3. Conclusion

This dissertation aims to offer a novel contribution to the modelling of power systems using variable generators specific to SA systems. It considers a simple power system model to simulate the economic and environmental effects of including a realistic penetration of PV technology into the system.

It consists of two parts:

- Part I focusses on a high level power system (PS) model, including PV projects from R1 & R2 of REIPPPP.
- Part II explores the C_r of PV generation for an expanded PV fleet, and the effect that geographic dispersion and penetration level of PV has on this value.

It is hoped that the results of this research will greatly enhance the knowledge on utility scale PV in South Africa and inform policy on long term energy planning. Furthermore, the results can be used to aid further research in this area.

2. CONTEXT: BACKGROUND AND THEORY

Solar PV technologies rely on energy from the sun as a fuel source, a resource that is cost neutral. However, because of high capital costs, historically PV has been a less economical option than conventional power generators. As a result the main drivers for investment in utility scale PV systems have most frequently been policy driven. In this chapter the context of solar PV technology, the recent growth of utility scale PV and the long term South African energy plan are discussed. The chapter begins with a short summary of the facts and figures about PV and its recent growth; and ultimately taking a brief look at the recent energy history of SA and incumbent Integrated Resource Plan released by the DOE in 2011 (DOE, 2011).

2.1. Solar Resource

Solar energy plants make use of the sun's energy to create electricity. The amount of energy reaching the earth surface in the form of sunlight is around 10 000 times the world's energy requirements (DGS, 2009).

The quality of solar resource that is available is arguably the most important factor when choosing a potential development site as it directly influences the project's economic viability and financial returns. Thus it is important that solar energy definitions are properly understood.

Most commonly the measurement of energy from the sun is defined in the following way (Brosz, et al., 2012):

- **Irradiance**: the measure of the power density of sunlight, in units of W/m^2. Often used interchangeably with "solar insolation"
- **Irradiation**: the measure of energy density of sunlight, in units of kWh/m^2 and is the energy content of solar radiation usually measured over a month or year
- **Peak Sun Hours** (PSH) (a.k.a. sun hours per day): length of time in hours at an irradiance level of 1000 W/m^2

In good weather at noon, irradiance may reach 1000 W/m^2 or more on the earth's surface. Counter intuitively, the highest levels of irradiance occur on partly cloudy days as a result of solar radiation reflected off passing clouds, where insolation levels can reach up to 1400 W/m^2 (DGS, 2009).

Solar radiation reaching the earth's surface can be split into a direct portion and a diffuse portion. These can be defined as direct normal irradiance (DNI) and diffuse horizontal irradiance (DHI) and are further explained below.

- **Direct Normal Irradiance**: the amount of solar radiation received per unit area by a surface that is always held perpendicular (or normal) to the rays that come in a straight line from the sun at its current position in the sky, in units of W/m^2 and kWh/m^2 for irradiance and irradiation, respectively. The majority of the available solar energy is DNI, and it is the only form of solar energy that can be concentrated (Brosz, et al., 2012).

- **Diffuse Horizontal Irradiance**: the amount of radiation received per unit area by a surface (not subject to any shade or shadow) that does not arrive on a direct path from the sun, but has been scattered by molecules and particles in the atmosphere and comes equally from all directions, in units of W/m^2 and kWh/m^2 for irradiance and irradiation, respectively (Brosz, et al., 2012).

Combining these two components gives you global horizontal irradiance (GHI)

$$GHI = DNI + DHI \qquad (1)$$

GHI can be defined as:

- The total amount of shortwave radiation received from above by a surface horizontal to the ground, in units of W/m^2 and kWh/m^2 for irradiance and irradiation, respectively.

GHI is of particular interest to us in terms of PV installations, as they utilize both DNI and DHI.

2.2. Solar Technologies

Converting energy from the sun into electricity can be done in two ways:

- Indirectly using concentrated solar power (CSP)
- Directly using photovoltaic modules

CSP systems make use of lenses or mirrors guided by tracking systems to focus the DNI along an axis which is used as a heat source for a conventional steam power plant thus indirectly generating electricity. PV on the other hand makes use of the photoelectric effect, which is the phenomenon by which semiconductor materials convert sunlight directly to electric current (Brosz, et al., 2012).

Solar cells are the key component in producing electricity and are most commonly made of silicon. The three main categories of PV semiconductors listed in terms of market share are as follows (Brosz, et al., 2012):

- Crystalline-silicon (c-Si): 80% – 90% of market share
- Thin film: 10% – 20% of market share
- Multi-junction

An overview of PV technologies and relative efficiencies can be found in Appendix A

2.3. Growth of Utility Scale PV

In recent years there has been a rapid increase in installed PV capacity globally. This has largely been due to the trend toward utility scale PV plants. A utility scale PV plant is one which generates energy

and exports it onto the grid, supplying the utility with energy through a Power Purchase Agreement (PPA) and in this case defined as being larger than 200kW (REN21, 2011). This in turn has had an economies-of-scale effect, quite drastically lowering module costs. In the U.S. installed prices of PV systems declined 5-7% per year on average from 1998-2011, and by 11-14% 2010-2011 (Feldman, et al., 2012).

Toward the end of 2010 approximately 9.7GW of utility scale PV had been installed worldwide out of an approximate 40GW total installed PV (REN21, 2011), as shown in Figure 1 below. This was an increase of over 3 GW during the year, around 50% growth. This meant that a quarter of all PV capacity at the end of 2010 was utility scale. This growth predominantly occurred in the EU, with 84% of the market (REN21, 2011).

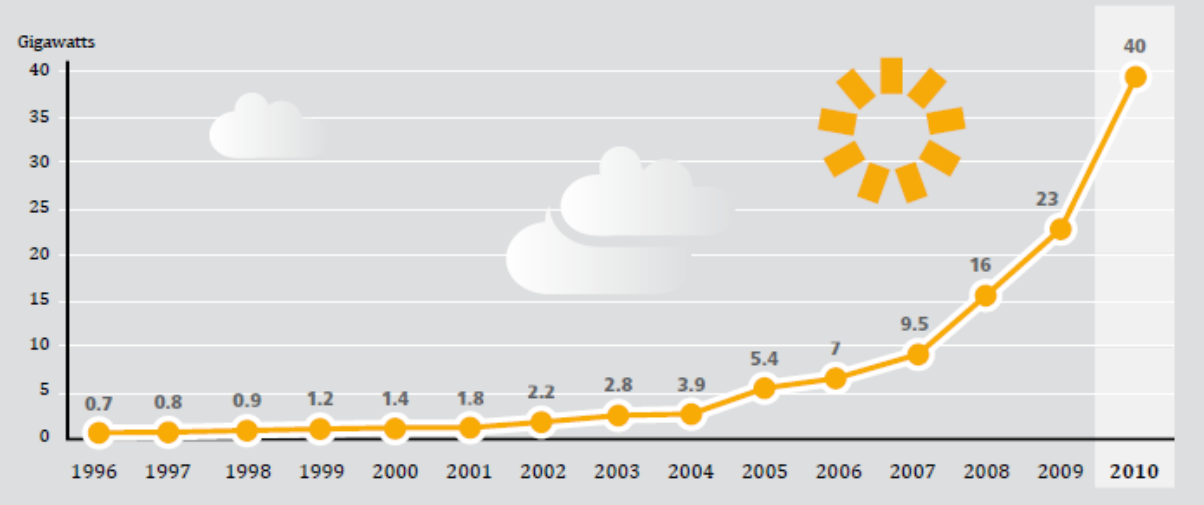

Figure 1: Growth of Total PV Capacity from 1996 - 2010 (REN21, 2011)

For 2011 the trend towards utility-scale projects became even more pronounced with a 60% increase in utility-scale installations over 2010 (REN21, 2011). Along with this great increase in installed utility scale PV, there is a trend toward bigger and bigger installations, which increasingly requires accurate modelling of power systems with a significant share of PV.

2.4. The South African Energy Context

Although SA has good wind and solar resources, as of 2010, given the historical access to large supplies of cheap coal, more than 90% of SA's electricity was generated using coal (Edkins, et al., 2010) and pre-2008 the country was able to supply the lowest electricity prices in the world at R0.25/kWh (Edkins, et al., 2010). In 2008 demand exceeded supply, which resulted in load shedding and caused Eskom to embark on an energy expansion plan involving return of service for mothballed coal plants; new coal-fired capacity in the form of Medupi and Kusile and the Ingula pumped storage scheme. In addition, the DoE initiated the renewable energy IPP procurement programme (REIPPPP) which placed an obligation on Eskom, being the system operator as well as the dominant utility, to enter into power purchase agreements (PPA) with Independent Power Producers (IPPs).

More than 100 countries have adopted renewable energy targets particularly focussing on wind and solar power. South Africa's aspirations, as outlined in the integrated resource plan (IRP), are particularly noteworthy because of a heavy historical reliance on coal.

The 2010 integrated resource plan (IRP) was finalised in March 2011. A least cost optimisation model under constraints was used to generate results, which were published along with assumptions made. This was then mediated and adjusted accordingly in a public consultation process, and finally allowed for 18.7 GW of renewables to be installed by 2030 (DOE, 2011) and integrated into the SA power system. Within this new energy mix, the DoE committed to procure energy from 8400 MW of solar PV, 8400 MW of wind and 1000 MW from CSP (DOE, 2011) through the REIPPP procurement programme. This amounts to wind and solar being 21% of generating capacity by 2030 (DOE, 2011). Furthermore ESKOM planning scenarios outline a potential of 40% penetration by 2040 (Eskom, 2012).

Prior to the IRP, SA's renewable energy policy was mostly driven by a renewable energy target of 10 000GWh by 2013 and subsidies offered through the Renewable Energy Finance and Subsidy Office (REFSO) and the 2009 Renewable Energy Feed In Tariff (REFIT) programme (Edkins, et al., 2010). 10 000GWh of energy is not a particularly large goal, given that in 2011 alone 240 528GWh of electricity was distributed (Stats SA, 2012). Even with all these measures, few renewable energy projects were undertaken until the IRP provided a structured energy plan that took SA's greenhouse gas reduction commitment into account as well as future learning rates for renewable technologies that projected them to become increasingly competitive.

The REIPPPP consists of rounds of competitive bidding and by December 2011 the DOE had received 53 bids across all technologies (DOE, 2012), from which 18 PV projects were awarded Preferred Bidder status, ranging from 5 MW to 75 MW in capacity with a total capacity of 632 MW. This was then followed up by Round 2 of the process which closed on March 2012, with 9 PV projects awarded with Preferred Bidder status at a total capacity of 417 MW.

Table 1 below describes PV project details from R1 and R2 of the REIPPPP process.

Table 1: PV Projects Awarded in R1 and R2 of the REIPPPP process

	PROJECT NAME	**CONTRACT CAPACITY**	**ANTICIPATED COD**	**PROVINCE**
		MW		
	Round 1			
1	SlimSun Swartland Solar Park	5	01-Jul-14	Western Cape
2	RustMo1 Solar Farm	6.8	15-Nov-13	North West Province
3	Konkoonsies Solar Energy Facility	9.7	13-Dec-13	Northern Cape
4	Mulilo Solar PV De Aar	9.7	01-Apr-14	Northern Cape
5	Aries Solar Energy Facility	9.7	13-Dec-13	Northern Cape
6	10MW Greefspan PV Power Plant	10	11-Apr-14	Northern Cape
7	Mulilo Solar PV Prieska	20	01-Apr-14	Northern Cape
8	Herbert PV Power Plant	20	11-Apr-14	Northern Cape
9	Soutpan (Erika Energy) (Pty) Ltd	28	30-Jan-14	Limpopo
10	Witkop Solar Park	30	25-Apr-14	Limpopo

11	Touwsriver Project	36	20-Jun-14	Western Cape
12	Mainstream PV De Aar	48.3	03-Apr-14	Northern Cape
13	Droogfontein PV	48.3	03-Apr-14	Northern Cape
14	Letsatsi	64	21-May-14	Free State
15	Lesedi	64	21-May-14	Northern Cape
16	Kalkbult	72.5	01-Jan-14	North West Province
17	Kathu Solar Plant	75	15-Aug-14	Northern Cape
18	De Aar Ilanga Lethemba	75	28-Feb-14	Northern Cape
	Round 2			
1	Vredendal	8.8	30-Nov-13	Western Cape
2	Upington Solar PV	8.9	01-Apr-16	Northern Cape
3	Aurora - Rietvlei	9	30-Nov-13	Western Cape
4	Linde	36.8	01-Dec-13	Northern Cape
5	Boshoff Solar Park	60	20-May-14	Free State
6	Dreunberg	69.6	01-Apr-14	Eastern Cape
7	Sishen Solar Facility	74	30-Jun-14	Northern Cape
8	Solar Capital Aggenys	75	01-Jan-14	Northern Cape
9	Jasper Power Company	75	30-Sep-14	Northern Cape

2.5. Conclusion

Up until 2011, when the IRP was gazetted, energy policy in SA had scant success in driving the development of a viable renewable energy market. This all changed in 2011, with the birth of the REIPPPP process and 27 successful PV bids commencing development in 2013. The IRP is a plan that directs expansion of electricity supply until 2030 in order to meet projected long term electricity demand. It details how electricity demand should be met in terms of generating type, capacity, timing and cost. It does not stipulate however, the location of the planned capacity and this could result in the case of all designated PV capacity concentrated in one solar rich area. This is particular relevant for wind and solar technologies for which production is dependent on variable weather patterns. The ramifications of this scenario are clear if one considers the example whereby one day of bad weather could result in the total PV capacity being offline. This would effectively minimise the availability of installed PV capacity, thus requiring back-up generators to cover the load, and effectively lowering the value that PV can added to the power system.

3. LITERATURE REVIEW

The objective of this research is to quantify the value that installed Solar PV capacity can add to the existing power system of South Africa for various levels of penetration and geographic dispersion. The value added will be quantified using a Capacity Credit (C_r) metric, which indicates the value a variable technology like PV can add to a power system when compared to that of an equivalent dispatchable generation technology.

In order to do this, utility scale PV plants need to be simulated; the existing power systems' level of reliability with and without the variable generators needs to be simulated and a dispatch model needs to be created. This chapter aims to explore important literature on these topics, focussing on papers that explore modelling tools for evaluating the integration of non-dispatchable technology into large grid power system.

3.1. Simulation of Utility Scale PV:

In order to effectively model the behaviour of a power system utilising a high penetration of PV, the hourly yield of the installed PV capacity needs to be simulated. PV power output is mostly dependent on the installed capacity (the nameplate capacity of the plant often referred to as the DC capacity), the ambient temperature on site and most importantly, the irradiance striking the collectors surface (Hart & Jacobson, 2011). Dragoon & Shumaker (2010) note that the method for calculating clear sky radiation is well understood and as a result the output of solar generators is highly predictable using satellite derived data. Nonetheless, predicting the output from a PV generator is complicated by a variety of environmental, solar cell technology and irradiance factors that are often dependent upon one another. This is illustrated in Figure 2 below, which shows a scatter plot of actual performance measurements taken over a five day period from a 165 Wp mc-Si[1] module in a study by Sandia Laboratories (King, et al., 2004) which displays variation in results based on the factors mentioned above. The vertical variation is mainly caused by change in solar irradiation level, while the horizontal variation is mainly caused by module temperature (King, et al., 2004).

1. Wp refers to the DC rating of the module, while mc-Si refers to the type of panel chosen, in this case a mono-crystalline silicon PV panel. There are a large variety of modules to choose from, which is further discussed in Appendix A

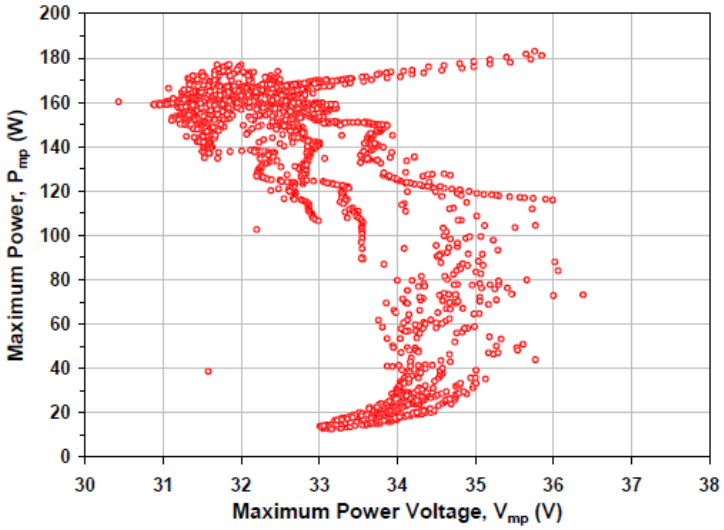

Figure 2: Scatter plot of performance measurements take over a five day period in January with both clear sky and cloudy conditions (King, et al., 2004).

In order to increase the accuracy of PV yield estimates, a large array of methodologies, models and computer packages have been developed.

Performance ratio (PR) is perhaps the most commonly used method for a comparison between projects and is a very approximate way of predicting yield of a PV system. The PR of a PV system is defined as the ratio of actual and theoretical performance (SMA, n.d.). It is mostly independent of orientation and incident solar irradiation and as a result is most effective for comparing plants that supply energy to the grid at different locations.

PR is used to calculate energy that can actually be exported to the grid after taking losses into consideration and is typically between 77 and 82% for a well-designed plant (Miller & Lumby, 2012). It is however more suited to comparison of average values over a given time period, such as a year or month rather than at an hourly resolution. This is because at an hourly resolution the PR of a system can fluctuate a great deal owing to the fact that the PR value is dependent on losses associated with the site. The main reason for this fluctuation is due to losses associated with cell temperature operating efficiency, which is largely dependent on ambient temperature and incident irradiation; factors which can vary a great deal over the period of a few hours. This has led to much effort spent on quantifying efficiency losses associated with the module cell temperature.

Models such as the Sandia Performance model calculate the electrical performance of individual PV modules (King, et al., 2004). This can then be scaled to apply to any system depending on the series/parallel combination of the array. The method uses three particular points on a module's I-V curve, an example of which is shown in Figure 3 below. These curves are usually provided by the module manufacturer:

- Short circuit current (Isc)
- Open circuit voltage (Voc)
- Maximum power point (MPP), or Pmax

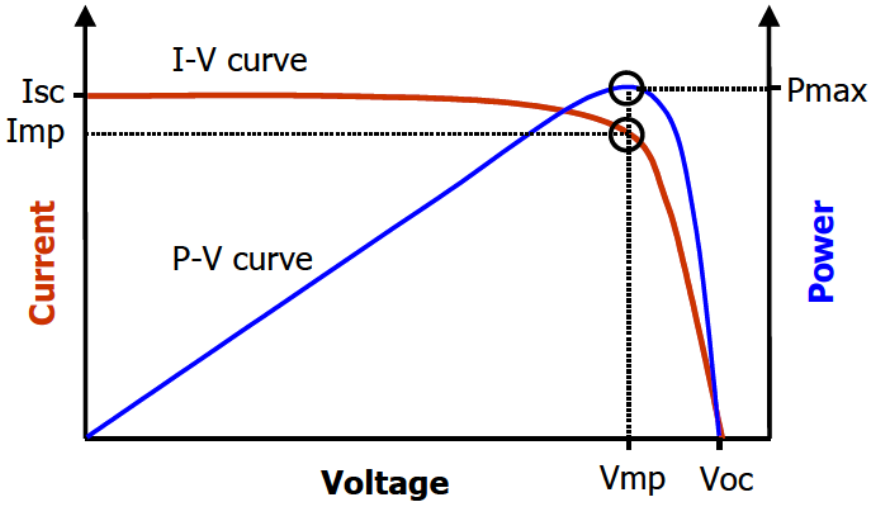

Figure 3: I-V curve for a PV module, showing Isc, Voc & MPP (Solmetric, 2011)

The I-V curve can then be used to calculate the P-V curve from which the power out can be determined using predetermined or measured module performance coefficients, such as cell temperature and efficiency characteristics. Access to this type of data is not always readily available however, and the data can be time consuming and onerous to generate.

Kou, et al. (1998) use a similar approach to *Sandia* in that they use a mathematical model to simulate the electrical characteristics of a PV module under various conditions using only information supplied by the manufacturer. To do this they theoretically reduce the PV cell to a simple electrical circuit, from which they can calculate parameters such as voltage, current and resistance. This simple approach is complicated however by many of the required parameters being dependant on incident radiation and cell temperature, but instead of using measured cell operating temperatures like Sandia, they make use of the manufacturer supplied NOCT (Nominal operating cell temperature) value to estimate the cell temperature (Kou, et al., 1998). Using the NOCT value by itself, while useful, does not take into consideration the mounting specifications of the module, such as fully ventilated or insulated mounting, which can have quite a significant impact on cell temperature. As a result alternative methods for calculation of cell temperature are now often used in many PV simulation programmes (PVsyst, 2012).

An alternative method to predict cell operating temperature is described by Jones & Underwood (2000). They make use of a simple thermal model to simulate an energy balance of PV cells based on climate variables. Theoretical methods are used to simulate the energy transfer process; involving short wave radiation, long wave radiation, convection and electrical energy production (Jones & Underwood, 2000). The method is found to be within 6 K of measured temperatures 95% of the time, and proves to be most accurate in periods of clear or overcast conditions, where irradiation is fluctuating least (Jones & Underwood, 2000).

Similarly, Bagen (2005) uses an iterative process to calculate the power out of a PV system using I-V curves and a thermodynamic model to estimate operating cell temperature based on the equation below.

$$P_O = \frac{V_r I_r}{H_{Tr} A} H_T \qquad (2)$$

Where A is the panel area, H_T is the solar insolation at a particular hour, V_r and I_r are reference voltage and current and P_o is the Power out.

In their approach, Hart & Jacobson (2011) combine the flexibility and simplicity of the PR method with a greater accuracy in loss calculation by using the following equation found in (Masters, 2004) to simulate PV output.

$$P_{PV}(t) = \sum_j \frac{V_j I j_{PV}(t) \eta j_T(t) \eta_{PV}(t)}{1000\ W/m^2} \qquad (3)$$

Where V_j is the installed capacity (DC) of the entire system at the *j*th PV site; $Ij_{PV}(t)$ is the incident irradiation that strikes the modules at time *t* for the site; $\eta j_T(t)$ is the efficiency coefficient associated with temperature losses at the site; and $\eta_{PV}(t)$ is the efficiency coefficient associated with site associated losses at time *t* for the site (Hart & Jacobson, 2011). These two efficiency coefficients are split into two distinct groups:

- **η_{PV}:** Generic losses associated with PV systems such as mismatch, soiling and inverter losses (Hart & Jacobson, 2011)
- **η_T:** Site specific temperature losses associated with hourly change in ambient temperature and incident irradiation (Hart & Jacobson, 2011)

The incident irradiation is a function of direct normal irradiance (Ij_{DNI}), diffuse normal irradiation (Ij_{DHI}), site location; tilt angle and time of year. It is approximated for time *t* by:

$$Ij_{PV}(t) = Ij_{DNI}(t)[cos\beta_j(t)cos\varphi_j(t)sin\sum_j] + Ij_{DNI}(t)[sin\beta_j(t)sin\sum_j] + Ij_{DHI}(t)[\frac{1+cos\sum_j}{2}] \qquad (4)$$

Where β_j, φ_j and $\sum_j$ are the solar altitude angle, solar azimuth angle and tilt angle respectively (Hart & Jacobson, 2010). This then allows for the approximation of temperature efficiency at time *t* as follows (Hart & Jacobson, 2010):

$$\eta j_T(t) = \frac{0.005}{°C} \times \left[T_j(t) + \frac{(NOCT - 20°C)}{800 \frac{W}{m^2}} Ij_T(t) - 25°C \right] \qquad (5)$$

Where T_j is the surface temperature in °C for the *j*th PV site and NOCT is the normal operating temperature value provided by the module manufacturer. Due to its flexibility this method lends itself to comparison of PV systems in multiple locations and of different capacities. This is because it relies only on installed capacity, incident irradiation and ambient temperature, and does not require factors such as number of modules in parallel and series and other site dependant variables, as some of the other methods do.

When considering the resolution of data required for modelling of PV systems it is important to consider the geographic footprint of the load. In their research on *Solar PV Variability and Grid Integration,* Dragoon & Shumaker (2010) found that cloud cover can cause variability in PV systems, with power fluctuations in the order of 50-60% over a period of seconds. Furthermore they found that this variability is greatly reduced through geographic dispersion. This has been shown to be true for relatively short distances of 20kms in US southern Great Plains, and just 9kms in Japan (Dragoon & Schumaker, 2010).

3.2. Power System Reliability: Theory

NERC (n.d.) defines a reliable power system as one that should be able to provide quality power to satisfy the system load with a reasonable assurance of quality and continuance of supply to its customers at all times.

Therefore the reliability of the system is a measure of ability of the system to provide this service and he defines the two key attributes of a reliable power system as:

- **System security**: the ability of the power system to withstand sudden disturbances
- **System adequacy**: the existence of sufficient facilities within the system to satisfy the consumer load demand or system operational constraints at all times

This is confirmed by Bagen (2005) in his work on *Reliability and Cost/Worth of Generating Systems Utilising Wind and Solar* where the author states:

> *"The reliability associated with a power system is a measure of the overall ability of the system to perform its basic function"* (Bagen, 2005)

In other words it is the measure of the ability of the power system to meet demand at all times, and ability to withstand sudden disturbances.

Billington & Allan (1996) recognised that before the 1960's simple and subjective criteria, or "rules of thumb", were used to approximate a power system's reliability. This is supported by Garver, et al (1964) who states that the reliability of the system was most usually approximated by looking at existing power systems, extrapolating their experiences and using the rules of thumb to estimate the reliability of the new system.

During the 1960's it was recognised that a more empirical approach was required and this resulted in much work assessing power system reliability methodology. From this two different branches of

reliability methodology emerged: Either using deterministic indices to reflect assumed situations, or probabilistic indices which deal with uncertainty in the system (Bagen, 2005).

Commonly, in deterministic methodology, the reserve capacity has been the preferred metric to determine reliability. There are various criteria to determining reserve capacity, with the following being the most common (Bagen, 2005):

- **Capacity reserve margin –** the difference between total installed capacity and system peak load expressed as a percentage of peak load
- **Loss of Largest Unit –** the required reserve capacity equal to that of the largest generating unit in the power system
- **Loss of Largest Unit + percentage margin –** similar to above, but with an additional fixed percentage; usually of total installed capacity or peak load
- **Dry year**: used in hydro dominated systems to determine effect of poor hydroelectric availability

These methods are easy to apply and understand, but generally do not look at the reliability of individual units, rather looking at the system as a single entity. This results in the methods becoming less efficient with increasing scale and complexity of the system (Hart & Jacobson, 2011). Furthermore, by their very nature, the occurrences of system failure, load demand and system behaviour are inherently uncertain, but this uncertainty cannot be taken into consideration when using deterministic methods (Bagen, 2005). As a result most utilities have adopted probabilistic approaches (Billinton & Allan, 1996).

In a probabilistic analysis, individual generating unit unavailability is an important parameter in the calculation of reliability (Billinton & Allan, 1996) and it allows for a quantitative analysis of alternatives on the system by taking parameters that directly influence reliability of individual units into consideration. Reliability indices are incorporated to help us understand the likelihood of an individual generating unit being offline. The most common of these are (Billinton & Allan, 1996):

- **LOLP**: Loss of load probability – % probability that load exceeds the available capacity
- **LOLE**: Loss of load expectation - the expected time duration that the load exceeds the available capacity
- **LOEE**: Loss of energy expectancy - the expected energy that will not be delivered when load exceeds capacity

Generally these indices look at the probability of loss of load as a result of supply being lower than demand. This is expressed in expected number of days over a prolonged period (usually 10 years) that insufficient generating capacity is available to serve load (Bagen, 2005). Furthermore they measure the value of an added unit's contribution to the system's capability. This is what is of interest to this dissertation, and will be looked at in depth in the next section.

The generic term for this method of modelling systems is called stochastic modelling. Stochastic modelling in general describes methods that are suitable for modelling complex systems that contain uncertainty (Karlsson, et al., 2009). In their report, Karlsson, et al. explains that contrary to deterministic methods, stochastic modelling will yield a range of results according to a probability distribution. The main disadvantage of stochastic modelling is increased complexity and data

analysis. The main advantage however is that stochastic modelling provides a more realistic description of a complex system (through a dispatch model).

Essentially probabilistic techniques can be separated into two groups: direct/analytical or Monte Carlo Simulation (MCS) (Bagen, 2005). Analytical methods use models to represent the system and mathematical solutions to evaluate the indices. MCS on the other hand, makes use of random numbers sampled from a distribution to simulate the actual process of random system behaviour.

There are costs and benefits to both methods. Direct methods employ a recursive technique to create an outage probability table, whereas MCS expresses available capacity at points in time, chronologically with a load curve superimposed to show points of risk (Bagen, 2005). The latter is an elegant way of portraying points of failure graphically, as seen in Figure 4 below. The energy not supplied can clearly be seen where the load curve surpasses the available capacity, shown in the shaded areas. The loss of load duration is shown by t_1, t_2 and t_3 in hours and the energy not supplied by e_1, e_2 and e_3.

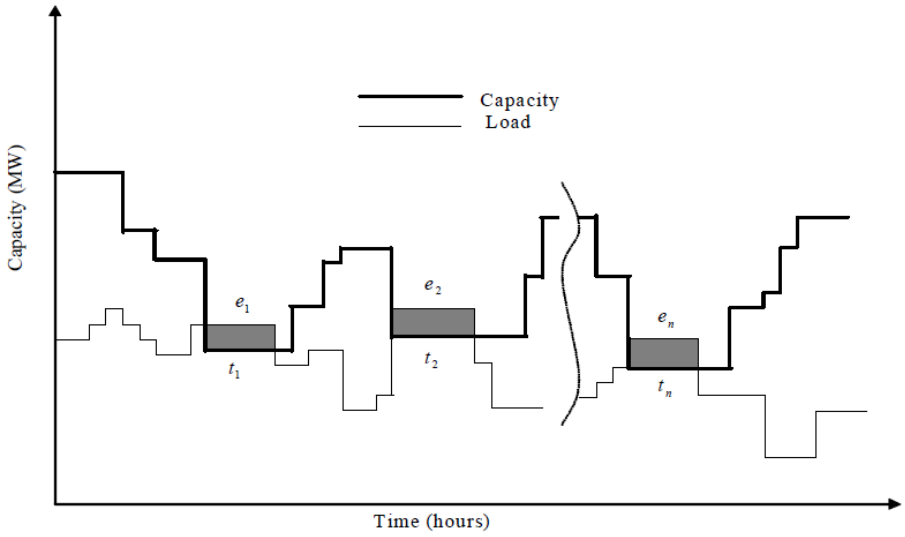

Figure 4: Superimposition of Load Curve on Hourly System Capacity (Bagen, 2005)

This chronological approach is particularly applicable when trying to incorporate the stochastic nature of variable supply renewable technologies into power system planning. This is because their random nature causes the approximation of the reliability in the system to become more complex (Bagen, 2005).

This point is further enforced by Hart and Jacobson (2011) who suggest that probabilistic methods that have traditionally been used to calculate the forced outage rate (FOR) of conventional generators have, in recent years been used successfully to model variable generators. This is particularly true for wind generation, with Holttinen, et al (2006) compiling a review of wind integration studies across Europe to date. The paper reviews projects from 10 countries and outlines studies made at the European Wind Energy Association and UCTE (Union for the Co-ordination of the Transmission of Electricity) and ETSO (European system operators).

With the majority of recent studies focussing on the integration of large scale wind, other technologies have received less attention, particularly solar PV. Much useful information on the

modelling of solar PV reliability can however be found in capacity credit studies, which focus on the general approach of integration of variable generators into power systems.

3.3. Capacity Credit (C_r)

With the increasing penetration of variable generators into power systems, it is becoming increasingly important to quantify the value that these generators can add to the system. This in turn will allow one to quantify the capacity of variable generators that can be added to an existing power system without negatively affecting its ability to supply demand in a reliable and adequate manner. In a modern power system that incorporates variable generators alongside conventional generators, a direct comparison is not always easy to make. C_r evaluation has become the best available tool for comparison of the value of generator capacities, and much research has been conducted in this area. Even so, currently there is no standard approach to C_r evaluation with results varying with the method chosen. This chapter discusses the different approaches used in this area of research, including evaluation of variable generators as a whole and then focusing on the C_r of PV generators.

In his paper Amelin (2009) uses an empirical approach to compare the properties of 4 typical and widely used C_r calculation methods. Significantly, he found that there can be large variation in C_r based on the method used to calculate it. He defines C_r as:

"The contribution of the additional generation unit to the generation adequacy of a power system"

A simple way to look at it is as the amount of conventional dispatchable capacity that can be "replaced" by variable generators without causing the system to become less reliable (Pudaruth & Li, 2008). C_r differs from the more common term Capacity Factor (CF), which represents the ratio of mean output to rated capacity (Perez, et al., 2008).

C_r evaluation was in existence before the integration of renewables into power systems became a heavily researched topic. Prior to this it was found to be useful in analysis of competitive electricity markets, such as in the U.S., where peaking plants often started to become unprofitable due to limited time use (Amelin, 2009). Therefore C_r calculations were used to quantify the capacity that peaking plants could add to the system during periods of high demand if required, and selling energy on this basis rather than in terms of kWh used (Amelin, 2009).

Amelin (2009) notes that with the increasing penetration of RE's into power systems worldwide, C_r evaluation has become the best available tool for analysing the effect of the integration of variable generators such as wind and solar power into a traditional power system. When a typical utility begins planning for additional generation capacity, different energy sources need to be compared. This is difficult to do directly, but can be achieved through C_r evaluation – a value that can be applied across all technologies. Simply put, 100MW of coal generation could be found to have the same capacity credit as 300MW of wind for a particular system and thus compared directly.

This analysis needs to be undertaken in order to maintain the same level of reliability in a power system when a conventional power plant is replaced by variable generators. For example, a variable generator that produces the same amount of energy on a yearly basis as a conventional plant does

not contribute to the system adequacy (the ability to satisfy the system load at all times) at the same level as the conventional power plant. Thus in order to maintain the reliability of the system, back-up capacity such as gas-peakers might be required (Amelin, 2009).

Previously it was thought the variable generators did not have a C_r value, a view that has now changed, recognizing the importance of quantifying the value added to the system from these generators (Pudaruth & Li, 2008).

Currently there is no set standard for C_r with a variety of definitions in use today (Amelin, 2009). The 4 definitions below are typically used in systems that use a classic probabilistic production cost simulation, similar to that approach taken in this thesis:

1. **Equivalent Firm Capacity** (EFC) – defined as the capacity of a theoretical 100% reliable generating unit that will cause the system to have the same LOLP as when the actual unit is added.
2. **Effective Load Carrying Capability** (ELCC) – defined as the additional load that can be carried by the system for a given reliability and a given additional capacity of new generating units.
3. **Equivalent Conventional Power Plant** (ECPP) – similar to EFC, but using a conventional power plant for comparison with conventional reliability levels, rather than a theoretical power plant.
4. **Guaranteed Capacity** – defined as the least capacity which can be expected to be available with a given probability (not to be confused with LOLP). It considers only capacity of the systems, not the load, with and without an added generator unit.

Perhaps the best known C_r methodology is the ELCC metric, first introduced by Garver in 1966. The method makes use of LOLP to graphically estimate the load carrying capability of a new generating unit (Garver, 1966). Initially a desired level of reliability for the system is chosen (often the level of reliability calculated for the system prior to the added generating unit). From this a reliability curve for the system is created by testing the reliability of the system at different loads. The new generating unit is then added to the system, and the reliability curve process is repeated at the defined reliability. The ELCC of the new unit is then the load increase the system may take within the desired level of reliability (Garver, 1966). This is perhaps best understood graphically, see Figure 5 below.

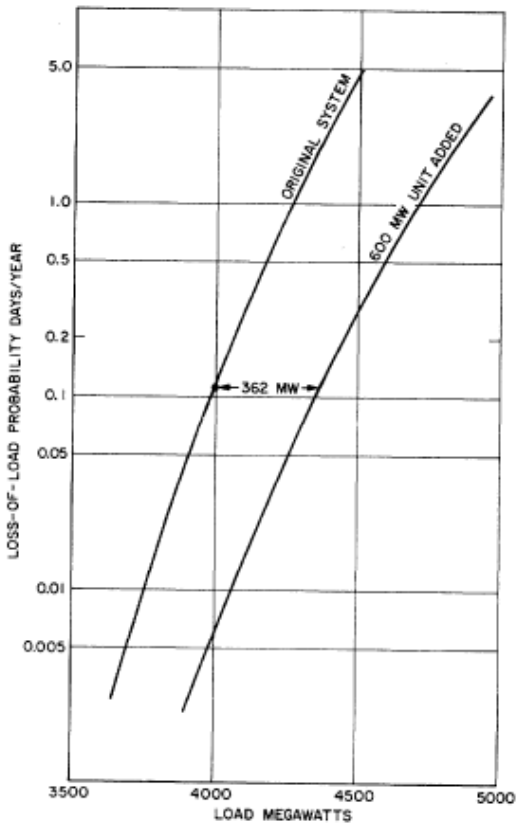

Figure 5: Annual Risk Expressed as LOLP after Adding a New Generating Unit (Garver, 1966)

In this example a new 600MW generating unit with a forced outage rate (FOR) of 5% is added to the system. A generating unit with a FOR of 5% will be offline for 5% of the year. As explained above, to find the ELCC of a new unit the reliability curves must be evaluated at various levels for the system as before and after the new unit is added as shown in Figure 5. The level of load increase at the defined risk level is the difference between the 2 curves (Garver, 1966). As a result at a system reliability of 0.11 days per year, the ELCC of 600MW generating unit is 363MW.

The one big disadvantage of using probabilistic approaches such as these is that it assumes that load and outages are independent of one another where in reality this is not the case (Amelin, 2009). In reality outages often are caused by high levels of load, which in turn can result in a higher loss of load occurrences then simulated in probabilistic scenarios. The first three definitions described above look to discover the effect of adding another generating unit on system adequacy based on how it affects the Loss of Load Probability (LOLP), which is the probability that the load exceeds available generation capacity (Amelin, 2009).

In order to test the definitions above Amelin (2009) set up a simple power system of a distributed load and existing generating units, which all had the same availability, based on 5 basic setups with distinct mean load, load variance and availability of existing units. The C_r of an added 1000MW conventional power and then an equivalent 2800MW of wind power were calculated using the different definitions.

Out of the 4 methods it was found that although there was a large variation in results with differences of up 30% observed, the first 3 were found to have consistent variations with ELCC

consistently slightly higher than EFC (see Figure 6 below). They followed a distinct trend of being dependant on the overall generation adequacy of the system and to a lesser degree the level of penetration (Amelin, 2009). In other words, the generating unit under scrutiny will have a higher C_r if added to a system with a higher LOLP, and if the generating unit capacity is small in comparison to total system capacity (Amelin, 2009). In contrast, for the last method he found that it is only dependent on size and availability of the system. Hence as can be seen in Figure 6 below, this method has correlated less than the other methods.

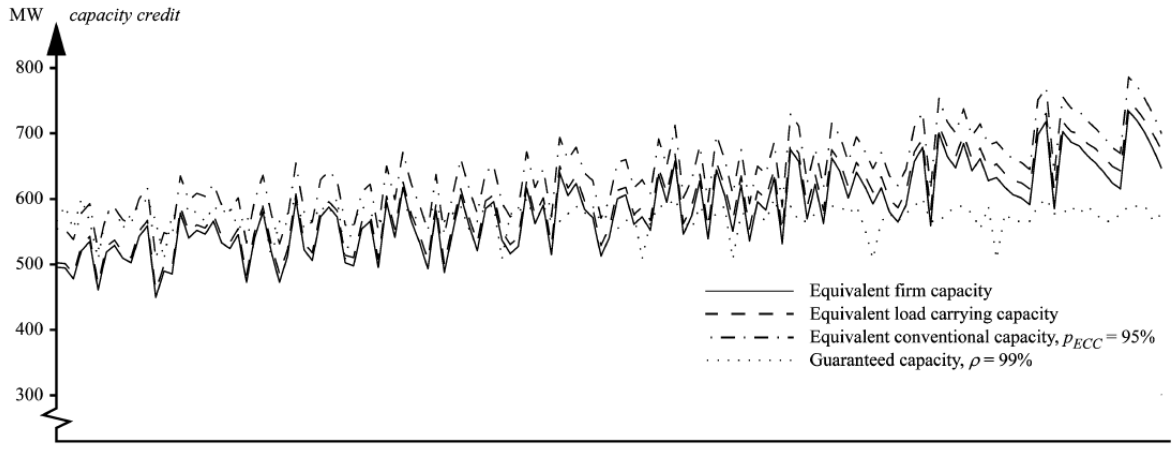

Figure 6: Capacity Credit Values for a block of 2800MW Wind Power for 135 Test Systems (Amelin, 2009)

The difference in results between methods 1,2,3 and 4 is mainly due to fact that 1,2 & 3 are based on how the last added unit affects the system adequacy(expressed by the LOLP of the systems); while 4 measures the impact of the added unit on guaranteed capacity of the system. This means that 4 does not take into account if the additional capacity is needed or not, since load is not included in the modelling (Amelin, 2009).

In similar research to Amelin (2009), Pudaruth and Li (2008) reviewed methods for determining C_r and emerging trends in industry favouring certain methods over others. In particular they looked at C_r for variable generators as a function of penetration for 2 typical approaches; EFC and ELCC. Similarly they discuss reliability indices such as LOLP, as well as forced outage rates (FOR) for conventional plants in their analysis.

In their review of academic literature they found that in order to calculate the C_r of an additional generation unit, the reliability of the existing system needs to be known. Furthermore they came to the conclusion that the majority of works completed on C_r studies made use of a probabilistic approach rather than analytical techniques, as the former accounts for the stochastic nature of intermittent generation for which the availability of its energy source is dependent on the variable nature of weather (Pudaruth & Li, 2008).

This is particularly true for PV systems, which can only generate power when the sun is shining. As a result PV technology is considered to be a non-dispatchable power source. However, in many studies (Particularly in the USA) it has been recognised that the variable supply from PV generators is not totally random in that there is correlation between summer peak demand for cooling and maximum output of PV plants (Perez, et al., 2008). Indeed one of the longer predictable weather cycles is that of seasons. Estimations of the C_r of PV systems vary greatly in range from 10% to 95% (Baker, et al.,

2013), mainly due to differences in physical settings and estimation methodology used. After applying the EFP and ELCC metrics to 14 PV locations around the U.S. Madaeni et al. (2012) found EFP and ELCC estimates during daytime peak load hours of 56-75% and 52-70% accordingly. These values are higher than expected however, and are mainly due to assumptions of broad geographic area, no generation constraints and a marginal increase in PV Capacity creating a very flexible power system (Baker, et al., 2013). Studies that focus on higher levels of PV penetration, a more detailed load model and a smaller geographic area have been shown to have lower C_r values (Baker, et al., 2013). This is vindicated by Lamont's (2008) evaluation of large scale PV in California, where a value of 17% was found, and by Gowrisankaran et al. (2013) who found values for large scale PV in Arizona of 17-35%.

Perez, et al. (2008) noted that for a demand side customer-owned PV system, the local C_r can readily be measured from energy used over a period of time. They note however, that on the supply side it is harder to quantify because its value is strongly reliant on three factors; C_r methodology, the geographic dispersion of the PV supply in terms of the load it serves and the time resolution used to measure the PV/load relationship. These factors are all related, particularly the latter two. If the PV supply is focussed in one area, cloud cover becomes a significant loss factor and high resolution data are required (at sub-hourly frequencies). If the PV plants are geographically dispersed however, hourly data becomes adequate because short term variability is mitigated (Perez, et al., 2008). This can be seen in Figure 7 below where a single location is compared to 20 locations spread across approximately 160km's.

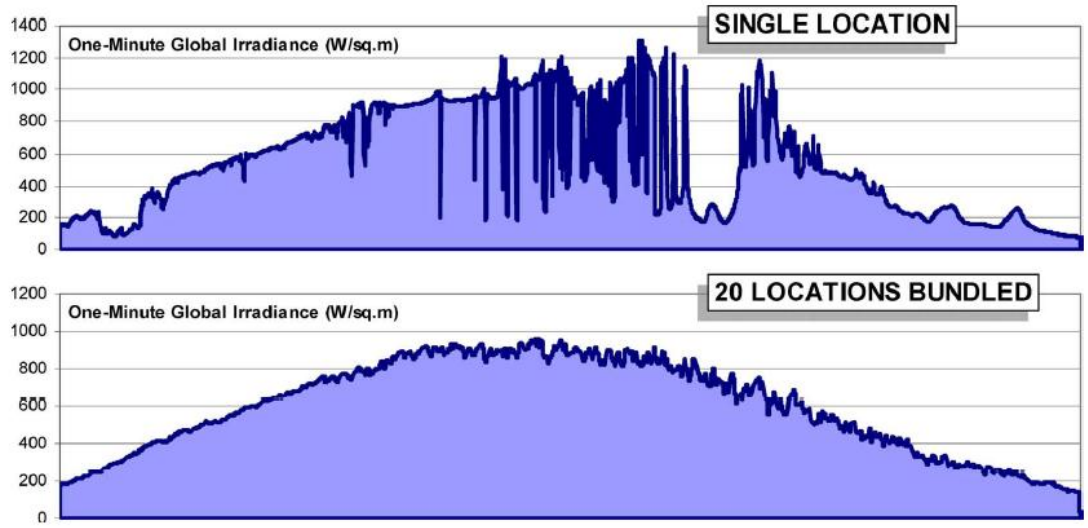

Figure 7: Effect of Geographic Dispersion on variability in Supply for a Single location and 20 Locations (Perez, et al., 2008)

In their work Perez, et al. (2008) present different methods to quantify C_r for PV systems using satellite derived data to simulate PV plant output at an hourly resolution. Similarly to Amelin (2009) they analyse a system using various C_r definitions, including the ELCC metric.

Significantly they found that the 3 input variables that affected the C_r metric the most are:

- Time resolution of data
- Number of generators considered

- Geographic dispersion of generators

In their simulations Perez, et al. (2008) analysed one year (2002) of load and PV generation for 3 US utilities. PV output was simulated for a fixed 30° tilt plant with penetration levels of 1% to 20% for each utility. Looking at Figure 8 below, it can be seen that the majority of methods used produce comparable results. All these methods are based on the physical measure of PV penetration except for the noticeable outlier, the Time Season Window (TSW) metric which has no dependence on penetration rates. This general agreement in C_r results between methods that are based on PV penetration rates is one of the most important findings of this study. Additionally it was found that the ELCC metric is a slightly more conservative approach than the other methodologies, and as such preferred by utilities (Perez, et al., 2008). Another important outcome of the study is that hourly satellite derived irradiation data at a 10 km resolution is appropriate for evaluation of geographically disperse PV systems, but not for single plants (Perez, et al., 2008).

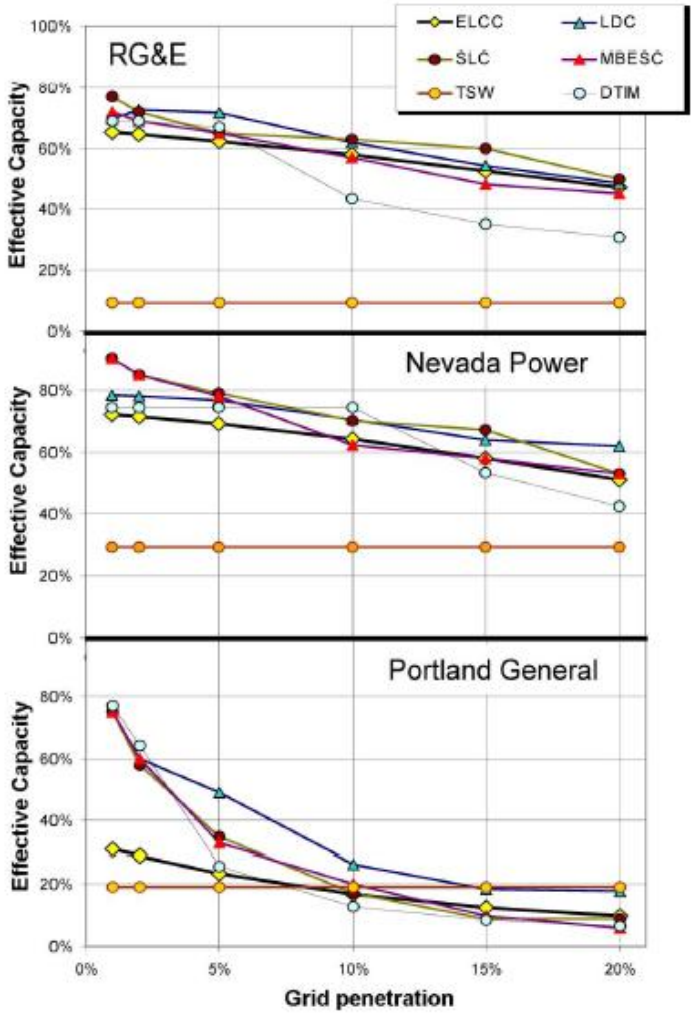

Figure 8: C_r as Function of Grid Penetration (Perez, et al., 2008)

The aim of Perez et al (2008) was to reach a consensus in the definition of C_r for PV systems, and the second half of the research was carried out through a workshop to gather information from the key stakeholders in the power system industry, such as utilities, government and developers from the solar industry who came together to exchange arguments and information in support of their

different viewpoints. A poll was taken and it was found that the preferred method for all parties concerned was the ELCC metric (Perez, et al., 2008). This is an important finding because methodologies have significant related impacts on monetary value of capacity, the cost of PV and long term capacity planning.

The findings of Perez et al (2008) are further vindicated by a study carried out by the National Renewable Energy Lab (NREL) in as early as 1997 (Milligan & Parsons, 1997) who thought it important to define a way for the energy market to measure C_r of new power plants, particularly with the dissolution of vertically integrated markets and the introduction of contracts with IPP's where C_r methodology will have to be agreed upon. The C_r evaluation allows for long term prediction of energy sales (Milligan & Parsons, 1997) and they recommend using the ELCC metric with the LOLP reliability method.

3.4. Dispatch models

An electrical power system's main function is to supply its customers with electricity in a reliable manner and as economically as possible (Bagen, 2005). Most conventional generating units are considered to be dispatchable because they have the ability to be dispatched with reasonable certainty, given that the plant is online.

A traditional dispatch model determines a number of configurations of plant dispatch that will meet demand and lists them in order of merit, merit being a combination of cost and the probability that the power can be dispatched. This usually results in generators being dispatched to minimize the hourly operating cost of electricity generation (Huber , 2011). The stochastic nature of systems utilizing renewable energy technology adds another dynamic to the dispatch of a power system however, but once reliability analyses, as presented above, are undertaken it allows for a cost optimisation of the system.

Hart & Jacobson (2011) optimised dispatch for a minimum LOLE requirement of 1 day in 10 years using MCS by least-cost optimisation to quantify the carbon emissions of systems incorporating high penetrations of high level renewables. The results of the optimised dispatch are displayed below in Figure 9 and provide a good example of a typical graphical example of a dispatch model output.

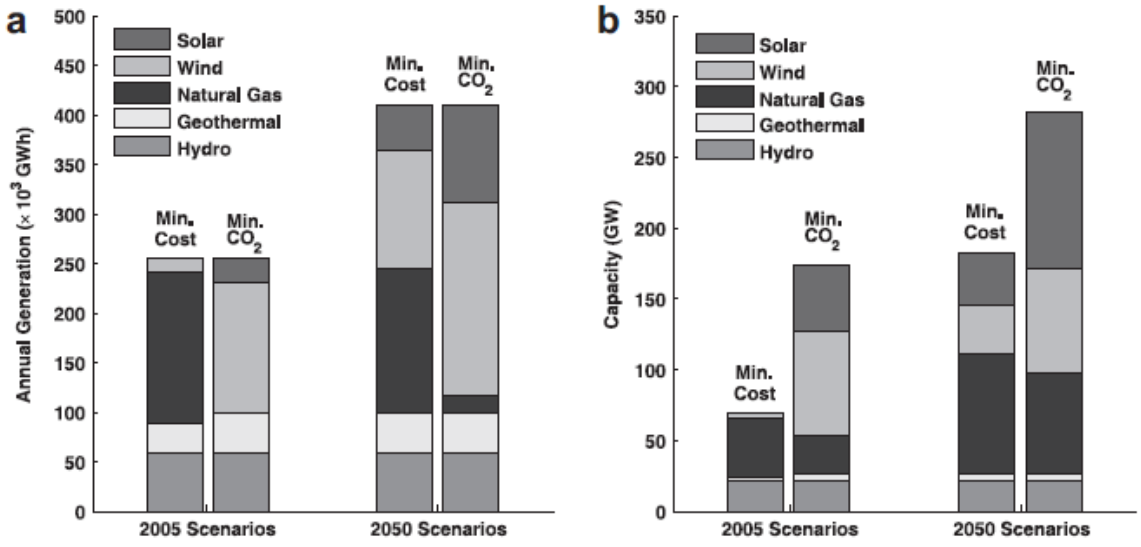

Figure 9: (a) Energy and (b) Capacity composition from the stochastic model (Hart & Jacobson, 2011)

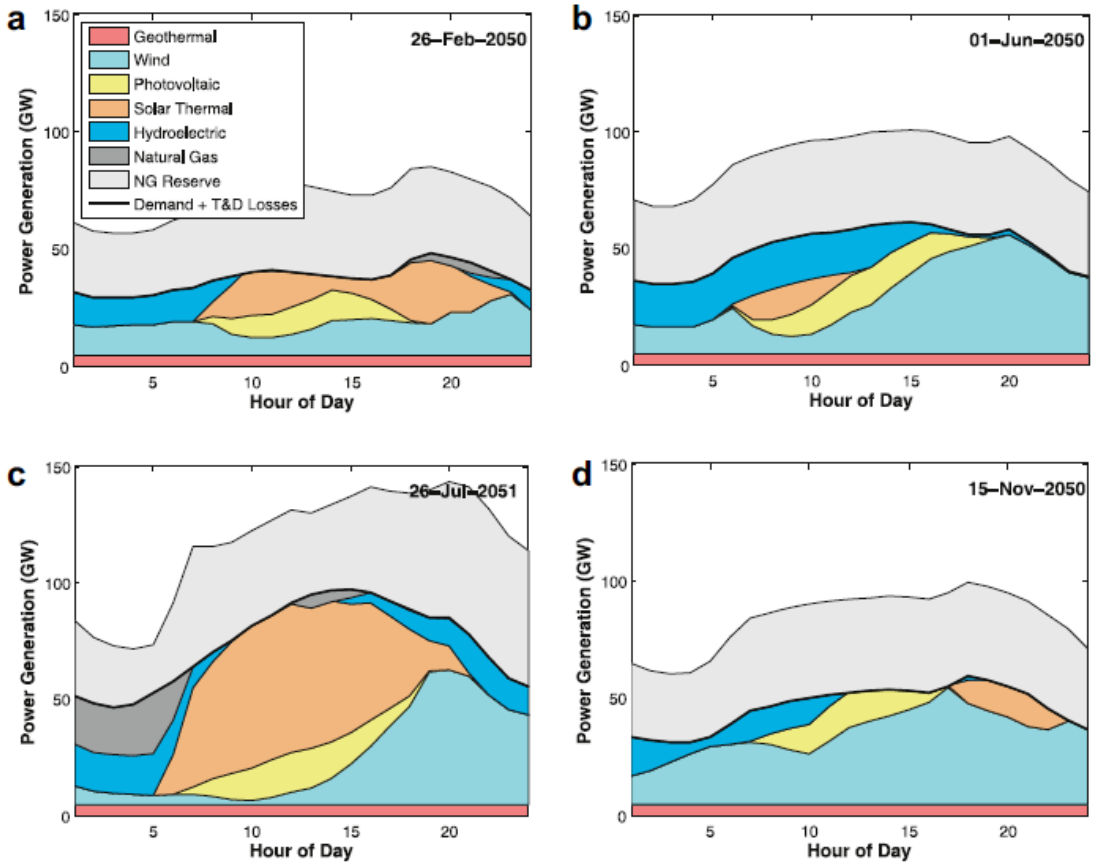

Figure 10: Dispatch by generation technology for a random day each season (Hart & Jacobson, 2011)

Figure 10 above shows the results of a typical dispatch model for a 24 hour period. It should be noted the system was optimised for least cost and least carbon scenarios and as result does not include conventional generators such as coal and nuclear. In this case the large back-up reserve requirements are in the form of natural gas to compensate for the low capacity factor of wind and solar. This is quite an extreme scenario and the authors note that mitigating intermittency with

conventional technology might require a new operating ideology; one that favours reliable capacity over cheap energy generation (Hart & Jacobson, 2011).

3.5. Publications on Power systems utilizing Variable Generators in South Africa

There have been limited modelling studies on the reliability and C_r of RE technologies in SA, with publications of note including two studies on wind integration; a GIZ report exploring the capacity credit of wind in SA (GIZ, 2011) and a paper on planning for large scale wind and solar power in SA by Kevin Ummel (Ummel, 2013).

The GIZ study (2011) sets out to quantify the capacity credit (C_r) of wind in South Africa using the Equivalent Firm Capacity metric (EFC) using the equations shown below:

$$EFC = CR(cp).Pav_{fl} \quad (6)$$

$$C_r = {}^{EFC}/_{Pr} \times 100 \quad (7)$$

Where, EFC is the Equivalent Firm capacity in MW, CR is the Capacity reduction factor, *cp* is the Wind Penetration level (ratio of installed wind capacity to conventional generation capacity), Pav_{fl} is average production during full load period, C_r is Capacity Credit in % and *Pr* is rated power of installed wind capacity in MW (GIZ, 2011).

The study defines capacity credit of wind as the percentage of installed wind capacity that adds to the firm capacity of the system. Through this paradigm they question how much conventional capacity is required for three scenarios, which are based on realistic assumptions with regards to wind farm sites, potential installed capacity and characteristics of the SA power system:

- Scenario 1: year 2015 – 2 000MW of installed wind capacity, a peak load 40 582MW and conventional capacity of 53 537MW
- Scenario 2: year 2020 – low wind scenario, 4 000MW of installed wind capacity, a peak load of 48 316MW and conventional capacity of 59735MW
- Scenario 3: year 2020 – high wind scenario, 10 000MW of installed wind capacity, a peak load of 48 316MW and conventional capacity of 59735MW

Thus, the report aims to explore how the level of wind penetration affects the C_r of wind.

The methodology of the report recognizes that the traditional method of determining reliability through an application of a reserve margin on total generation capacity to calculate total required capacity is not applicable in this case. They note that if this were applied to the total system, including wind, this would tend to underestimate the required capacity due to wind's low availability (GIZ, 2011). Secondly, if the reserve margin metric was applied to conventional capacity only (hence taking winds C_r as zero) it would tend to overestimate required installed capacity because the wind generation will in the end improve the systems reliability of supply. This then would effectively be ignored in this simple approach (GIZ, 2011).

Thus for the three scenarios presented above, the LOLP at daily peak load is calculated and used as the reliability index assessing the capacity credit of wind generation in SA. Load data was based on the 'moderate load growth scenario' from the IRP 2010 (DOE, 2011) for 2015 and 2020, shown in Figure 11 below.

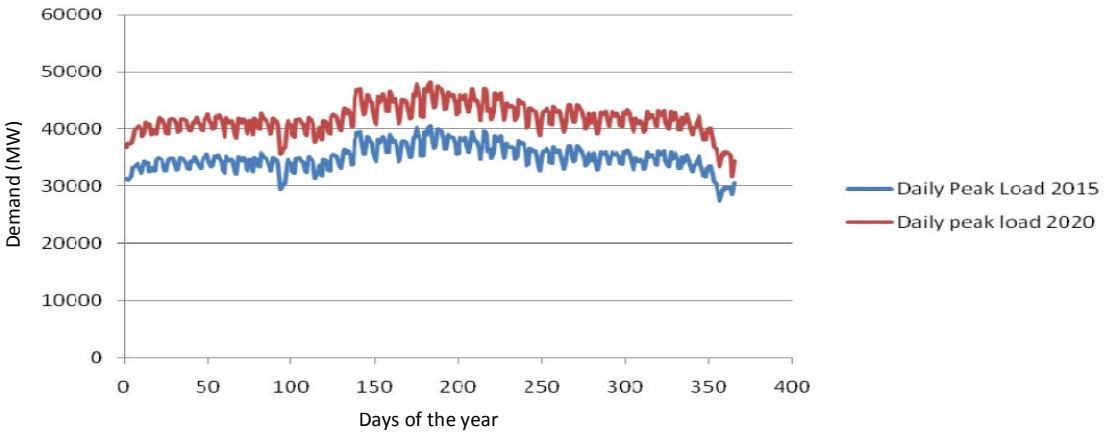

Figure 11: Moderate load growth scenario used in the GIZ report (GIZ, 2011)

C_r has been defined in terms of EFC with the following results:

- Scenario 1: C_r = 26.8%
- Scenario 2: C_r = 25.4%
- Scenario 3: C_r = 22.6%

Thus the authors found that C_r of wind decreased as levels of penetration increased (GIZ, 2011). In other words the increased capacity acts to lower the C_r. However, the report does not test the effect of geographic dispersion in the scenario analysis, which is a major shortfall in the results. Even so, it was found that variable generators such as wind present a viable economic alternative for generation of electricity in SA. Furthermore, they add to the firm capacity of the system and it was shown that by incorporating wind farms into the power system the reliability of the system increases and that it is possible to replace some of the conventional power generation capacity completely (GIZ, 2011).

Perhaps the most applicable work to this dissertation is the recent study by Ummel (2013) which identifies cost-effective deployment strategies for wind and solar power (WSP) in SA. It presents a novel way of including the complexities of electricity generation planning over space and time and it successfully captures the complexities of having large penetrations of variable weather-dependent technologies in a power system.

The objective of the report is to quantify how and where to deploy WSP such that it is reliable, efficient and cost minimising (Ummel, 2013). It achieves this by using a simple power system model that simulates environmental and economic performance for the case of achievable spatial deployment of WSP with maximum reliability in 2040. Additionally it models the expected generating efficiency for key WSP technologies over a 10 year period.

Of particular interest to this dissertation, SAM[1] software is used to simulate hourly generating efficiency time series for 176 cells across SA. Locations of the chosen cells have been optimised through various exclusion screens and in particular, mean yearly resource. The screens are a tool used to exclude areas that are deemed unsuitable for location of sites. The screens consider land cover, terrain slope, proximity to human populations, geomorphology and protected areas and parks. From this Ummel (2013) generated typical diurnal patterns in generating efficiency for each season, as seen in Figure 12 below.

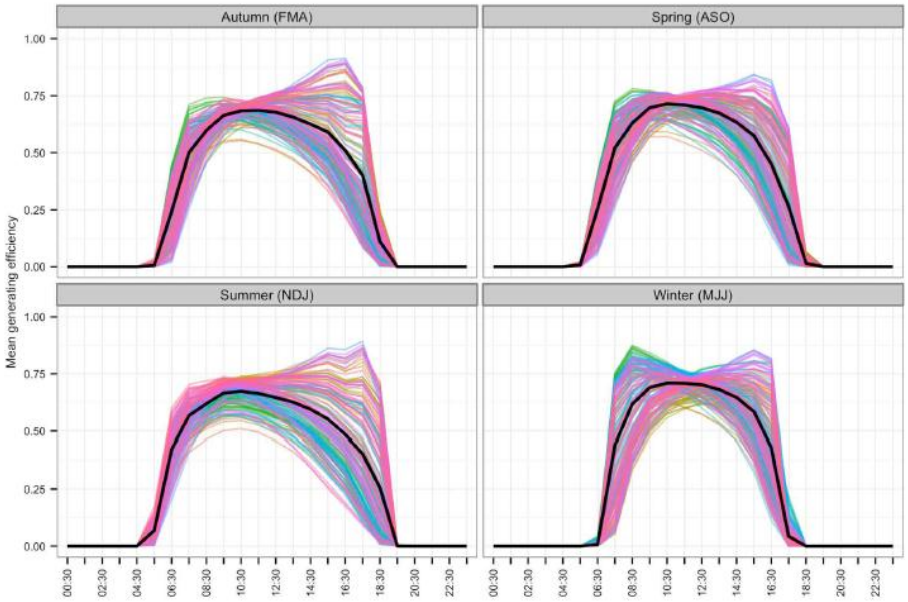

Figure 12: Mean diurnal generating efficiency, by season, for 176 modelled PV sites (1996-2005) (Ummel, 2013)

Predictably PV shows a simple diurnal pattern with the mean shown in black above. However, there are significant differences in the results due to geographic dispersion and seasonal differences, the former being reflect in the variation of curves present. Ummel (2013) found that, in general, summer efficiency remains high into the evenings, with some of the locations show capacity factors of 50% and above for 18h00-19h00. Winter efficiency decreases earlier in the day, but there are no significant seasonal differences in peak efficiency over the course of the day, with peak values occurring around 10h00.

Ummel's (2013) optimisation focuses only on one year (2040) with the default green scenario showing the WSP deployment patterns for a capacity of 46.5GW based on the projections of the IRP (DOE, 2011). The IRP outlines the expected installed capacity and level of penetration for each technology by 2040. Furthermore, development 'zones' identified by Eskom for likely future development of WSP forms the basis for allocation of WSP capacity, with PV particularly being evenly distributed across the zones.

The above scenario is then varied to create two alternative scenarios. Variation A is similar to the green scenario with the exception being that the location of installed capacity is optimised to minimise the cost of CO_2 abatement (Ummel, 2013). Variation B on the other hand allows for quantity of WSP capacity to be additionally optimised (max 46.5GW) (Ummel, 2013).

1. SAM refers to NREL's System Advisor model, which is a performance and financial model used to facilitate the decision making process (NREL, 2013).

LOLP is then calculated on an hourly basis and summed over a predefined period which yields LOLE as a reliability indicator. The model then automatically adjusts OCGT (Open cycle gas turbine) capacity to reach a desired reliability level of LOLE = 0.1 (Ummel, 2013).

The results of this research suggest that optimisation of geographic dispersion of WSP has potential to significantly reduce CO_2 emissions. Below are the results, showing deployment pattern for WSP and mean diurnal generation trends for the green scenario and variations.

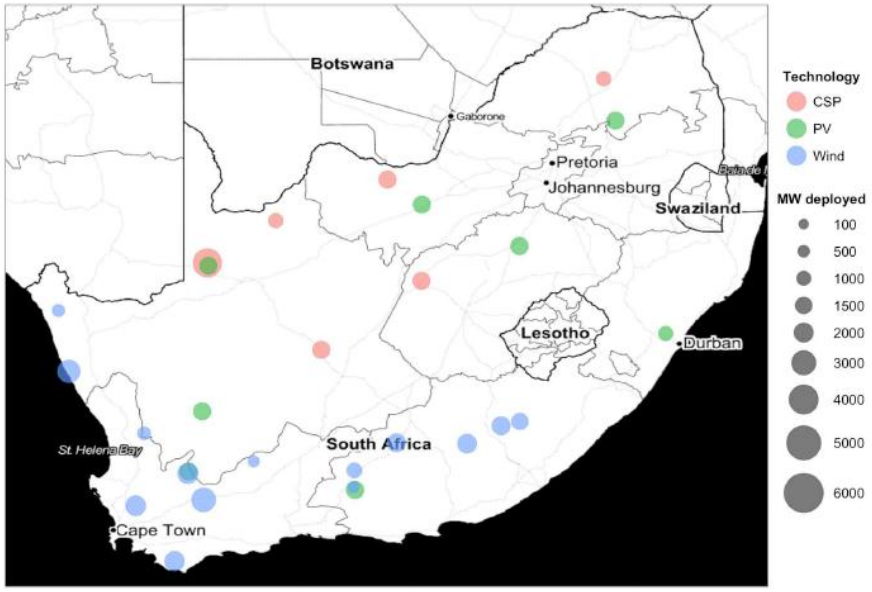

Figure 13: Green Scenario – deployment of WSP for 2040 (Ummel, 2013)

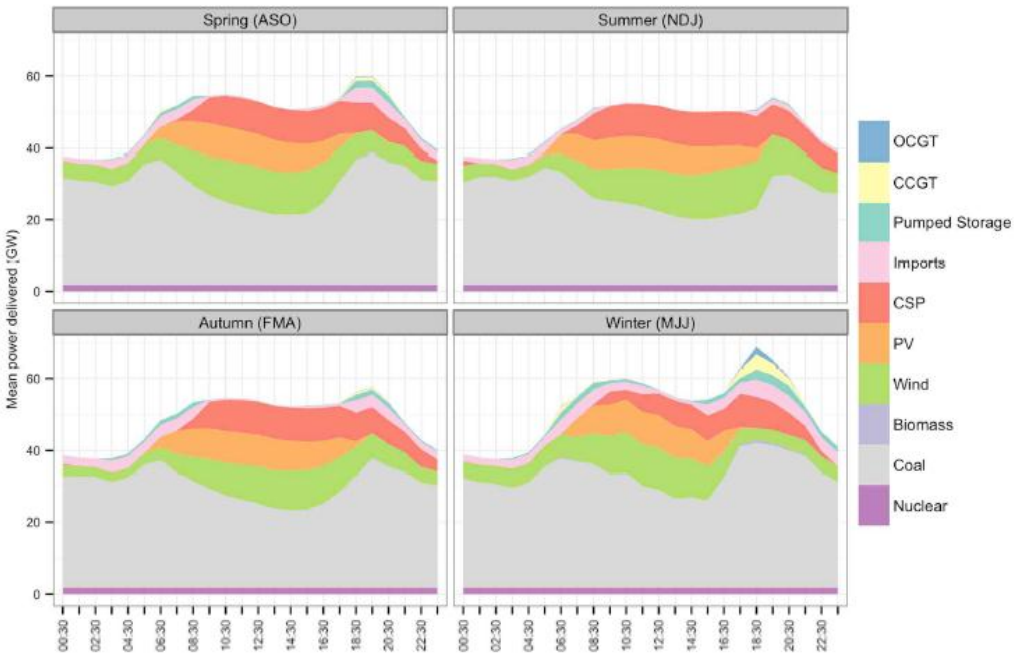

Figure 14: Mean diurnal generation profile for green scenario in 2040 (Ummel, 2013)

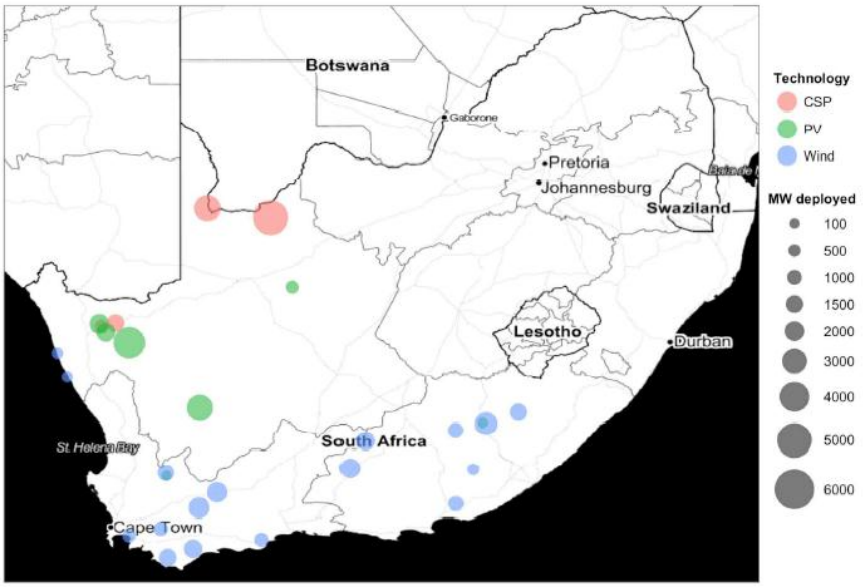

Figure 15: Variation A – deployment of WSP for 2040 (Ummel, 2013)

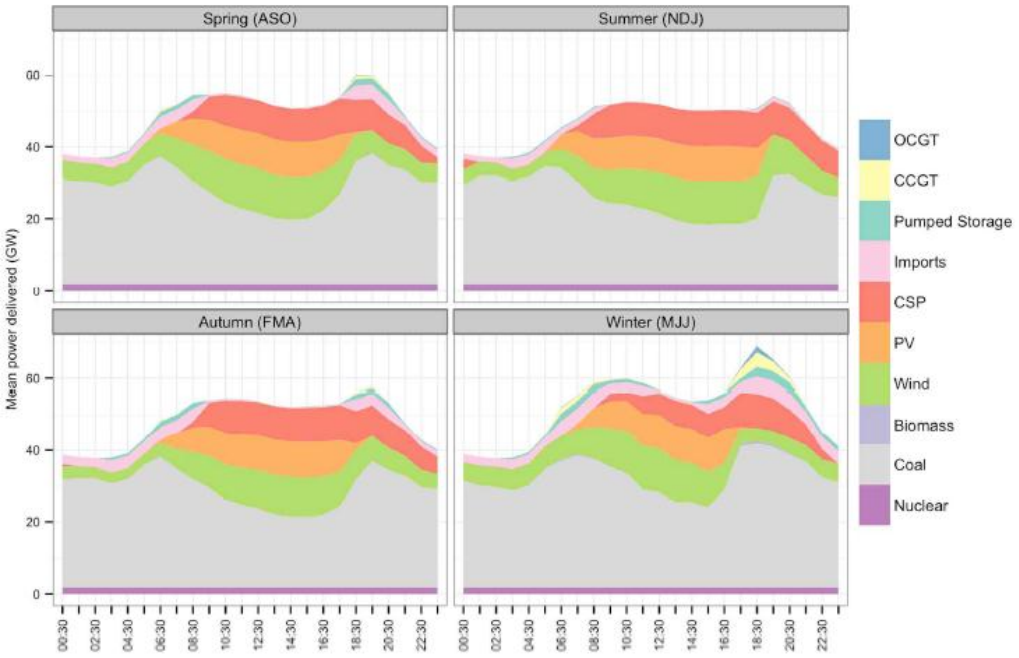

Figure 16: Mean diurnal generation for Variation A in 2040 (Ummel, 2013)

While the deployment for the green scenario and variation A are quite different, the mean diurnal generation is quite similar. Alternatively, looking at Figure 17 and Figure 18 below showing variation B we can see that the optimisation of capacity allows for a much different result. Significant to this dissertation, daytime generation is dominated by PV with large deployment in the Northern Cape. Comparatively the green scenario and variation A allow for an even generation spread with the former being the most geographically disperse.

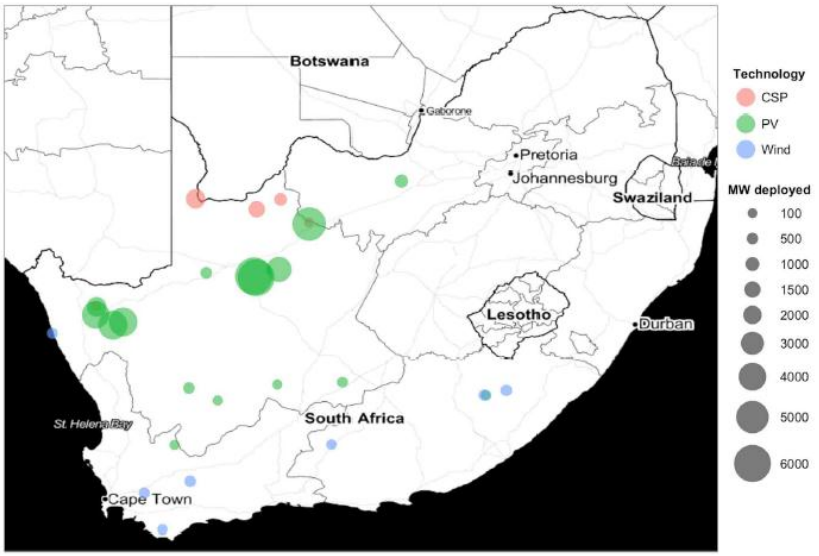

Figure 17: Variation B: Deployment of WSP in 2040 (Ummel, 2013)

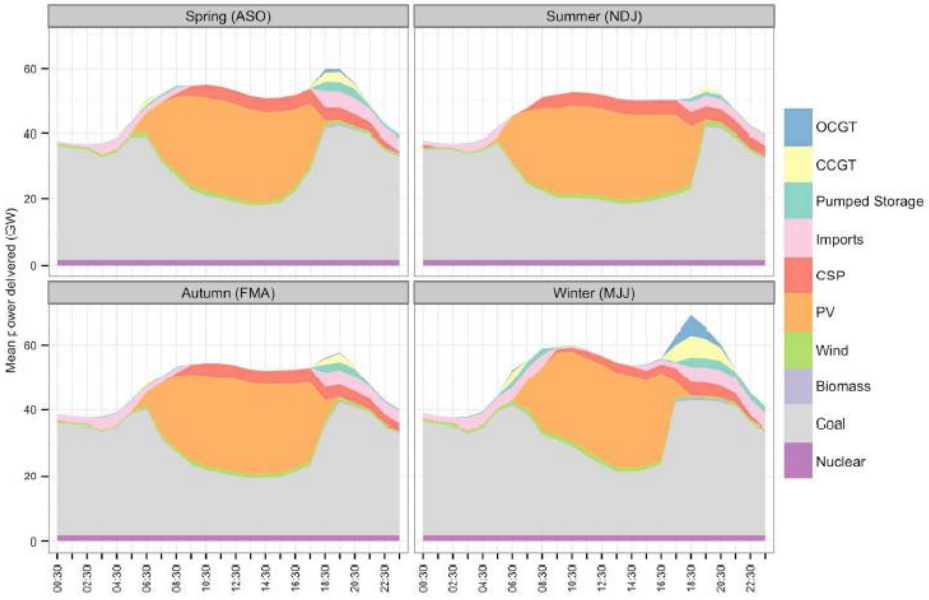

Figure 18: Mean diurnal generation for Variation B in 2040 (Ummel, 2013)

On the other hand, variation B, shown in Figure 18 above, shows deployment of WSP and particularly PV in highly concentrated areas. This suggests that the model is not constrained by the effect of geographic dispersion on reliability of the system. Another minor shortfall is that ramp rates and spinning reserves have not been taken in consideration signified by the steep increase in dispatch of coal seen in Figure 18 above. This could significantly affect CO_2 emission results. However, Ummel (2013) recognises this point, estimating that $100 million could be saved by 2040, through use of more advanced modelling efforts. He recognises that this is because as power systems adapt with higher penetration of variable RE's, so should the analytical tools used to try understand them.

Thus along with the GIZ report mentioned earlier, these are important publications in the context of RE development in SA. They provide a good basis of information and provide deep insights into the characteristics of the SA power system.

3.6. Conclusion

From the review of the literature above it is clear that much has been done in bringing together PV yield simulation, reliability and C_r indicators for variable generating units included in traditional power systems and the dispatch modelling of power systems. This is particularly true for wind in general and for power systems from the U.S. and Europe. However, there are good works on the C_r of PV systems, which along with general studies on the integration of variable generators in power systems provides a solid platform and large amounts of information for constructing a similar study relevant to the SA context.

In the SA context, work has been carried out on the wind C_r through the GIZ study (2011), along with a dispatch model that optimises WSP deployment for least-cost and CO_2 mitigation parameters (Ummel, 2013). There is space for further research in these areas however, as the GIZ study only considers C_r at peak demand for a few typical days a year, and Ummel (2013) does not specifically consider scenarios of geographic dispersion in his work.

In light of the above, it is clear that there is space to optimise long term energy planning in SA. As a result this study will undertake to determine the reliability of solar PV in the SA power system through the creation of a dispatch model using C_r methods similar to that discussed above (this will be discussed in more detail in the methodology chapter). While similar studies have been done elsewhere in the world, this work is original in that it is looking specifically at the South African situation including the effect of the REIPPPP process and the correlation between geographic dispersion and C_r. A study on this basis has not been published in SA and it is hoped the results can therefore contribute to national power system planning and a growing role for PV in SA.

4. METHODOLOGY – SOLAR DATA AND PV YIELD

The goal of this research is made up of two parts. The first part is to effectively simulate the performance of utility-scale PV plants in the South African context, the methodology of which will be discussed in this chapter. The second part is to model a South African power system that includes variable solar PV generators, in order to determine PV's Capacity Credit (C_r) for a variety of scenarios. This will be discussed in the following chapter (Methodology – Modelling).

The accurate simulation of utility-scale PV plants requires large amounts of solar irradiation data. As a result the purpose of this chapter is to (1) discuss and analyse the overall research design, (2) explain the sources of data, (3) discuss PV yield methodology and (4) describe the assumptions and limitations of the research design, particularly focussing on aspects that are unique to this thesis.

4.1. Research Design

Hourly irradiation data was used to simulate the yield of utility-scale PV plants. It is purely a desktop study approach that simulates PV yield through a performance calculation described by Hart and Jacobson (2011) (see equations 3-5). The performance calculation in question relies only on installed capacity, incoming irradiation and efficiency and temperature coefficients derived from parameters usually provided by the module manufacturers. There are both strengths and weaknesses to this approach. The biggest strength is that it is simple, flexible and robust, with no site dependant variables. This makes it suited for the purpose of comparing multiple independent PV plants across SA and the manipulation of data in a scenario analysis.

One weakness of this approach is that in its simplicity it takes factors such as shading as an average over the whole day, where in reality these losses would only be experienced late in the evening and early in the morning. Similarly it uses aggregate values in its calculation of the thermal efficiency parameter. This would be of concern if this method was used to evaluate a single plant in depth, where results were sensitive to small changes in the performance of the plant. In this case this is not significant however, as the SA power system was studied at high level. Thus, when considering the margin of this error against the installed capacity of the whole SA power system, it becomes trivial, and instead lends itself to a more conservative estimate of the potential of PV in SA. There are of course a myriad of alternative simulation methods (discussed further in the literature review), including many computer programmes. These tend to investigate the performance of PV plants more in depth and are reliant on site specific parameters, such as number of modules in parallel and series, making them cumbersome and unsuitable for use in evaluating multiple scenarios. Thus at this high level, the approach chosen is suitable for the performance of PV plants across SA where hourly irradiation data are available.

When evaluating the C_r of solar PV it has been found that the time resolution of data, the number of generators considered and the geographic dispersion of these generators can significantly affect the outcome (Perez, et al., 2008). Irradiation data at an hourly resolution was used to evaluate the performance of PV systems in this research, which is well suited for use in a power system dispatch model as the demand is usually also in this format. Furthermore because of the high level approach

and the evaluation the of multiple dispersed PV plants, data at this resolution is suitable. This point is confirmed in a similar study carried out by Perez, et al. (2008) who recognized that the effect of cloud cover becomes significant at a sub hourly level when considering performance of PV in a concentrated area. There are many sources of irradiation data, with the most common and useable being satellite derived.

A number of research instruments were used in this design to reach the goal of creating reliable PV yield data for sites around SA. Microsoft EXCEL was used as the platform to model the yield for all the sites and Meteornorm v.7 meteorological database (Meteotest, 2013) was used to collect primary and secondary variables for PV performance analysis. These results were then ratified using PV modelling software packages, NREL's System Advisor Model 2013 (SAM) (NREL, 2013) and PVSyst 6.1.0 (Mermoud, 2013). Both of which are recognised as industry standard modelling tools, with the former being used frequently for research purposes.

These tools were used to provide easy analysis of data and reliable results, but in PV systems analysis the factor that can have the biggest effect on producing reliable results is usually the source of meteorological data, given uncertainty in annual GHI of up to 22% (SolarGIS, 2013).

4.2. Sources of Data

There are two main sources of solar irradiation data incident on the earth (JRC, 2012):

- Ground measurements
- Satellite derived data

Neither of these options are perfect, with both having strengths and weaknesses. Ground measurements are usually carried out using a measurement instruments such as a pyranometer. When considering the solar radiation for one place, this is the preferred option, as measurements of high time resolution can readily be obtained. Potential problems with site measurements can occur when there is dirt or other matter obscuring the measurement sensor, or when the sensor is shaded for parts of the day. These can be avoided with regular maintenance and careful siting of the equipment.

If a site considered has no measurements, but there is data for a site nearby, it is possible to estimate the solar irradiation for the site from this data, but the accuracy of this decreases with distances (JRC, 2012).

Irradiation from satellite data can be derived using a number of methods. Most often the satellite measures light coming from the earth, which is usually light reflected off the ground or clouds. Thus the derivation needs to take the light absorbed by the atmosphere and that reflected by the clouds into consideration (JRC, 2012). Additionally data can come from two types of satellites; Geostationary and Polar-orbiting. Geostationary satellites take regular pictures of the earth allowing for high time resolution data, but usually each pixel in the image is equal to a rectangle a few kilometres across (JRC, 2012). This results in the data for that rectangle being the average for the area. Polar-orbiting satellites on the other hand fly closer to the earth, but as a result are moving fast relative to the earth's surface and can only take a few images a day (JRC, 2012).

The main benefit of satellite derived data is that it gives uniform coverage across large areas; whereas ground-measured data is usually used for particular locations situated far apart (JRC, 2012). There are however, a few drawbacks to using satellite derived data. The first of these is that snow can often be mistaken for cloud cover, skewing the results. Secondly, in mountainous areas one pixel may cover areas of various altitudes, something not catered for in satellite derived data (JRC, 2012). Fortunately, in the case of this research, these drawbacks do not apply as the sites chosen for evaluation are not in areas that are mountainous or prone to snowfall.

With the competitive renewable's market in SA brought about by the REIPPP process at the time of writing this thesis, solar data has become a valuable and proprietary commodity. As a result not much sharing of information has occurred. This is particularly true for site measured data, as unlike the wind projects, site measured data was not a requirement for prospective bids, and satellite derived data from reputable resources could be used instead.

Efforts were made to obtain measured data from public resources, such as the national utility, Eskom and the South African Weather Service (SAWS), but the data was found to be partial in terms of annual coverage and most often did not cover representative sites. In SAWS's case the data was limited to weather station sites. Furthermore, only a portion of the weather station sites had hourly measurements of irradiation data and generally these sites are not suited for PV simulation as they are most often found in built up areas or at local airfields. Additionally the stream of data was found to be unreliable in most cases as often the recording equipment was offline, or provided unreasonable data for lengthy periods of time. Therefore, with the uniform coverage across the whole of SA and its preferred use by prospective IPP's in their bid process, it was decided that satellite derived data would be the preferred tool.

There are various satellite resources that are readily accessible via the internet. One of these is *Soda-is,* which provides links to resources located in various countries, particularly radiation databases (CEP, 2013). A certain amount of data can be accessed free of cost, but is quite limited. Global and direct irradiation values are available in the *Helioclim3* (HC3) format, but are restricted to just under two years over 2004 and 2005. HC3 is a service provided by MINES Paris / Armines (France) that provides 15 minute to monthly irradiation using the heliostat satellite images from 2004 at a 3km resolution for the European and African regions (Helioclim, 2009). This is a valuable resource, but when it comes to calculating the yield from the incoming irradiation (discussed further below) it has a few shortfalls. The data provided does not include certain secondary parameters that are dependent on the irradiation values such as ambient temperature that are necessary for the calculation of PV yield. Thus these would have to be further modelled in proprietary software, and this source is thus not suitable for the scope of this thesis.

Fortunately then, access was granted to use the Meteonorm v.7 database. Meteonorm is a reputable meteorological database currently used by many of the parties involved in the REIPPP process and included in the DOE's request for proposal (RFP) as one of 7 reputable and allowable sources for use in PV simulation (DoE, 2012).

Alternatively to Meteonorm, NASA also provides a meteorological database that has been active for the past ten years. This dataset uses long-term satellite-derived monthly averages from 22 years of data over the period 1983 to 2005 (NASA, 2013). However, results are only provided for 1° latitude by 1° longitude grid cells which translates to approximately 110km x 110km rectangles over the

globe. Due to this low resolution, the data is more suited toward approximations of solar potential and feasibility studies rather than performance of PV plants.

The Meteonorm database is compiled by *Meteotest*, a private company started in 1981 (Meteotest, 2013). They make use of data from nearby ground based weather stations along with satellite data and interpolate the data to produce a set of data for the specific project site. Meteonorm stochastically averages ground and satellite data for the period of 1986-2005 from a database of approximately 1800 weather stations to provide a typical mean year (TMY) of data for any site in the world (Meteotest, 2013), see Figure 19 below. A TMY does not represent a real historical year but rather a hypothetical year that statistically represents a typical year for the desired location (Meteotest, 2013).

Irradiation uncertainty is generally found to be in the range of 8% (Meteotest, 2013) and this figure is reportedly based on over 25 years of experience in the development of meteorological databases for energy applications (Meteotest, 2013).

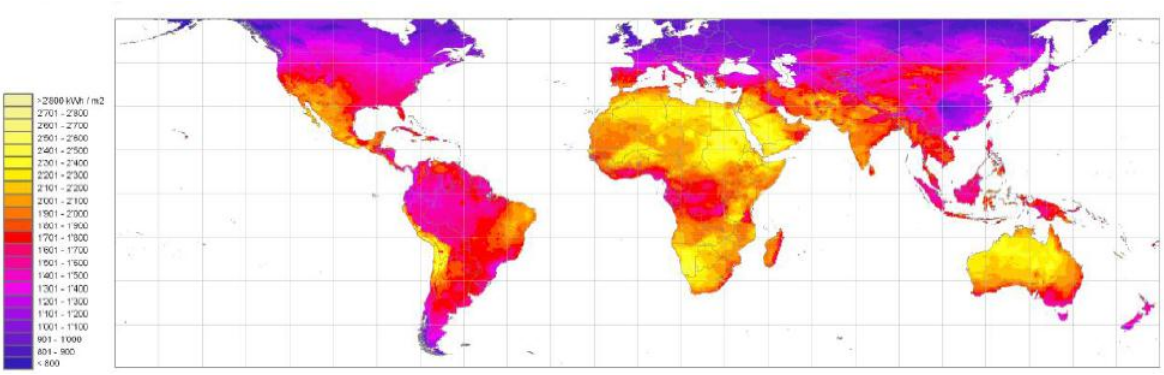

Figure 19: Map of mean yearly sum of global irradiation in kWh/m² based on satellite and ground information for the period 1986–2005 (Meteotest, 2013).

Meteorological data relevant to this research from Meteonorm can be split into primary and secondary variables.

Primary Variables:

- Month
- Day
- Hour
- Global Horizontal Irradiation
- Diffuse Irradiation
- Direct Irradiation
- Ambient Temperature

Secondary Variables

- Wind speed
- Relative Humidity
- Relative Pressure

From the above it can be seen that short of actual site measurements, Meteonorm was the best available tool for this analysis, as it provides statistically generated information for individual sites in a robust manner. This allows for flexibility in site selection and scenario analysis, points which are very important to this research.

4.3. Site Selection

When choosing potential PV sites, one of the most important factors is the solar resource. Looking at Figure 19 above it is clear that SA has an extremely good solar resource across the majority of the country. Thus it would be understandable to draw the conclusion that sites could be selected anywhere across the country. There are however many other factors contributing to the best available PV site. Many of these are related to economic and practical matters to do with connectivity and evacuation of power to the grid with minimal losses. Additionally, there are socio-economic ramifications such as job creation and possible diversion of arable land which have to be taken into consideration. Furthermore, a goal of this thesis is to develop realistic scenarios for deployment of PV as closely as is reasonably possible. Finding potential sites while sticking to the constraints mentioned above, among others, is an arduous process. Fortunately running concurrently with this research is the DoE's renewable energy IPP procurement (REIPPPP) process, where many of the bidders have already been through this process in their site selection (see chapter 2.4). Thus it was decided to build on this work and follow the trends of IPP's with preferred bidder status from the first two rounds of bidding.

Thus REIPPPP based PV sites were subsequently used as sites for modelling purposes in this thesis. Furthermore, capacities outlined in the programme were carried through for the base case scenario and treated as variable in the rest of the scenarios. Data for these sites was then generated using Meteonorm and manipulated to estimate the yield of PV systems.

4.4. Analysis of Data

For the analysis of PV yield Hart & Jacobson's (2011) method for PV estimation has been used. It combines the flexibility and simplicity of comparing PV plant's Performance Ratios (discussed in more detail in the literature review) with a greater accuracy in loss calculation by using equations found in (Masters, 2004) to simulate PV output (see equations 3 - 5 in the Literature review).

This method effectively removes site dependant variables, and replaces them with efficiency parameters. As a result it relies only on installed capacity, incident irradiation and ambient temperature. These can be further split into dependant and independent variables.

The independent variables include:

- Site selection
- Capacity
- System Design

The dependent variables include:

- Irradiation data
- Ambient temperature
- Loss assumptions

This gives this approach numerous strengths:

- Due to its flexibility this method lends itself to comparison of PV systems in multiple locations and of different capacities
- Using efficiency parameters reduces computational and data collection time drastically
- It allows for design of one standard system that can then be placed at any site
- It provides robust and reliable data

This approach is not without its weaknesses however:

- In its simplicity it takes loss factors such as shading as an average over the whole day, where in reality these losses would only be experienced late in the evening and early in the morning
- It uses aggregate values spaced over an hour in its calculation of the thermal efficiency parameter

These would be of consequence if this method was used to evaluate a single plant in depth, but since a high level viewpoint is desired it is less of a concern.

In order to validate the chosen method used to evaluate PV performance discussed above, the results for 6 random sites were compared for the base case using two separate PV modelling software packages. These were NREL's System Advisor Model 2013 (SAM) and PVSyst 6.1.0. Both of which are recognised as industry standard modelling tools, with the former being used frequently for research purposes.

4.5. System Design

A generic fixed tilt PV system design was used in the yield calculation. The system was based on the following design and the thermal and loss parameters were taken from the datasheets for the module and inverter stipulated below:

- Tilt angle of 30°
- Orientation of 0°
- Suntech STP280-24vd Polycrystalline modules (See Appendix C for more detail)
- SMA SC800CP XT Central inverter (See Appendix C for more detail)

A fixed tilt system was chosen as a representative design, as it was the most popular design in the first round of the REIPPPP. As suggested by Bekker (2007) the latitude of the location is a reasonable tilt angle. Looking at Table 2 below, we can see that generally speaking South Africa spans from

approximately 25°S to 35°S, with the 30°S latitude passing through the middle of the country and close to De Aar.

Table 2: Latitude of various locations across SA (Matshoge & Sebitosi, 2010)

Data set	*Latitude (S)*
Calvinia	31.5°
Cape Town	34.0°
De Aar	30.7°
Durban	30.0°
P Elizabeth	34.0°
Polokwane	23.9°
Pretoria	25.7°

Thus, a tilt angle of 30° was chosen as representative of PV plants for various sites across SA. Furthermore, the optimal orientation of plants changes with longitude and latitude i.e. the angle from the azimuth. For the sake of a generic plant, a standard 0° orientation has been adopted. Of course the method suggested by Bekker (2007) above is a simplification with the optimum tilt angles varying slightly from the latitude. This value is further altered if maximum yields are required for different seasons.

The model of 280 Watt panel chosen for the yield simulation is produced by Suntech power, the world's largest producer of silicon solar modules and recommended for utility scale plants (Suntech-Power, 2013). Similarly a SMA central invertor was chosen in the design. SMA is one of the best known names in the invertor industry, and a global leader in the development and sales of PV invertors (SMA, 2013). Again a typical central inverter was chosen designed for multi-megawatt situations.

4.6. Assumptions

In creating a purely theoretical performance model of a PV system many assumptions need to made in order to run the simulation. Perhaps the most significant of these are the loss assumptions that were used in the calculation of the PV performance, shown in Table 3 below (see Appendix B for more information).

Table 3: Loss assumptions

Category	Loss Description	Assumption	Source / Desciption
Shading and Spectral	Near side shading losses	2.50%	Based on design limiting shading losses to 2-4% (Luque & Hegedus, 2011)
	Reflection losses (IAM factor)	2.50%	PVSyst Standard (Mermoud, 2013) based on a b_0 value of 0.05*
PV Modules	PV loss due to irradiance level	1.20%	Dependent on module selection. Average value taken from PVSyst results of 0.6% loss, thus doubled to take a more conservative approach.
	Quality loss	0.80%	PVSyst Standard (Mermoud, 2013)
	Array soiling loss	2.50%	Sharma (2011) suggests a value of 1%, but a more conservative value has been chosen based on a low cleaning regime and low rainfall.
	Module array mismatch loss	1.00%	Assumption of positively sorted modules, value taken from manufacture data sheet (Suntech-Power, 2013)
	DC Ohmic wiring loss	1.25%	PVSyst Standard (Mermoud, 2013)
AC electrical components	Inverter efficiency loss	1.90%	Taken from Inverter manufacturer (SMA, 2013)
	AC Ohmic wiring loss	0.50%	PVSyst Standard (Mermoud, 2013)
	Transformer loss	1.20%	PVSyst Standard (Mermoud, 2013)
	Total	15.35%	

*the b_0 value refers to a parameter developed by ASHRAE (American Society of Heating Refrigeration and Air Conditioning) using to quantify the light effectively reaching the PV cells surface after going through various refractions while passing through the layers of glass and protective coating (PVSyst SA, 2012).

The losses shown above are, where possible, taken from the data sheets for inverter and module shown above. Otherwise they are taken from PVSyst standard values for typical systems (PVSyst SA, 2012) and in the case of site specific losses, such as soiling, the values correspond as close as possible to industry standards used currently for SA and assumed to be the same for all plants.

Nameplate capacity of the individual plants is taken as 15% above the contracted capacity, as outlined in Table 1, and suggested in the RFP (DoE, 2012). Nameplate capacity refers to the summation of the individual modules wattages and is the DC capacity of the plant. This is not the same as the AC capacity as this refers to the power output capabilities after all losses have been taken into consideration. Oversizing by 15% allows the AC capacity to be around contracted capacity.

4.7. Limitations

One of the major limitations to this part of the research was the use of a typical mean year of irradiation data. Although in itself a good and reliable source of data, a distribution collated from

multiple years would give a greater field to sample from, thus increasing the robustness of the data. This relates to the secondary goal of this thesis, discussed in the next chapter, which involves stochastically analysing the performance of PV plants. Another limitation of this research is related to the system design. Only one type of system is analysed, whereas in reality there are various design options available to IPP's. This choice could conceivably affect the yield experienced by the plants at different times of the day. If, for example, an east-to-west tracking system was being simulated compared to a fixed axis system; the tracking system would have an increased yield over the fixed tilt system in the afternoon and the mornings as a result of it tracking the direction portion of the irradiation. A third limitation is the lack of access to ground measured meteorological data for potential PV sites across SA. This lack of data is quite understandable in that the RE market is in its infancy in SA, with the first utility-scale PV plants in the planning stage at the time of this research. Access to this type of data, along with actual recorded performance data for the sites would however greatly increase the validity of the results of this research.

4.8. Conclusion

The goal for the first part of the thesis is to accurately simulate the yield of utility scale PV plants across SA. The overall research design is based on a simulation of PV plants using hourly irradiation data for various sites across SA. This simulation was carried out using a performance calculation based on equations 3 - 5, which depends only on installed capacity of the plant, incoming irradiation and ambient temperature at the site. Its main strength is in its simplicity and flexibility, which allows for robust manipulation of the data and scenario analysis for a variety of different sites and installed capacities.

Satellite derived hourly resolution irradiation data, ambient temperature and other secondary parameters were obtained using Meteonorm v.7, a reputable source recognised by the DoE (DoE, 2012). Meteornorm is a meteorological database that stochastically blends ground data from nearby weather stations (if available) and satellite data for the period of 1986-2005 to provide a typical mean year of data for any site in the world (Meteotest, 2013).

Site selection was based on preferred bidders from round 1 and 2 of REIPPPP as it accurately reflects trends in IPP's and PV deployment across SA. These sites have the added benefit of other considerations taken by the developers in site selection, such as proximity to the national grid for evacuation of power and job creation etc. Yield was then calculated for these sites using a north facing fixed 30° tilt system, and for the base case, the capacities as laid out in the REIPPPP bids.

The results of these simulations were then ratified using two PV modelling software packages, NREL's System Advisor Model 2013 (SAM) and PVSyst 6.1.0. Both of which are recognised as industry standard modelling tools, with the former being used frequently for research purposes.

From this whole process, reliable data with a few limitations was obtained. The main limitation is that there is only one year of data to sample from, whereas data that spanned a number of years would provide more robust results. Thus we won't be able to account for some extreme events in our dispatch model. The year of data is however, a typical mean year which has been stochastically

assimilated from just under 20 years of data. Other minor limitations include the system design of only one typical PV system, and a lack of access to ground measured data.

Even with these limitations it is safe to say that the goal of the first part of this research was reached, in that reliable data was produced from the accurate simulation of utility-scale PV plants across SA. This data then feeds into part 2 of the research methodology, which is modelling of the SA power system including solar PV for various scenarios of geographic dispersion.

5. METHODOLOGY – MODELLING

The goal of this research is made up of two parts. The first part is to accurately simulate the performance of utility-scale PV plants in the South African context (discussed in the previous chapter). The second part is to model a South African power system that includes variable solar PV generators, in order to determine its Capacity Credit (C_r) for a variety of scenarios. Secondary goals include calculation of reliability indices; Expected energy not served (ENS) and Loss of Load Expectancy (LOLE); and CO_2 emissions for these scenarios. This will be discussed below.

The purpose of this chapter is to discuss and analyse (1) the overall research design, (2) the meaning of C_r and the reliability indices used to evaluate it, (3) C_r modelling Methodology, (4) scenario analysis, (5) modelling of the dispatch model including PV, (6) Analysis of SA's load profile and (8) assumptions and limitations of the design. This chapter focusses particularly on aspects that are unique to this thesis.

5.1. Research Design

The overall approach of this research design is a stochastic simulation and system analysis of the power system of SA with and without variable PV generators. This was done in order to evaluate the amount of conventional power that is possible to be avoided or replaced through the use of PV. This is referred to as the C_r of PV and is a way of measuring the 'value' (in terms of reliable generation capacity) that can be added to the power system from PV generation.

In the case of this modelling exercise, conventional generators can be considered to be a 2 state system (Voorspools & D'haeseleer, 2005). They are either on or offline depending on technical availability (due to maintenance or forced outages). Thus from this the available online capacity can be extrapolated and made available for the system operator to dispatch. The available capacity of variable generators like PV or wind on the other hand, is reliant on weather patterns, which have an inherent randomness. As a result the available capacity for dispatch can fluctuate between 0 and 100% of installed capacity over a relatively short time period. This is the main difference between conventional and variable generators, and is the reason for stochastic simulation.

Stochastic simulation is a process that is commonly used in modelling of systems that incorporate random behaviour. It is a process that considers uncertainty in a system through the application of probability theory. The behaviour of a generating system is often described stochastically using probability and cumulative distributions from chronological load data. Power based reliability indices are then used to describe the level of reliability, or risk in the system, and can be used to evaluate the C_r of PV. The most popular of these indices include:

- Loss of load probability (LOLP)
- Loss of load expectancy (LOLE)
- Expected energy not supplied (EENS)

Of course to avoid the modelling effort and time series data required by stochastic modelling, a conservative approach could be adopted, and the value that PV can add to the system could be ignored altogether (Voorspools & D'haeseleer, 2005). This would allow for a simplified deterministic analysis of the system, a process that requires less complexity. It has been found, however, that particularly in the USA and other parts of the world that there is an increasingly positive correlation between PV output and summer midday peak demand (usually from cooling demands) and thus there is a high probability that PV must add some value to the system (Perez, et al., 2008). As a result, a conservative approach would result in large inefficiencies in the system, resulting in overspending, curtailment and a suboptimal dispatch of energy.

Alternatively, one could fully account for the total installed capacity of PV (Voorspools & D'haeseleer, 2005), but as explained above power output from PV is fluctuating and as such the system would be undersized and unreliable. Thus, it can be argued that in order to take the uncertainty of power systems including variable generators into consideration, stochastic modelling using time-series load data and generator capacity outage probability tables is a superior method for optimal evaluation of these systems.

Stochastic modelling was used to obtain these main outcomes:

- The firm capacity of the conventional system at a predefined reliability level
- The available PV capacity online at the same predefined reliability level at certain times of the day and periods of the year
- The C_r of PV using the effective load carrying capability (ELCC) metric to test the effect of geographic diversity and level of penetration on the C_r of PV through scenario analysis
- A Dispatch model of the SA power system with and without PV, to calculate reliability indices (EENS and LOLE), average capacity factor, CO_2 avoided and cost implications.

These main outcomes were calculated with a final goal in mind – to graphically show the correlation between C_r and geographic dispersion, and C_r and level of penetration.

To do this, essentially two systems were compared, one employing only conventional generation, the other including the additional PV capacity using LOLP calculations (see Appendix F for in depth description). LOLP was used in Monte Carlo Simulation (MCS) to probabilistically calculate the firm capacity (or LCC) of each system. The LOLP calculator treats existing thermal units as discrete binary systems (i.e. individual units that are either on or off) and through MCS samples forced outage rates (FOR) for each technology and an array of random numbers between 0 and 1 to simulate number of units online. The units online are then summed and make up the LCC of the system. Thus at a given reliability the effective load that the system can be assured to supply is calculated. This is known as the firm capacity.

The addition of PV generation to the system was then analysed. This was done by formulating distributions of likely PV yield from chronological yield data for interesting temporal subsets such as midday in summer. These distributions were then added into the LOLP calculation and from this the effective load that the new system could carry at these times was found. From this the two systems were then compared to find the change in firm capacity using the ELCC metric (discussed in more detail below) and then used to create a third system and find a typical thermal unit that will give you

the same change in firm capacity. The capacity ratio of the resultant equivalent thermal unit and installed PV is then the C_r.

Scenarios testing the effect of geographic dispersion for the base case year were created using existing demand and power system dynamics, while geographic dispersion is manipulated. This was tested both through the C_r and the dispatch model. The effect of penetration levels on the other hand was explored through C_r calculations alone by consecutively adding PV capacity to the existing system and recording the results.

The dispatch model then allowed for the calculation of average capacity factors, LOL indices, CO_2 avoided and cost ramifications of the different geographic scenarios.

5.2. C_r and reliability modelling context

The purpose of a C_r is to evaluate the value of a variable generator to a power system. In other words, how much conventional generation can be replaced or avoided by the deployment of PV? Another way of looking at it is how much of the installed capacity of PV doesn't need to be backed up by conventional means.

The effective load carry capability (ELCC) metric was used to evaluate the C_r in this research. The ELCC method was first introduced by Garver in 1966. LOLP is used to quantify and graphically estimate the load carrying capability (LCC) of a new generating unit (Garver, 1966). The LCC of the system is essentially the ratio of firm capacity and available capacity of the system expressed as a percentage. The firm capacity refers to the portion of available capacity that can be guaranteed to be served at a set confidence level.

Initially, in Garver's (1966) method a desired level of reliability for the system is chosen as the benchmark for the new system (this is often the level of reliability calculated for the existing system prior to the added generating unit). The existing system is then tested to evaluate the reliability of the system at different loads, creating a risk or reliability curve (see Figure 20 below).

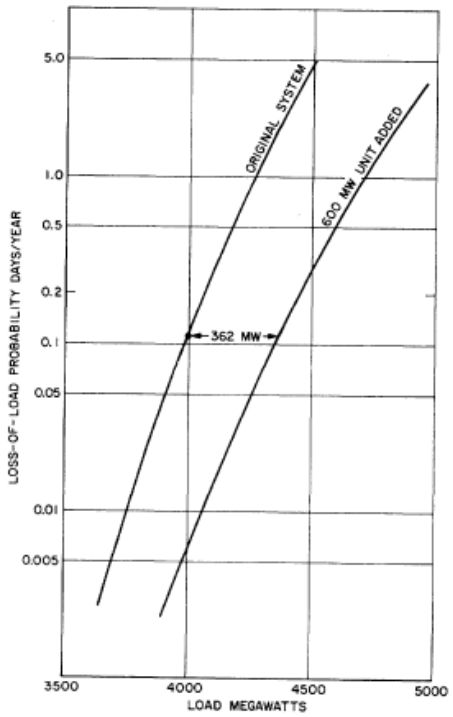

Figure 20: Annual Risk after Adding a New Generating Unit (Garver, 1966)

The new generating unit is then added to the system, and the reliability curve process is repeated. The LCC of the new unit is then the load increase the system can meet within the desired level of reliability (Garver, 1966).

In the example above, a new 600MW generating unit is added to the system. The level of load increase at the defined reliability level is the difference between the 2 curves (Garver, 1966). As a result at a LOLP of 0.11 days per year, the ELCC of the 600MW generating unit is 363MW.

5.3. C_r Modelling Methodology

Similarly to Garver's (1966) method, the LCC for this research was estimated using LOLP reliability indices. Initially it was thought that generating capacity outage tables based on the forced outage rate (FOR) (Bagen, 2005), developed and employed in the dispatch model could be used to simulate the systems firm capacity. However, it was found that individual LOL probabilities for each generation technology could not be summed at the same reliability level due to the difference in unit size. In effect, adding distributions in this manner overestimates the probability of outages happening simultaneously. Thus, as suggested by Garver (1966), the LOLP of the whole system needs to be considered.

Therefore a method similar to Garver's is employed to compare the changes in ELCC, or firm capacity of three systems as follows:

- Existing system made up of existing conventional units
- Existing system with additional PV generation

- Existing system with an equivalent thermal unit that gives you the same change in firm capacity as that of the PV system

5.3.1. ELCC for conventional system

The FOR can be defined through the following equation and is the probability that a generating unit will be offline at some time in the future after planned outages have been considered (Bagen, 2005):

$$FOR = \frac{\sum[down\ time]}{\sum[down\ time]+\sum[up\ time]-\sum[Planned\ outages]} \qquad (8)$$

In other words it is the chance of unplanned outages for a unit expressed as percentage. In the case of this research, the FOR of each technology was an exogenous input taken from Eskom's recent integrated strategic energy plan (ISEP10) (Eskom, 2006)and are displayed in Table 4 below.

Table 4: FOR of conventional technologies

Generating unit type	FOR
Cahora Bassa Hydro - Regional	10.0%
Mini-Hydro - Local	8.5%
Hydro – Local	6.4%
PWR nuclear	6.5%
Large Coal	8.7%
Large Coal Dry-cooling	6.4%
Small coal	4.6%
Open-Cycle Gas Turbine – Diesel	12.2%

From the FOR, probability distributions are calculated for each conventional generation technology, describing the probability that units will go offline. These distributions are created using a uniform distribution.

Existing thermal units are treated as discrete binary systems i.e. individual units that are either on or off. The number of units online is simulated through MCS by sampling of the FOR's for each technology and an array of random numbers between 0 and 1. If the random number is smaller than the FOR then the unit is offline. The reverse is also true. This simulates the inherent randomness of forced outages experienced in reality. The subsequent units online are then summed and make up the LCC of the system. This can perhaps be better portrayed mathematically as follows:

If, for a discrete unit:

$$x = Rand() \qquad (9)$$

For an FOR of 10%,

$$if\ x < 0.1 \quad c = 0 \quad unit\ is\ offline \qquad (10)$$

And,

$$if\ x > 0.1 \quad c = 1 \quad unit\ is\ online \qquad (11)$$

Where c = 0, or c = 1 is the binary system denoting whether a unit is on or offline. Thus at a given reliability the effective load that system can be assured to supply is calculated. This translates into the following equation:

$$LCC_{th} = \frac{Available\ firm\ capacity\ online\ at\ 98\%\ Reliability}{Total\ Installed\ Capacity} \qquad (12)$$

"98% reliability refers to a state where the system will supply the LCC 98% of time"

This gives us:

$$LCC_{th} = \frac{C_f}{C_{th}} \qquad (13)$$

Where LCC_{th} is the LCC of the thermal or conventional units, C_f is the firm capacity, or available capacity online and C_{th} is the total installed capacity. Thus at a chosen reliability level the ELCC of the conventional system can be calculated as shown in the example below:

Table 5: LCC of Existing System

LCC - Thermal	
Total Installed Capacity	43468 MW
Reliability Target	98%
LCC	37918MW
LCC %	87.2%
Inflation on demand	13%

Thus at a reliability level of 98% the existing system with an installed capacity of 43468 MW was found to have a LCC of 37918 MW, which translates to 87.2%. A reliability of 98% is relatively conservative, but is in range of Eskom 2013 reliability levels. These were inferred from Eskom weekly adequacy reports and shown to be 90% for the worst case scenario (mid-winter) and 98.5% under lower loads (summer) (Eskom, 2014).

5.3.2. ELCC for system including PV

While LOLP for the conventional system can be derived from the FOR for each conventional generator, this method is not applicable to variable generators such as PV. There is no defined FOR for PV as the available capacity is dependent on variable meteorological patterns. Thus distributions were created from chronological yield data over a given time period instead. Furthermore, unlike a conventional generator, there is little point in calculating the LCC for PV over the whole time period.

The reason for this is a simple one, considering that the power output from a solar plant is dependent on sunlight and over a whole year, approximately half of that will be night time. Furthermore, the trends in output differ from season to season. Thus this would greatly skew the distribution values, in turn skewing the ELCC results. To counteract this, distributions for a variety of interesting subsets were generated.

Similarly to the thermal system random numbers between 0 and 1 are used to look up values from the inverse cumulative distribution (1-CDF) and scaled up by the capacity of installed PV. Below is a condensed sample from 12h00 annually:

Table 6: PDF and CDF for PV – Annual 12h00

Annual: 12h00			
Capacity	Frequency	PDF	CDF
0.0	0	0.000	0.000
105.5	0	0.000	0.000
210.9	0	0.000	0.000
316.4	4	0.011	0.011
421.8	8	0.022	0.033
527.3	47	0.129	0.162
632.8	110	0.301	0.463
738.2	146	0.400	0.863
843.7	50	0.137	1.000
949.1	0	0.000	1.000
1054.6	0	0.000	1.000

Table 7: Inverse CDF of PV – Annual 12h00

Inverse CDF		
	Probability	Capacity
10	0.000	1055
9	0.000	949
8	0.000	844
7	0.137	738
6	0.537	633
5	0.838	527
4	0.967	422
3	0.989	316
2	1.000	211
1	1.000	105
0	1.000	0

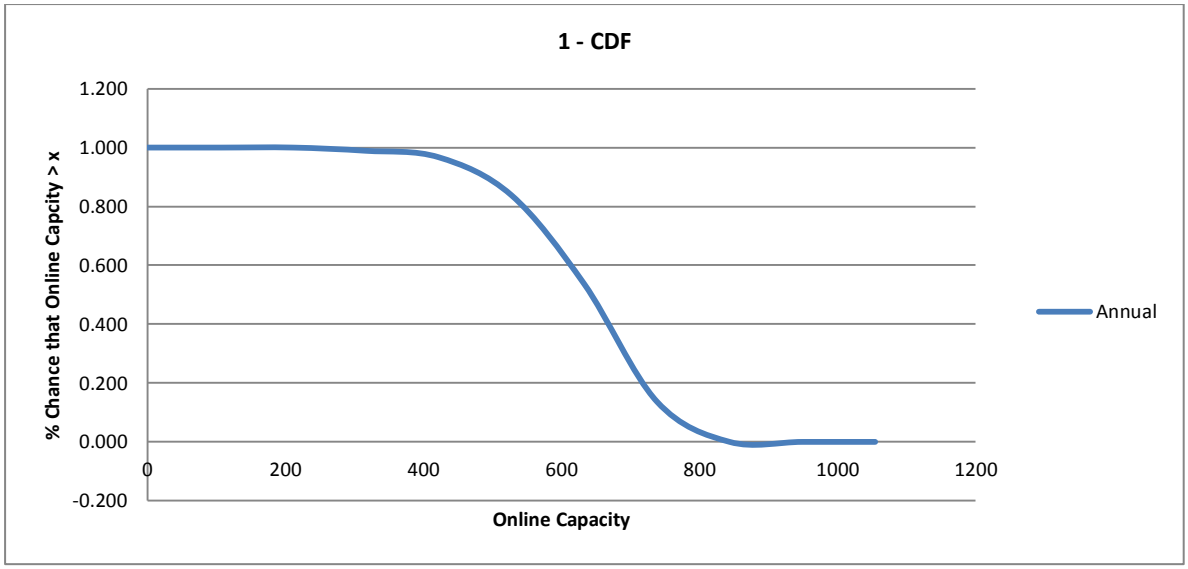

Figure 21: Inverse CDF for PV – Annual 12h00

More specifically the PDF describes the probability of likely capacity being online, while the CDF describes the % chance of having less than that capacity online. While the information provided by the CDF is useful, we really want to know the % chance of having *more* than a particular capacity online. Therefore the inverse distribution is used.

The sum of available thermal and PV is then tested against a singular demand and from this the ELCC is calculated for the new system:

$$LCC_{PV} = \frac{Available\ capacity\ online}{Installed\ conventional\ Capacity + Installed\ PV\ Capacity} \qquad (14)$$

This gives us:

$$LCC_{PV} = \frac{C_f}{C_{TH} + C_{PV}} \qquad (15)$$

Where LCC_{pv} is the LCC of system including PV, C_f is the firm capacity and C_{pv} is the installed PV capacity.

Unlike for conventional units, adding the PV LOLP distribution directly to the calculation is acceptable, as it is the probability for a point in time and as a result considered an event occurring in the system.

Subsets were chosen on the basis of where they might add value to the system. An obvious example is the hours over midday during summer, where there has been shown to be a correlation between summer peak cooling demands and maximum PV yield (Perez, et al., 2008). Furthermore it is useful to observe the variation in diurnal and seasonal trend for C_r using these subsets. Each subset is a separate calculation which is described in the scenario analysis below.

5.3.3. Calculating the C_r

Since the LCC, and hence the firm capacity has been calculated for both the conventional system and subsets of the PV adjusted system, the C_r can now be quantified. Equation 16 below is perhaps best understood with the aid of the following graph.

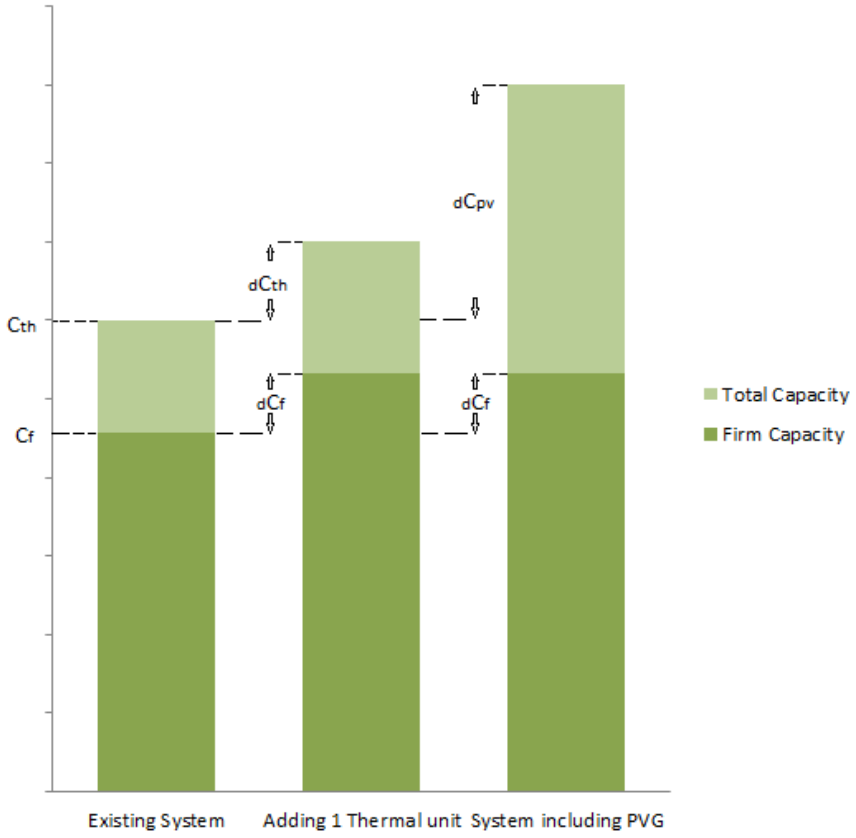

Figure 22: Graph displaying the effect of adding a thermal unit and PVG to the firm capacity of the system

Essentially, to calculate the C_r we want to find out the capacity of PV that would be required to increase the systems firm capacity by the same amount as if a conventional thermal unit was added. For example, 300MW of PV might increase the firm capacity of the system by the same amount as 100MW of coal. This is displayed graphically in Figure 22 above, which shows an existing system in the first column with its corresponding firm capacity C_f, and the next column displaying the same system with an additional thermal unit dC_{th} and the corresponding increase in firm capacity dC_f. The third column displays the alternative option of additional PV capacity, dC_{pv}, required to reach the same dC_f. This ratio of PV to theoretical thermal unit is the C_r and is described mathematically below.

$$C_r = \frac{dC_{th}}{dC_{pv}} \qquad (16)$$

This is simple in theory, but in practice requires a large amount of arduous iteration. This is due to the fact that when adding thermal capacity to the system the firm capacity increases in a granular manner because of individual unit size. In other words the firm capacity only increases when there is enough capacity online for another unit. In the case of this simulation, small coal was used as the typical thermal unit at a unit size of 154.9MW and is represented in Figure 23 below where the blue curve shows the jump in firm capacity.

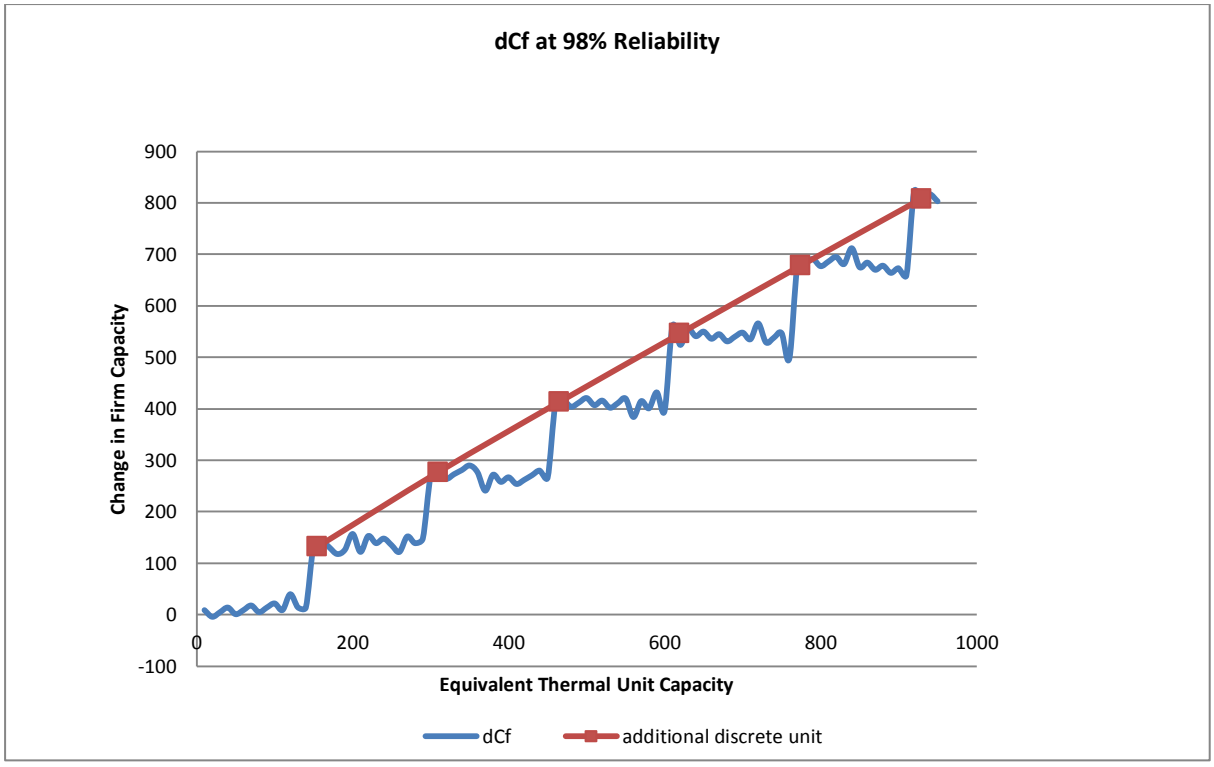

Figure 23: Change in firm capacity with addition of thermal units

This granularity causes a number of problems when trying to iterate the equivalent thermal capacity as much of the time a small change in thermal capacity can cause a huge variation in firm capacity.

Thus in order to mitigate this granularity and to calculate the C_r in an accurate and efficient manner the following process is proposed.

- Calculate firm capacity for existing system at defined reliability level
- Generate a table of incremental changes in firm capacity brought about by the additional of thermal units (represented by the red dots above)
- Calculate the resultant change in firm capacity from the additional PV
- Compare this to the closest change in firm capacity in the thermal table above
- Instead of iterating the thermal capacity, iterate the installed PV capacity until the change in firm capacity is equal to that of the closest thermal unit chosen

The C_r is then

$$C_r = \frac{C_{thermal\ unit} \times n}{C_{pv\ res}} \qquad (17)$$

Where, $C_{thermal\ unit}$ is the unit capacity of the typical thermal unit (small coal: 154.9MW), n is the number or units (n=1,2,3.. i) and $C_{PV\ res}$ is the resultant PV that gives the same change in capacity as the closest equivalent thermal unit.

Alternatively the trend of change in firm capacity from additional thermal units can be plotted and used to formulate a C_r algorithm. This was done for 98 % reliability (see Figure 23 above) and the following equation was formulated:

$$dC_f = 0.8699dC_{th} + 4.0667 \quad (18)$$

Where dC_f is the change in firm capacity from the additional PV and C_{th} is the equivalent thermal capacity that will give you the same change in firm capacity independent of the thermal unit granularity. The results of equation 18 can then be substituted back into equation 16 to calculate the C_r.

C_r's were calculated using both methods described above and compared. Results were found to have 2% uncertainty in the worst case, and as a result the latter method was deemed acceptable. Thus, from this we calculated the C_r of PV for various scenarios and subsets.

5.4. Scenario Analysis

The main goal of this thesis is to calculate the C_r of PVG in the SA power system for a variety of geographic dispersion and penetration scenarios. The reason for the scenario analysis is to test the effect that geographic spatial diversity has on the C_r and as a secondary goal test the C_r at different levels of penetration. As discussed above, before any scenarios can be analysed, relevant temporal subsets need to be chosen.

5.4.1. Subsets

Subsets were chosen to reflect interesting parts of the day and year from which meaningful results and trends could be drawn. Thus firstly, for the base case, diurnal trends were explored. This was done by calculating C_r every 2 hours of the day starting at first light and ending in the evening.

These were then calculated for following periods:

- Annual Period
- Summer, Autumn, Winter and Spring
- High Demand Period
- Low Demand Period

The subsets above were all carried out for the base case. For the geographic scenarios analysis the C_r were calculated for annual, low demand and high demand periods.

C_r for levels of penetration was calculated at midday for the annual demand period.

The seasons used in this research are based on those Eskom use in their tariff breakdowns (Eskom, 2013). Eskom's (2013) year is split into two seasons; high demand (1 June – 31 August) and low demand (1 September – 31 May). Thus, in this research, winter is based on the period of high demand, and summer, spring and autumn are split equally across the period of low demand as follows:

- Spring: 1 September – 31 November
- Summer: 1 December – 31 February
- Autumn: 1 March – 31 June

This then allowed for the evaluation of the above subsets for different levels of penetration and geographic dispersion.

5.4.2. Penetration Levels

C_r for different levels of penetration were calculated at midday for the annual demand period to simply show the effect of penetration level on PV's C_r. The installed capacities considered include:

- 1054.6 MW (base case)
- 2000 MW
- 4000 MW
- 6000 MW
- 8000 MW
- 10 000 MW

5.4.3. Geographic dispersion

The scenarios testing geographic dispersion were simulated for the base year of this research (2010) by systematically moving from a diverse spread of new plants added to the system to a singular location. Installed capacity remains constant and as the diversity is reduced the extra capacity is shared equally amongst the remaining plants. The current IPP projects, as described in the previous chapter are spread out across the Northern Cape, Limpopo, Free State and Western Cape provinces for the base case, as can be seen in Figure 24 below.

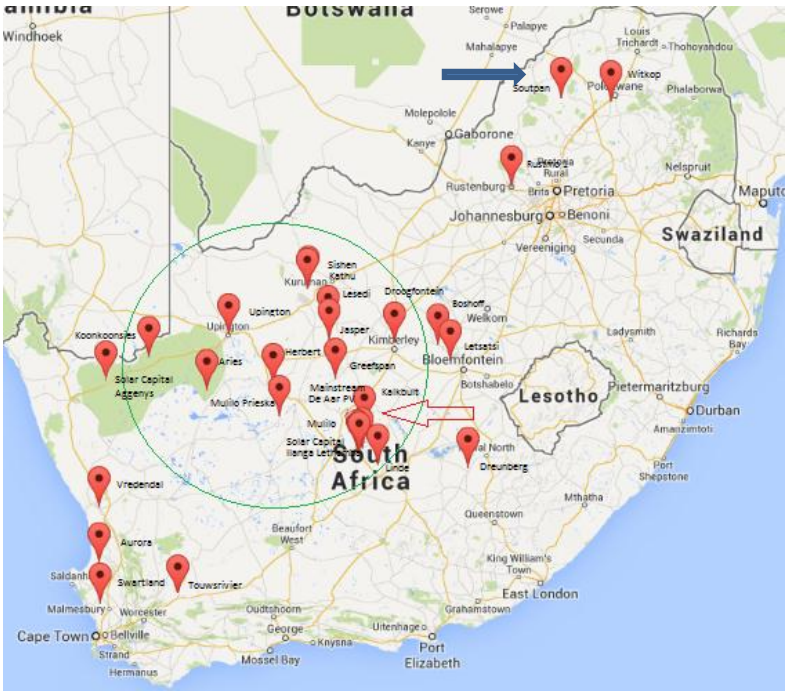

Figure 24: Spread of PV plants across SA (The Energy Blog, 2013)

Thus looking at Figure 24 the following scenarios were evaluated:

- **No PV –** Existing System
- **Scenario A -** Base Case, Total spread of PV plants based on R1 and R2 of REIPPPP

- **Scenario B** – Only plants located in the Northern cape (Circled in green)
- **Scenario C** – Total capacity concentrated in De Aar (Pointed out by red arrow)

Focussing all PV capacity in a singular location potentially causes the C_r to follow the climatic trends of that particular location. De Aar has a high probability of good all year round performance, thus potentially producing relatively high C_r values. This was tested by moving the singular location to Soutpan (Pointed out by blue arrow), in the Limpopo province, which while still a good solar location, showed relatively high variation in monthly yield. Therefore:

- **Scenario D –** Total capacity concentrated at Soutpan

These scenarios were then used in the dispatch model to quantify CO_2 produced, LOL indices and associated cost implications.

5.5. Design of the Dispatch Model

The SA power system has been modelled using an economic dispatch model. This model was used to simulate how a variable generator might be practically dispatched in combination with conventional generators and to quantify loss of load indices; CO_2 emissions avoided and associated cost implications. The model uses short run marginal cost as driver to dispatch available capacity in order to meet demand.

Much of the foundation of the dispatch model was used in conjunction with modelling of the C_r and is explained below.

Parameters used in this model come from a variety of sources:

- Hourly load data was drawn from Eskom's MYPD2 scenario for 2010 (Eskom, 2010)
- Power plant data was taken from the IRP 2010 (DOE, 2011), and parameters for existing plants were taken from Eskoms ISEP10 of 2006 (Eskom, 2006)

Further, the basic structure of the model was based upon work done on the ERC's SNAPP model (ERC, 2010), which mainly analyses periods of peak demand.

5.5.1. Overview

At the highest level a power system is made up of two parts; supply and demand. A certain amount of capacity is required to meet demand after accounting for considerations such as maintenance, forced outage rates (FOR) and reserve margin (RM).

The power system considered consists of a portfolio of conventional generators and the addition of a variable generator in the form of PV capacity. As a result of the additional PV a day ahead forecast model is employed to take the inherent uncertainty into consideration. A day-ahead forecast predicts what will be received from the variable generator, thus enabling an approximation of the resultant load that must be met by conventional means. Thus unit commitment for each hour is pre-determined a day ahead of time based on forecasted load and PV generation. The logic of this is shown in Figure 25 below.

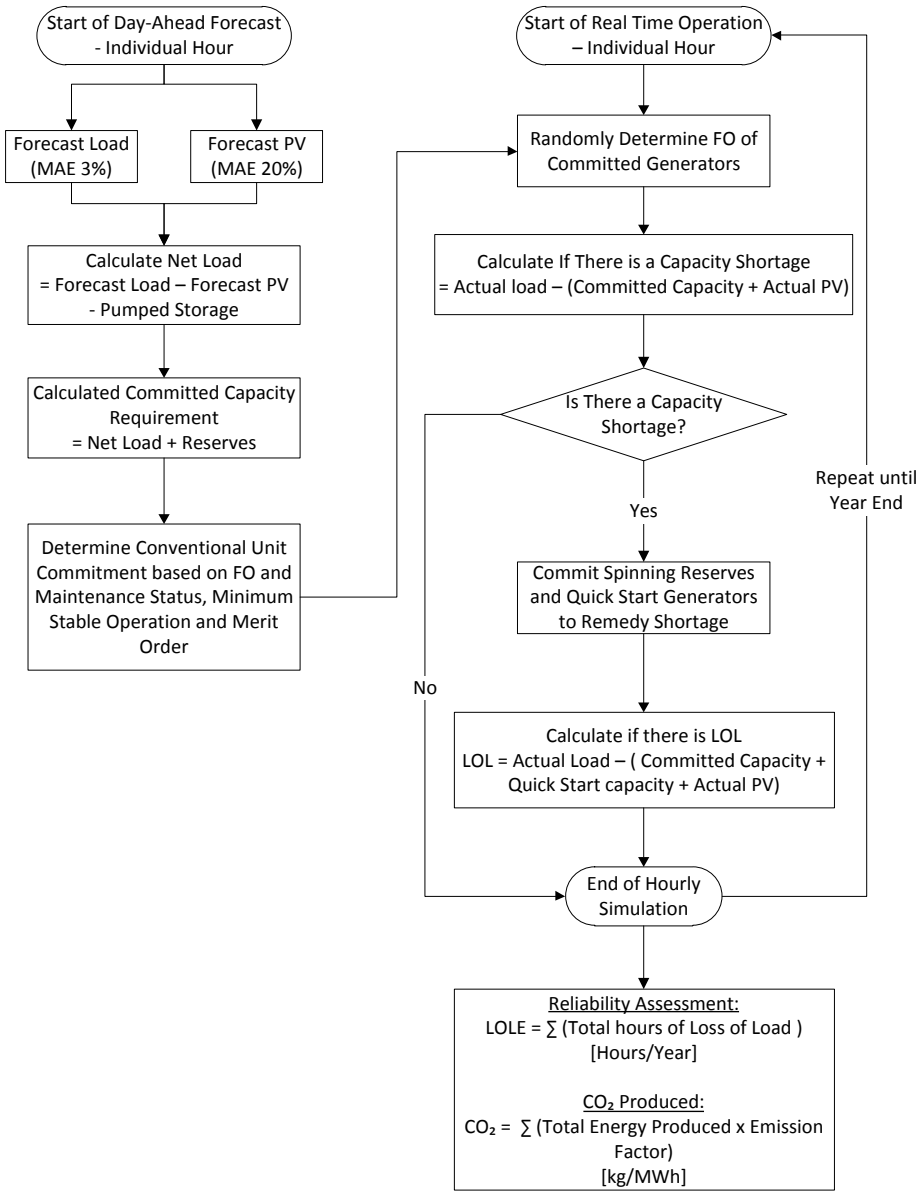

Figure 25: Logic of day-ahead commitment and real time operation

During real time operating hours, available capacity based on the day ahead forecast is ready to meet the net load (total load less actual PV yield). However, the system is subject to randomly generated forced outages and deviation from predicted and actual PV yield. Thus, if the resulting capacity is insufficient emergency actions such as spinning reserve and quick-start generators are employed. This is then completed for a year, calculating CO_2 produced and LOL indices. The individual processes are described in more detail below.

5.5.2. Day ahead forecast

The day ahead forecast pre-determines the generation requirements of conventional generation for the following day. It takes the variability of the added PV generation into consideration by forecasting the load and capacity generated by PV a day ahead of time. The difference between these two values results in the net load:

$$Net\ Load = Forecast\ Load - Forecast\ PV \qquad (19)$$

The resultant net load is the load that needs to be met by the conventional system and this allows for early commitment of generation resources, some of which require hours of advanced warning to come online.

In reality load forecasts are not perfect and will generally differ from real time operation. A mean absolute error (MAE) can be used to recognise uncertainty in the forecast, but was avoided due to the fact that in this analysis demand is known. Thus a safety factor is added into the prediction by inflating load by the LCC. At a chosen reliability of 98% the predicted load was inflated by an LCC of 87.2%, through the following equation.

$$Forecast\ load = \frac{(Predicted\ Load)}{LCC_{TH}} \qquad (20)$$

Where, LCC_{th} is the LCC for the thermal system as calculated in chapter 5.3, and the predicted load is the forecast load before uncertainty has been taken into consideration.

MAE's for weather forecasts particularly that of wind generally fall into the region of 15-20% (Lew & Milligan, 2011). In reality the accuracy of solar forecasting is quite high with hourly forecast errors in the range of 6-10% (Norris & Dise, 2013). However remaining consistently conservative we have opted for a 20% MAE to simulate the worst case scenario. This can be easily changed by future users of the model. Even with uncertainty in forecasts, studies have shown that day-ahead forecasts drastically reduce the need for curtailment due to oversupply of energy from lack of foresight. Thus:

$$Forecast\ PV = Simulated\ PV\ \times (1 - MAE) \qquad (21)$$

From this the net load is calculated on an hourly basis (using equation 19), and can be used to determine the operational procedure of pumped storage.

Net load is ranked from hour of lowest demand to highest demand, and used to govern when pumped storage will consume or generate energy. Energy is generated in the 6 hours of lowest demand and consumed in 6 hours of highest demand, while the remaining hours of the day are spent dormant. Pumped storage is not considered a true dispatchable generator as it both consumes and produces energy. Thus pumped storage is represented differently to the rest of the conventional system.

The resultant load must be met by conventional generators, and is used to determine the number of units that are to be committed for the following day. The choice of unit is decided by a combination of merit order approach and a minimum stable operation of 30% (GIZ, 2011). Non-thermal units such as nuclear and hydro are committed first due to their low marginal cost and inherently continuous energy production. While thermal plants are also committed in merit order, but with an additional constraint of minimum stable generation. This reflects the reality that a generator unit, such as coal can only run at a minimum of 30% of capacity and is used to calculate the "spinning reserves" of each technology to be committed first. This is reflected in Figure 26 below:

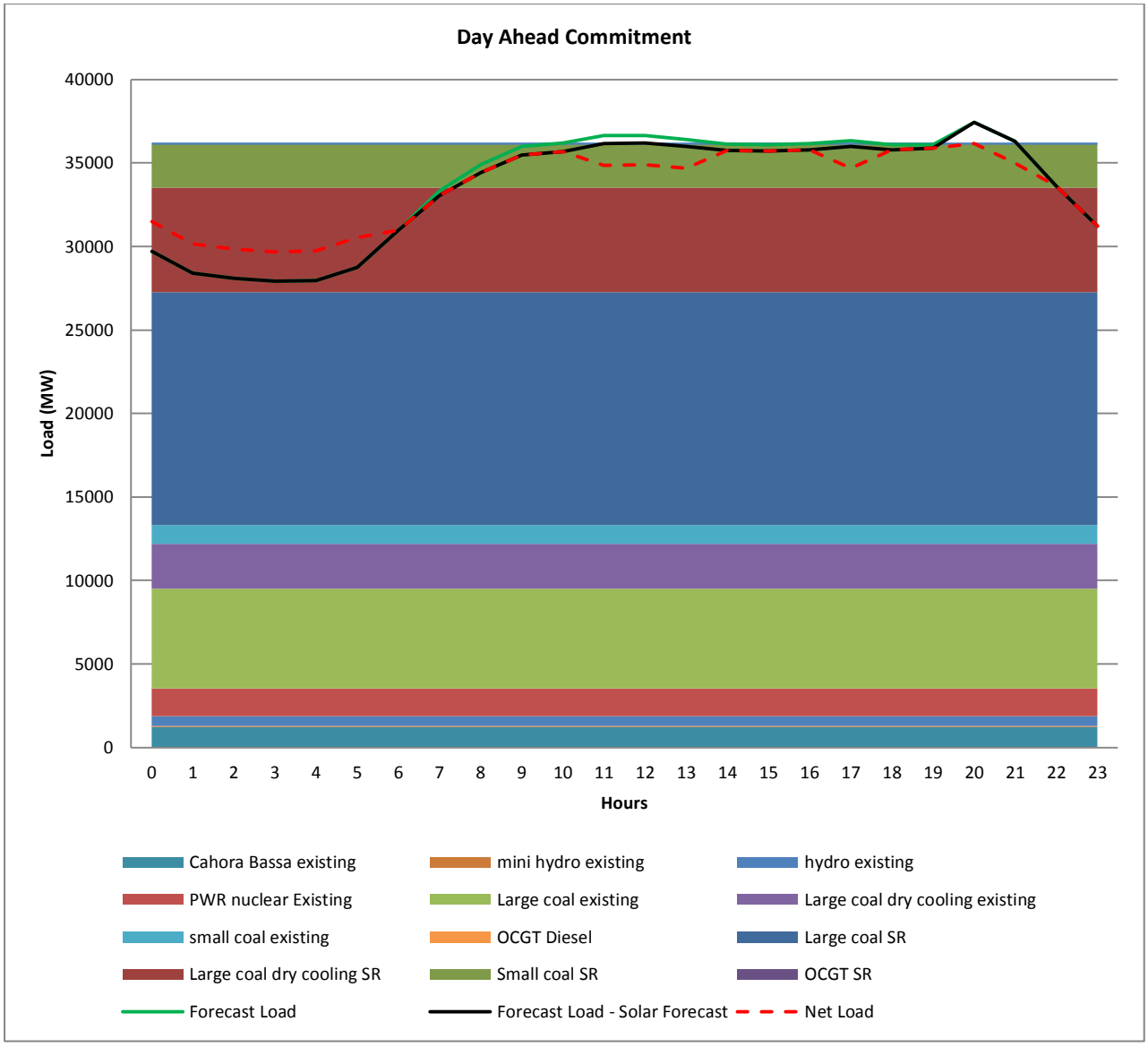

Figure 26: Day-ahead model for the base case showing spinning reserves, forecast load, net load and committed thermal capacity

At the beginning of generation commitment unit availability is decided by maintenance and forced outage status. This in turn is governed by the desired reserve margin and maintenance regime.

5.5.3. Availability and load forecasting

The dispatch order of conventional generation is decided through the so called merit order system. It considers the short run marginal cost for each technology in the existing generation fleet available in SA and dispatches units in order of least cost first. Short run marginal cost can be broken down into variable costs (running cost excluding fuel costs), fuel costs and carbon costs (carbon taxes).

$$Short\ Run\ Marginal\ Cost = Variable\ Costs + Fuel\ Cost + Carbon\ Cost \quad (22)$$

Conventional generation technologies considered in the simulation were:

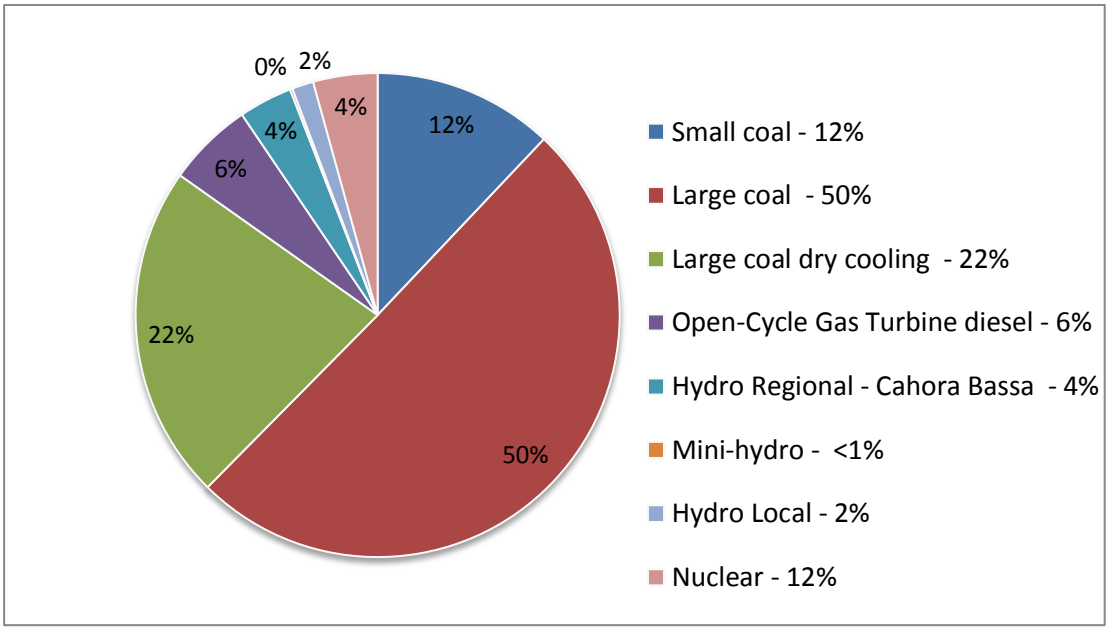

Figure 27: Generation mix of dispatchable technologies

Considering the short run marginal cost resulted in the following merit order:

- Cahora Bassa Regional Hydro
- Mini-hydro
- Local Hydro
- Nuclear
- Large Coal
- Large Coal dry cooling
- Small Coal
- OCGT - Diesel

In reality the individual generating units (GU) that fall into the categories shown in Figure 27 above, vary in capacity. In this dissertation the capacity of these units was assumed to be the same across each technology and averaged out.

Unit availability is decided in two parts; (i) by outage status based on maintenance and (ii) by forced outage rates, the latter being simulated during real time operation. Using planned outage rates (POR) the maintenance adjusted capacity is determined. The amount of capacity [MW] that can be under maintenance varies per month and is determined by the difference between the total installed capacity and monthly peak demand adjusted by RM (including maintenance) for each month as follows.

$$Monthly\ Maintenance = Total\ Installed\ Capacity - (Monthly\ Peak\ Demand \times (1 + RM(incl.maintenance)) \quad (23)$$

Where RM (including maintenance) is:

$$RM\ (including\ maintenance) = \frac{\left(\sum_{1\ to\ 12}^{i} Available\ for\ Downtime_i - \sum_{1\ to\ x}^{n}\left(POR_n X\ Capacity_n X 8760 \frac{hours}{year}\right)\right)}{\sum_{1to12}^{i}(Peak\ Demand_i\ X\ monthly\ hours_i)}$$

(24)

Where *i* denotes a month number from 1 to 12, POR is the planned outage rate and *n* denotes the number of generating technologies in the system and where;

$$Available\ for\ Downtime_i = (Total\ Capacity - Peak\ Demand_i)\ X\ monthly\ hours_i \quad (25)$$

And;

$$Monthly\ hours_i = The\ number\ of\ operating\ hours\ in\ month\ i = days\ in\ month/365\ X\ 8760\ hours/year \quad (26)$$

In order to simulate forced outages probability and cumulative distribution functions (PDF and CDF) were calculated from the FOR for each conventional generation technology, describing the probability that units will go offline. These distributions were obtained using a binomial distribution function shown below, and allowed for the generation of the capacity outage tables.

$$f(k;n;p) = \binom{n}{k} p^k\ (1-p)^{n-k} \quad (27)$$

Where *k* = 0, 1, 2 … *n*; *n* is the number of tests and *p* is the probability of success in each test (Lacey, 1998).

More specifically the PDF describes the probability of likely capacity being online, while the CDF describes the % chance of having less than that capacity online. Below is a condensed sample taken from the working model of the PDF and CDF for 'Small Coal':

Table 8: PDF and CDF for Small Coal

Plant Type	small coal		
# of Units	46		
Max Unit Capacity	108		
Total Available Capacity	4980		
FOR	4.6%		
# of units offline	**Capacity**	**PDF**	**CDF**
11	3789	0.000	0.000
10	3897	0.000	0.000
9	4006	0.000	0.000
8	4114	0.001	0.001
7	4222	0.004	0.005
6	4330	0.013	0.018
5	4439	0.041	0.059
4	4547	0.101	0.160
3	4655	0.195	0.355
2	4764	0.276	0.631

1	4872	0.254	0.885
0	4980	0.115	1.000
Note: CDF refers to the probability of capacity online being < x			

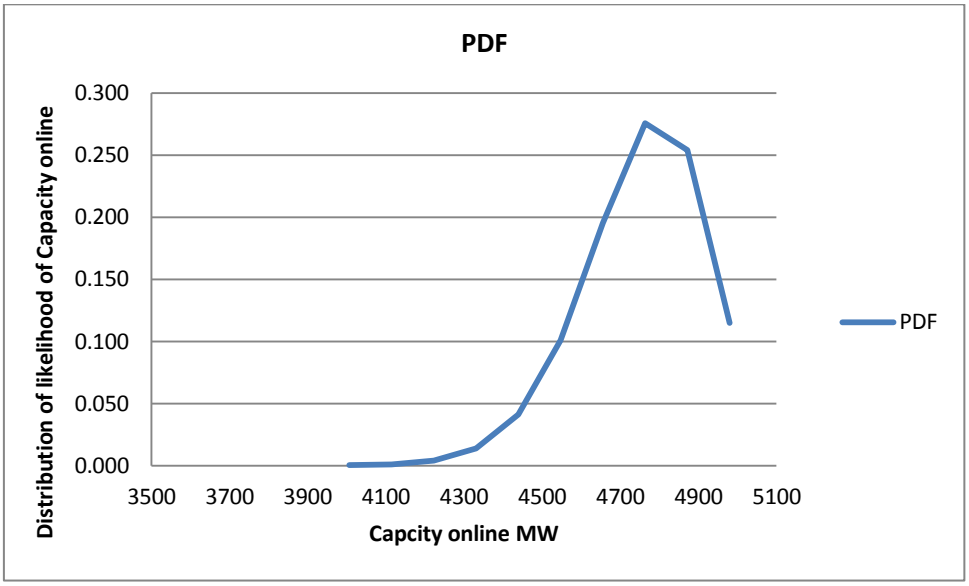

Figure 28: PDF for Small Coal

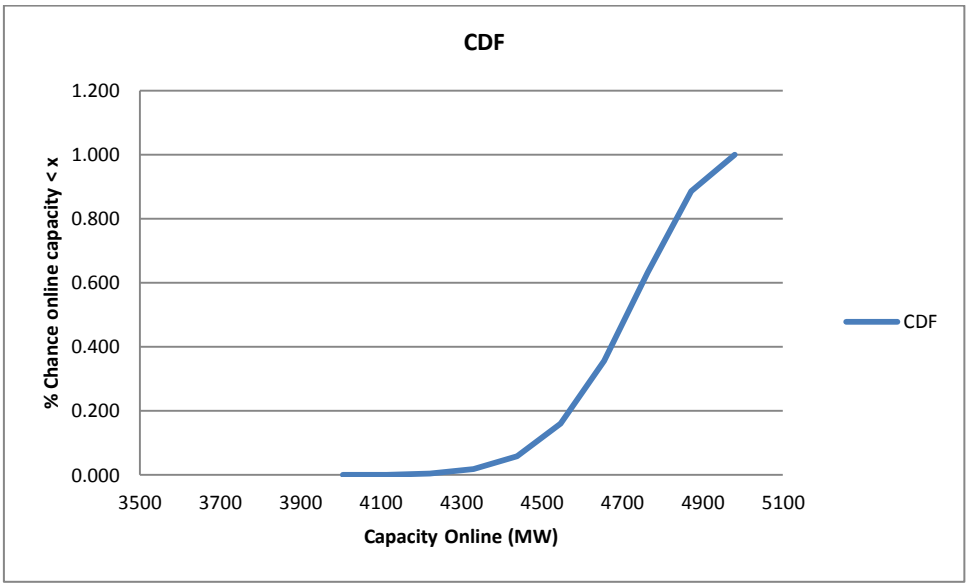

Figure 29: CDF for small Coal

Where total available capacity is maintenance adjusted capacity. Similar to that described in chapter 5.3.1, random numbers are used to decide the capacity that is online for each technology. Looking at Table 8 above for example, if the random number happened to be greater than 0.16, but less than 0.355, then this means that 4547 MW of small coal will be online at that time. This is then used in the real time operation of the dispatch to simulate the real-life randomness of forced outages.

5.5.4. Real time operation

For real time operation actual hourly demand for the day is to be met by available capacity otherwise loss-of-load will occur. Real time simulation for an individual hour begins with the availability of the committed units (from the day ahead forecast) being adjusted for maintenance and randomly generated forced outages. The latter is done to simulate the random behaviour of outage occurrences in real life. After actual PV generation has been accounted for initial commitment of non-thermal generators and minimum stable generation of thermal generators is implemented. This then allows for scheduling of pumped storage.

At this point if there is capacity shortage this needs to be calculated:

$$Capcacity\ Shortage = Actual\ Load - (committed\ capacity + Actual\ PV) \quad (28)$$

Where, committed capacity is committed minimum stable generation and non-thermal plants. If there isn't a shortage of a capacity, that is the end of the hourly simulation. If there is a shortage however, emergency spinning reserves are required to remedy the situation. If there is still a shortage in capacity however, loss-of-load will occur:

$$LOL = Actual\ Load - (committed\ capacity + spinning\ reserves + Actual\ PV) \quad (29)$$

An example of real time operation for the base case is represented in Figure 30 below:

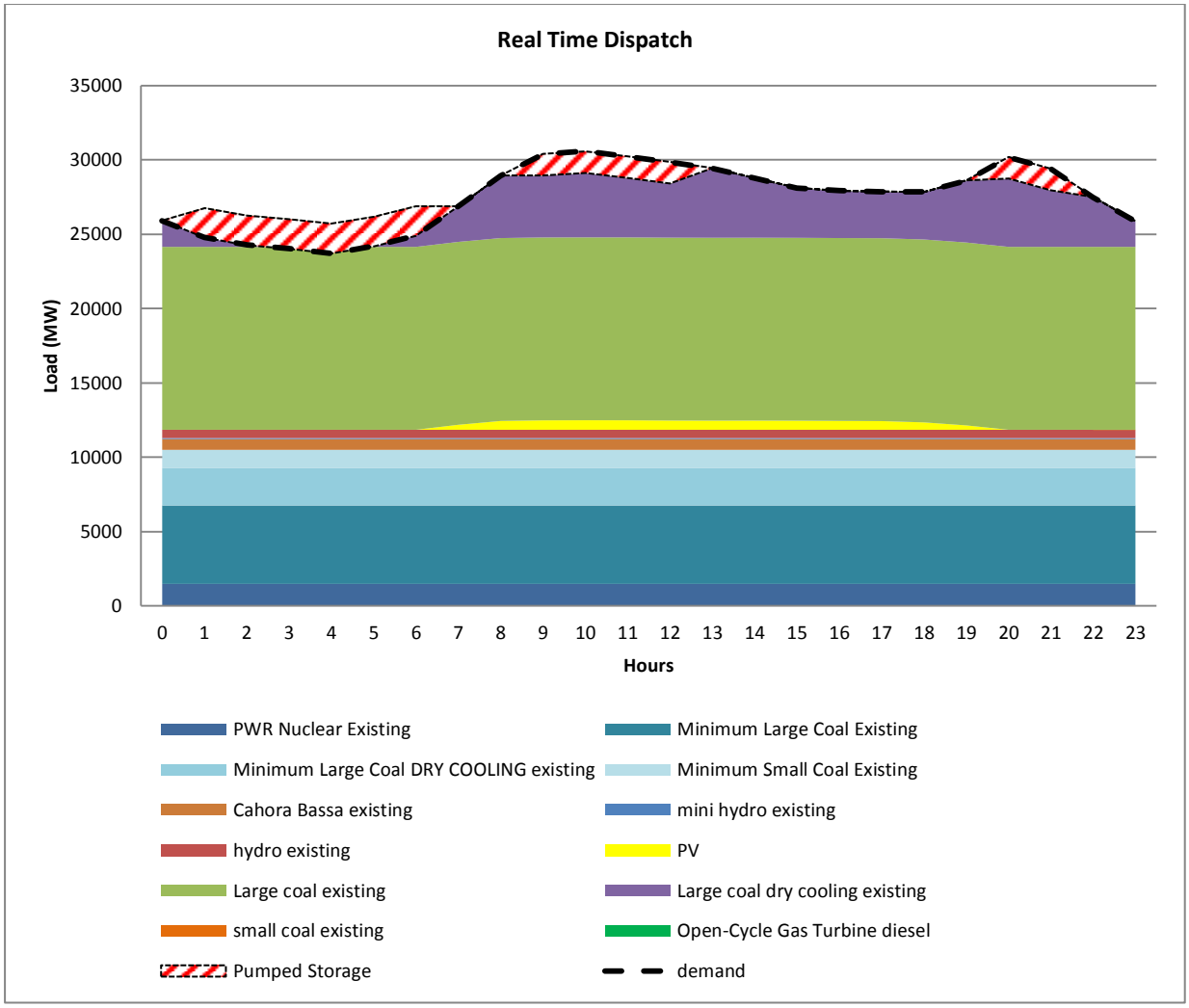

Figure 30: Example of real time dispatch for the base case

5.5.5. Dispatch model outputs

The dispatch is designed to meet load economically on a daily basis and has been set up to calculate various outputs that can be compared across the scenarios discussed in 5.4.3. These include:

- Hourly capacity factors for each technology
- Hourly un-served energy, or EENS
- Hourly LOLE
- Hourly Energy value of fuel used for thermal generators
- Hourly cost of fuel
- Hourly CO_2 produced

These are then summed for the day and Monte Carlo Simulation (MCS) was again employed to simulate the output that would be reached over a year. This is done by randomising the day of the month, running 100 simulations for each month while recording each runs results (see appendix F for the visual basic code). These results are then averaged and multiplied by the number of days in the month considered to get monthly results. These are then summed for the year.

Hourly capacity factors are generated for each technology by the following equation:

$$CF = \frac{Dispatched\ capacity}{Available\ Online\ Capacity}$$

LOL on an hourly basis is quantified through the reliability indices LOLE and EENS:

$$LOLE = \sum_{y=1}^{n}(Total\ hours\ of\ LOL) \quad (30)$$

$$EENS = \sum_{y=1}^{n}(Total\ kWh\ not\ served) \quad (31)$$

Where the LOLE is the total hours where LOL is experienced, while EENS is the total kWh not served during those hours. If calculating the per unit value of LOLE over the total period considered we get LOLP:

$$LOLP = \frac{\sum_{y=1}^{n}(Total\ hours\ of\ LOL)}{Total\ hours\ of\ period\ considerd} \quad (32)$$

In general we quantify the period considered in number of peak occurrences for that period. So for a year, if there is only one peak hour per day, then the period considered would be 365.

Energy value and cost of fuel and CO_2 produced are calculated in the same process. When a typical plant is online efficiency and hence fuel used is dependent on the operating load. This is depicted for sub-critical coal in Figure 31 below:

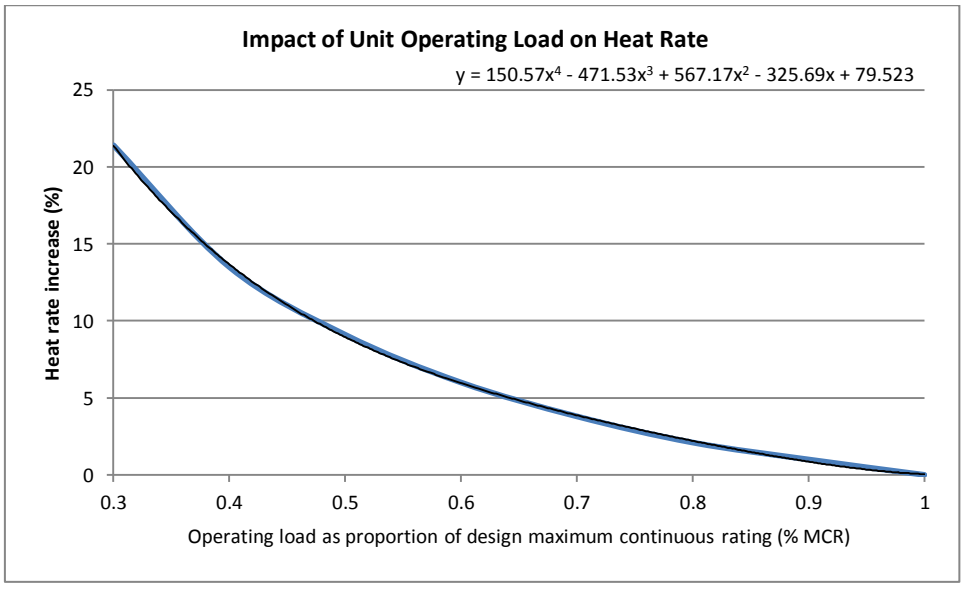

Figure 31: Impact of Unit Operating Load on Heat Rate (IEA, 2010)

The curve above shows that as the operating load decreases the relative heat rate (kJ/kWh) increases. This means that the efficiency decreases and the relative fuel use and CO_2 production increases. From the curve above, the following equation was formulated describing operating load vs. heat rate increase.

$$y = 150.57x^4 - 471.53x^3 + 567.17x^2 - 325.69x + 79.523 \quad (33)$$

Where y is the heat rate increase (%) and x is the operating load. The change in heat rate can then be used to calculate the efficiency of the unit at the hourly capacity factor:

$$Eff = \frac{3600}{Heat\ Rate} \qquad (34)$$

This then allows for the energy value of fuel used (GJ) to be calculated for each technology:

$$Energy\ of\ fuel\ used = \frac{Dispatched\ Capacity \times 3.6}{Eff} \qquad (35)$$

Cost and CO_2 parameters from the IRP (DOE, 2011), shown below, were then used to calculate the associated emissions and cost implications for each scenario.

Table 9: Cost and CO_2 Parameters for thermal units (DOE, 2011)

Technology	Cost	CO_2 produced
	R/GJ	kg/GJ
Large coal existing	15	96.25
Large coal dry cooling existing	15	96.25
Small coal existing	15	96.25
Open-Cycle Gas Turbine diesel	145.66	74.0667

All the above outputs were used to quantify the value of PV in the SA power system.

5.6. Load Profiles for SA

Eskom differentiates between 2 seasons in SA. A period of high demand (1 June – 31 August) and Period of Low demand for the rest of the year (Eskom, 2013). The load and particularly the peak load vary greatly across the year as can be seen in Figure 32 below.

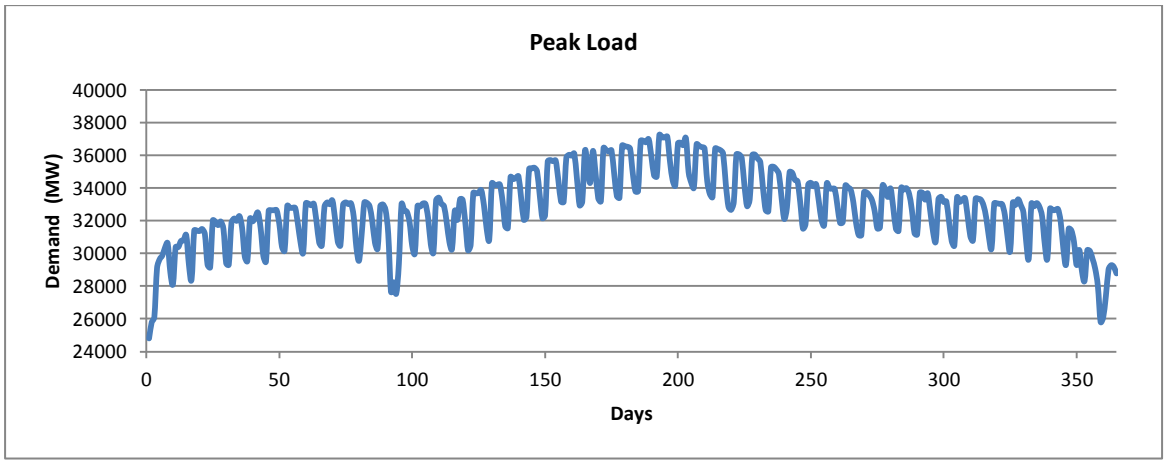

Figure 32: Trend of Peak load over a year

This results in different load profiles for these two periods.

The period of high demand in SA falls during the winter months. Months, where although there is still ample levels of irradiation, the days are shorter and ambient temperatures are significantly lower. This temperature drop particularly coincides with sun down and sun up, which results in an increased demand for lighting and heating overlapping with commercial requirements. Thus there is a particularly large peak demand in the evening, between 17h00 and 19h00, as can be seen for the typical July load profile in Figure 33 below.

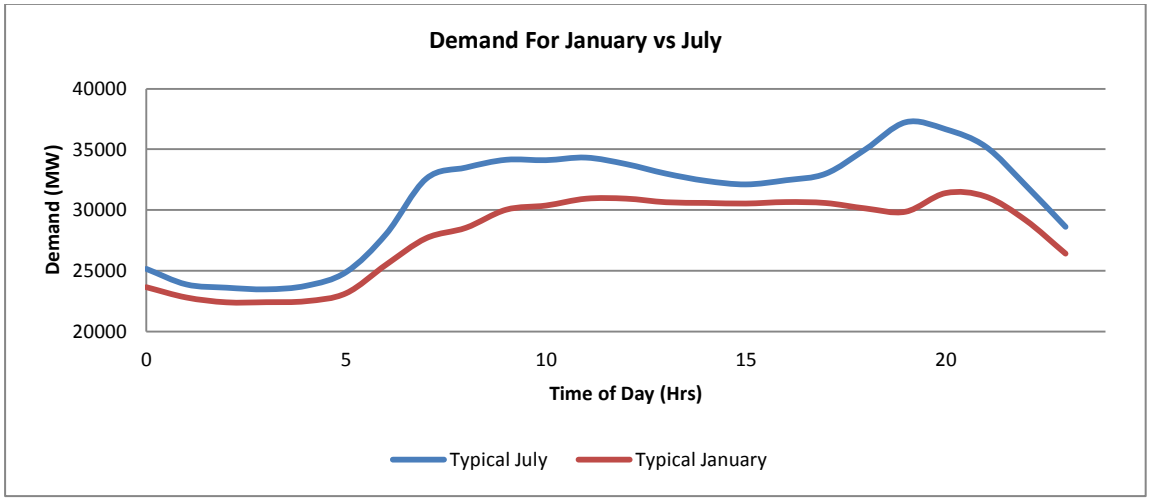

Figure 33: Demand for January vs. Demand for July

Furthermore there is a minor peak in load from 7am to 12h00 in the morning, before levelling out during the day. Significantly, the evening peak is noticeably higher than the rest of the daily demand.

On the other hand the demand profile experienced in periods of low demand is typified by examples taken from January (see Figure 33 above). In comparison to the demand experienced in the winter months, there is only a minor peak in late evening (toward 21h00). Further, midday requirements are fairly flat and nearly as high as that of the daily peak. This difference in shape is highly significant when one considers the economic dispatch of generators and the value that PV can add to the system during this midday period.

The load profiles for the two months contrast significantly. However, of particular interest to this research are the relatively high levels of demand shown during the daylight hours for both periods and the potential for PV to replace conventional generation options during these times.

5.7. Assumptions and Limitations

When tackling a complex system problem such as this one, many assumptions and limitations are applied when reaching a solution. The main limitations to this research are that it is considered for one year of data only, and that the C_r results have not been ratified using and alternative approach. This is because C_r research is fairly immature, particularly in SA.

Furthermore the one big disadvantage of using probabilistic approaches such as these is that it assumes that load and outages are independent of one another where in reality this is not the case (Amelin, 2009). Additionally, the model's outage table reflects the number of available units

unadjusted by the number of units offline due to maintenance and forced outages. To include this in the model would however have been outside of the scope of this research and was estimated to have a marginal effect on the results.

The dispatch model is governed by certain constraints, as discussed above. This is still a simplified version however, as ramp rates and efficiency adjustment rates have not been included, particularly for coal. Including this would quite significantly affect CO_2 emissions.

Currently the scenarios are constrained to locations chosen in round 1 and round 2 of REIPPPP. In reality, future build will likely be in more disperse locations. In further research it might be profitable to include more widely spread sites in the evaluation of geographic dispersion and at higher penetration levels.

Even with these limitations the power model is a simple but adequate simulation tool.

5.8. Summary

A model was set up to evaluate the C_r for PV in SA testing the effect of geographic diversity and penetration level on C_r through scenario analysis. Stochastic simulation was used along with LOLP mathematics to probabilistically simulate the LCC of a conventional power system and that of a power system including PV at a reliability level of 98%. These two power systems were then compared to calculate the change in firm capacity from adding PV. An equivalent thermal unit that would bring about the same change in firm capacity was then calculated through iteration. The ratio of the equivalent thermal unit and the additional PV capacity is then effectively a measure of the C_r of PV using the following formula:

$$C_r = \frac{dC_{th}}{dC_{pv}} \qquad (36)$$

C_r's were calculated for subsets of different times for month and seasonal periods through the scenario analysis. The effect of geographic dispersion was tested for a fixed capacity in 2010 by starting with a base case scenario (based on round 1 and round 2 of REIPPPP) and slowly decreasing the dispersion until all capacity was focussed in one area.

Similarly C_r's at different levels of penetration were simply calculated for incremental changes in PV capacity for midday over a year on the existing system.

A simple power model was then created to simulate the dispatch of a PV adjusted power system. Dispatch was economically optimised through short run marginal cost and includes a day-ahead load and PV yield forecast to commit conventional capacity ahead of time. Load is inflated by the LCC at 98% reliability, while a conservative MAE of 20% was used to cater for PV forecast uncertainty accordingly. This allowed for calculation of required spinning reserves and minimum stable generation to be used in the dispatch.

For the real time simulation, these were then dispatched first along with actual PV, after which conventional capacity was dispatched economically to meet the load. If the load cannot be met, loss

of load occurs and is quantified for the year, along with CO_2 avoided; average capacity factors and associated cost implications.

Demand profiles of the SA power system were then analysed showing a positive correlation between PV production and the relatively high levels of demand during the day across the year.

This methodology has resulted in a simple, but adequate analysis of the C_r for PV in SA, along with a simple and robust power system model.

6. RESULTS & DISCUSSION

The effect of geographic dispersion and penetration levels on the C_r of utility scale PV were tested for the SA power system. This was simulated using the effective load carrying capability (ELCC) method, while an energy dispatch model was used to simulate real time operation from which yearly output of CO_2 avoided; average capacity factors and associated cost implications were measured.

As a result the following results will be explored:

1) PV Generation
   a) Individual yield trends
   b) Overall yield trends
2) C_r results – Base Case
3) C_r results – Geographic Dispersion
4) C_r results – Penetration Levels
5) Dispatch model outputs

6.1. PV generation yield

For the base case, 27 individual PV plants were modelled. Site locations and capacities were based on preferred bidders as decided by round 1 and 2 of REIPPPP. Yield was modelled using a simple method outlined by Hart & Jacobson (2011) (see equations 3-5). Below are the main results from the yield analysis. Table 10 below describes the yearly yields for each site.

Table 10: Maintenance Adjusted yearly yield for Base Case

Maintenance Adjusted Yearly Yield for Base Case Scenario						
	Name	**Contracted Capacity AC**		**Actual Yield**	**Theoretical Yield**	**PR**
		MW	**KW**	**GWh/yr**	**GWh/yr**	**%**
1	Letsatsi	64	64000	136.5	181.6	75%
2	Lesedi	64	64000	142.3	189.7	75%
3	Witkop	30	30000	57.6	76.2	76%
4	Touwsrivier	37	37000	75.5	99.3	76%
5	Soutpan	28	28000	49.3	66.0	75%
6	Mulilo - De Aar	10	10000	20.4	27.1	75%
7	Mulilo - Prieska	20	20000	46.0	61.8	74%
8	Konkoosies	10	10000	23.2	31.3	74%
9	Rusmo1	7	7000	12.8	17.0	75%
10	Kalkbult	72.5	72500	162.0	216.4	75%
11	Aries	10	10000	22.5	30.4	74%
12	Swartland	5	5000	9.4	12.3	77%
13	Mainstream - De Aar	50	50000	107.9	143.6	75%
14	Greefspan	10	10000	21.8	29.2	75%
15	Kathu	75	75000	173.3	236.4	73%

16	Ilanga Lethemba	75	75000	161.4	214.9	75%
17	Droogfontein	50	50000	101.1	135.2	75%
18	Herbert	20	20000	44.7	60.8	74%
19	Aggenys	75	75000	183.2	244.5	75%
20	Sishen	74	74000	170.9	233.1	73%
21	Aurora	9	9000	17.7	23.2	76%
22	Vredendal	8.8	8800	18.6	24.5	76%
23	Linde	36.8	36800	78.4	104.3	75%
24	Dreunberg	69.6	69600	148.3	196.7	75%
25	Jasper	75	75000	156.0	206.8	75%
26	Boshoff	60	60000	126.1	168.0	75%
27	Upington	8.9	8900	20.3	27.7	73%
	total	**1054.6**	**1054600**	**2287.4**	**average**	**75%**

Samples of the results above were then compared against, *PVSyst* and *SAM*, 2 software packages commonly used in research and industry today. The results shown below in Table 11 further ratify the results.

Table 11: Ratification of Yield Results

Ratification of Results						
Name	**AC Capacity**	**Manual**	**Pvsyst**	**%diff**	**SAM model**	**% difference**
	MW	**GWh/yr**	**GWh/yr**		**GWh/yr**	
Letsatsi	64	143.69	146.74	-2.1%	145.92	-1.6%
Mulilo - De Aar	10	21.48	21.68	-0.9%	22.90	-6.6%
Rusmo1	7	13.53	14.919	-10.3%	14.60	-7.9%
Kathu	75	182.46	179.18	1.8%	176.41	3.3%
Ilanga Lethemba	75	169.92	172.58	-1.6%	173.57	-2.1%
Upington	8.9	21.36	21.22	0.7%	20.96	1.9%
			Ave Dev.	**2.9 %**		**3.9%**

On average, a deviation of 2.9% and 3.9% was found on yearly simulations for PVSyst and SAM respectively, which is within acceptable range. Additionally, the majority of the simulated results were found to be slightly more conservative than PVSyst and SAM results.

Furthermore the performance ratio (PR) for each plant has been calculated. It was found that for the base case scenario 2287.4 GWh/yr of energy will be produced at an average performance ratio of 75%. The PR is a useful tool for comparing performance between plants independently of site location or setup. A PR of 75% is indicative of healthy performance, and in line with values from modern plants, which indicates that the yield results are acceptable.

6.1.1. Individual yield trends

The PV plant locations, as outlined by REIPPPP, are spread out across SA and situated mainly in and around three regions of the country (see Figure 24):

- Limpopo province
- The Northern Cape and Freestate provinces
- Western Cape province

The following graphs show the key trends found in the three different areas:

Limpopo:

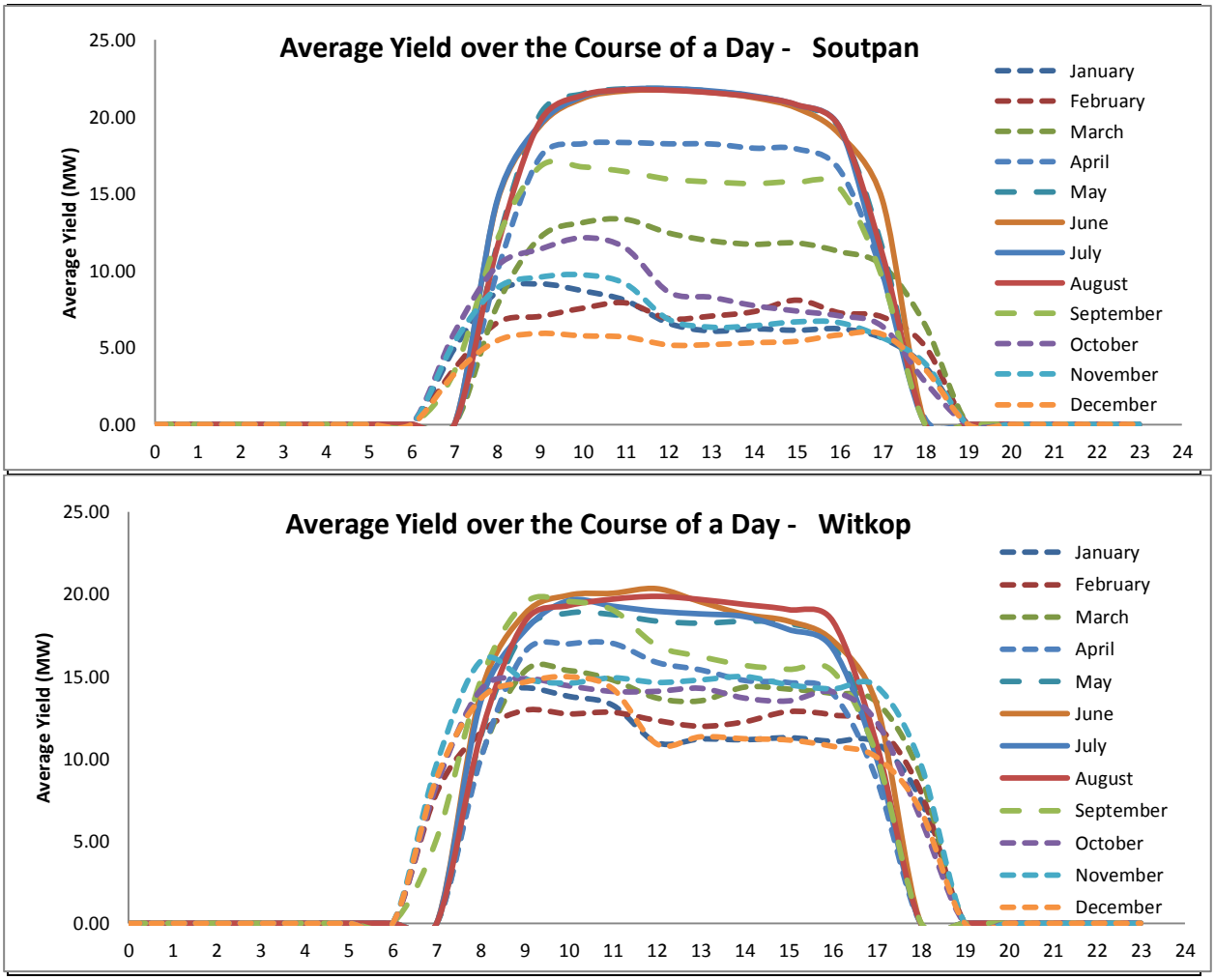

Figure 34: Average yield for Soutpan and Witkop PV plants

Western Cape:

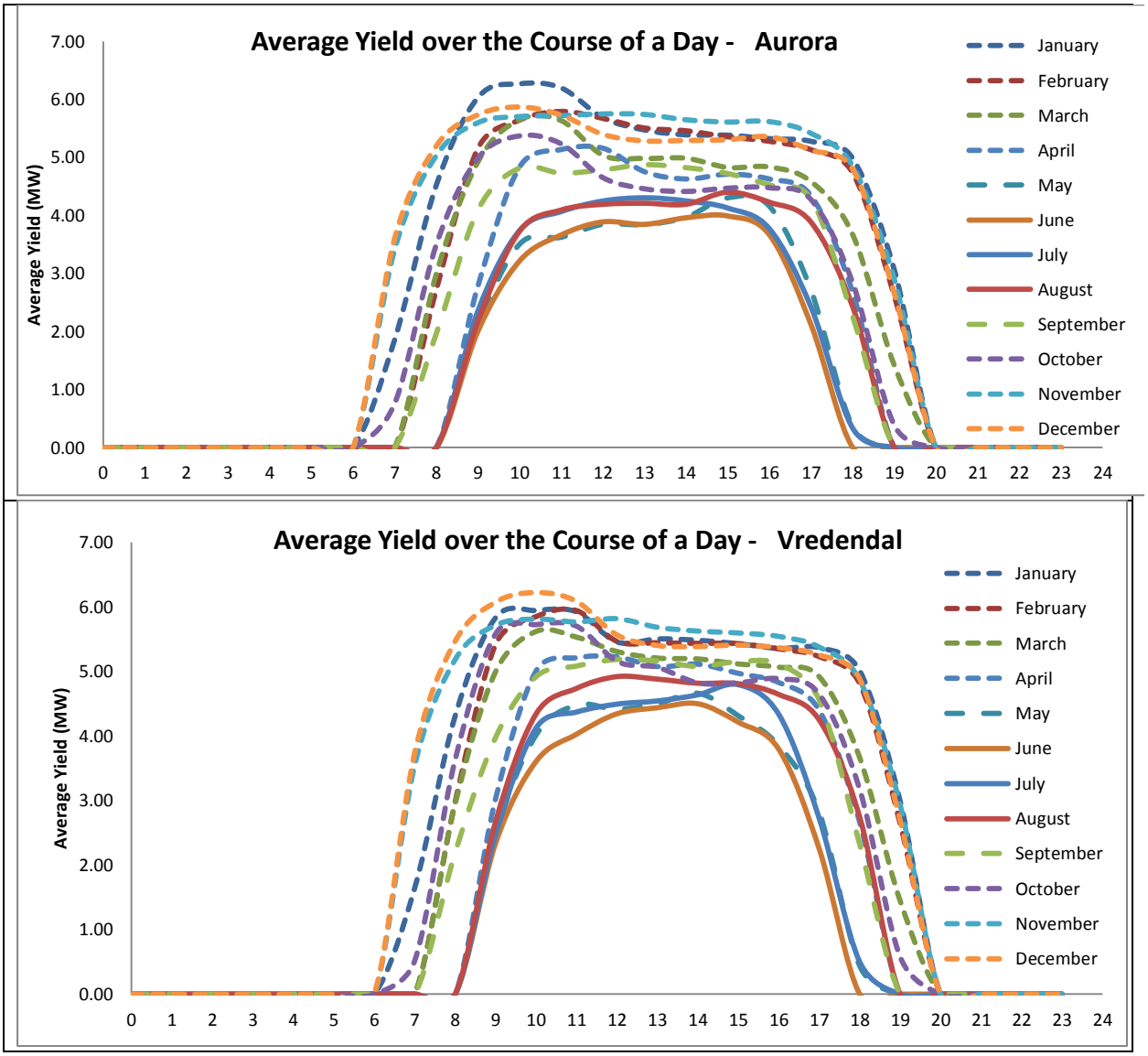

Figure 35: Average yield for Aurora and Vredendal

Northern Cape:

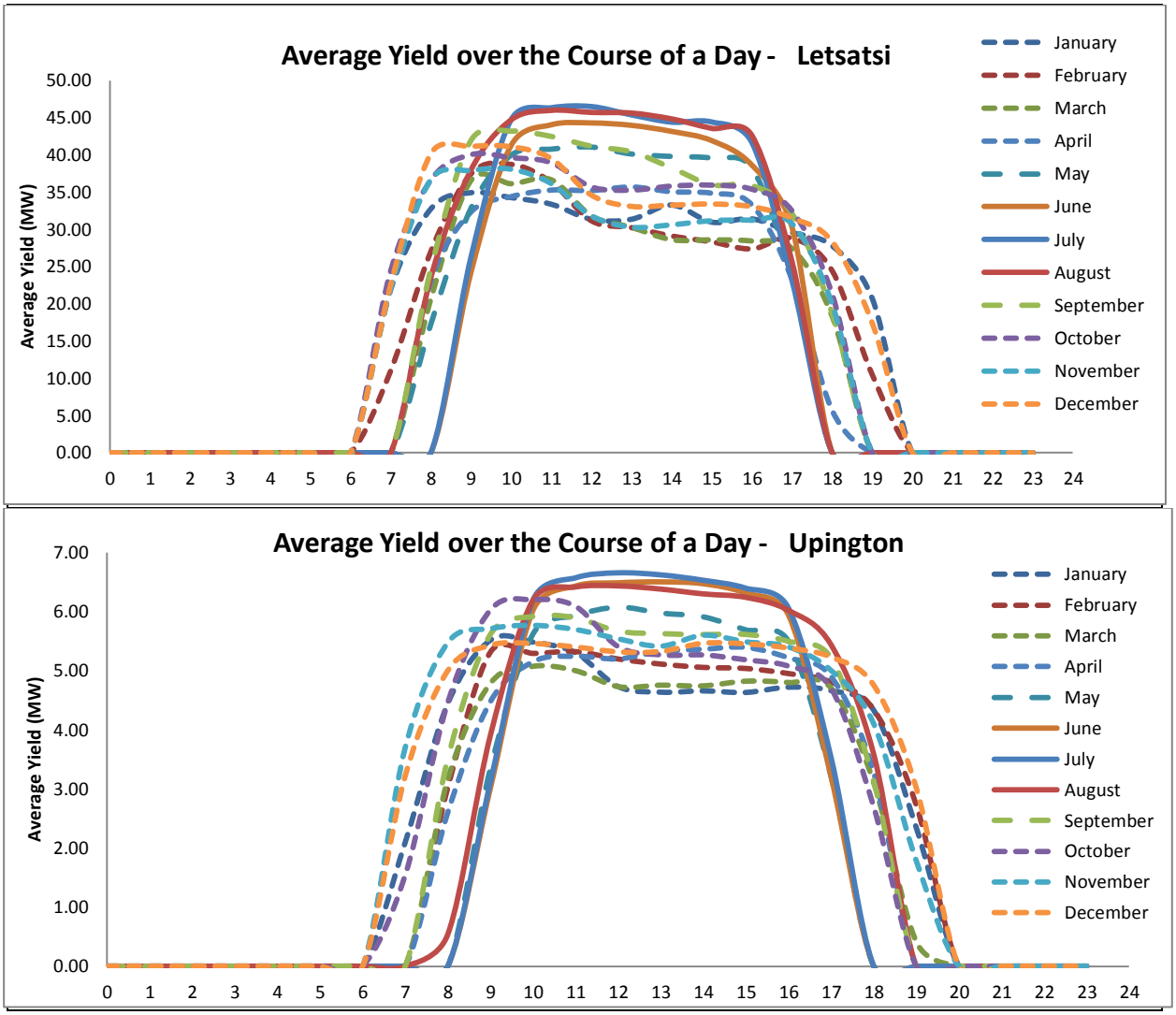

Figure 36: Average Yield for Letsatsi and Upington

Although the winter and summer months are the same for all plants across the country, rainfall, cloud cover and periods of maximum ambient temperatures occur at different times of the year. When considering yield from typical plants from each region this becomes more apparent. Furthermore several interesting correlations can be found.

Looking at the average daily yield for two typical sites from the Limpopo region in Figure 34 above, several points of interest emerge. Looking at the graphs it can be seen that while the average yield for the low demand period (signified by dashed lines) is spread over a greater part of the day, the peak yield is predominantly found during the winter months (solid lines).

Furthermore, the maximum yield in the months of low demand shows a distinct trend of peaking at 10h00 and 11h00 and then tapering off in the afternoon. Conversely the winter months peak is fairly constant, plateauing over the middle of the day. This would suggest periods of rainfall and cloud cover during the summer months.

On the other hand, looking at typical yields from the Western Cape (see Figure 35 above), a slightly different trend emerges

Similarly to the plants in Limpopo there is a definite peak before midday during the summer months. However, in the Western Cape this trend starts earlier in the day with majority of the dashed lines peaking between 09h00 and 11h00, before dropping off slightly and flattening off until approximately 18h00.

Unlike Limpopo, yield is greater on average in summer for the Western Cape, with fairly consistent average yields for both periods of high and low demand. This suggests that the irradiation levels are higher in summer, spring and autumn with winter being slightly lower, with a few days of cloud and rain occurring in the winter period.

The majority of PV plants are sited in or on the border of the Northern Cape Province. Thus the patterns found in this area will have the most significant effect on the overall results.

Looking at Figure 36 above, again it was found that for many of the summer months there was a distinct peak between 10h00 and 11h00 before yield flattened off for the afternoon. Similar to the Limpopo sites, maximum yield tended to be higher in the winter months for the Northern Cape. However, the difference in yield levels between the two is less pronounced. Counter intuitively, it was found that some of the lowest periods of yield occur during the hot summer months of January and February.

Looking at all three regions as a whole there are few clear trends:

- A definite peak in the months of low demand between 10h00 and 12h00 before tapering off into the afternoon
- High constant yields in the winter months, which apart from the Western Cape has generally higher peak values in the winter months

There are several likely reasons for these trends. Firstly, the tilt angle of modules for all the PV sites has been fixed at 30°. This is not the optimum for each site as this changes with season and longitude and latitude (Matshoge & Sebitosi, 2010), but produces a good all year output and optimises on shading and area usage. This tilt angle will inversely affect summer yields for the more northern located plants to a greater extent as the suns position in the sky increases in height the closer to the tropic of Capricorn you become. Conversely, this effectively increases the winter yields of the more northern plants to a greater extent for similar reasons.

Secondly, much of the northern parts of SA experience afternoon storms and rainfall in the summer months caused by the extremely high temperatures found in these regions. These seasonal weather patterns become apparent when looking at meteorological data for the Letsatsi site, located north of Bloemfontein, shown in Figure 37 below.

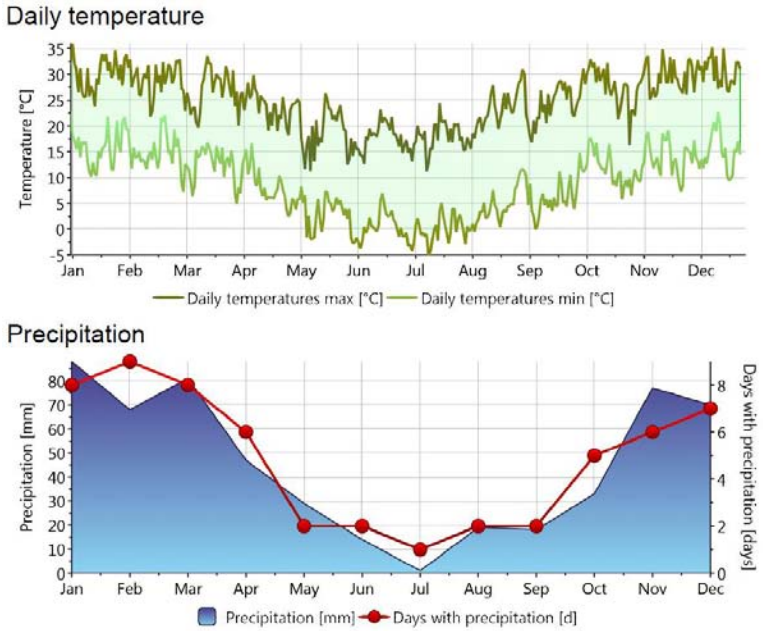

Figure 37: Temperature and Precipitation profile of Letsatsi (Meteonorm V7.0, 2013)

It was found that months with maximum temperatures (Jan, Feb, Mar, Nov and Dec) coincide with months of both maximum precipitation and maximum days with precipitation. This effectively shortens the sunshine duration for these months, as displayed in Figure 38 below, thus negatively affecting yield in these months.

Furthermore, while the actual sunshine duration (shown in red below) is fairly consistent throughout the year, the daily global radiation is much more variable during the months discussed above. This causes short periods of particularly low yield dispersed amongst periods of high yield.

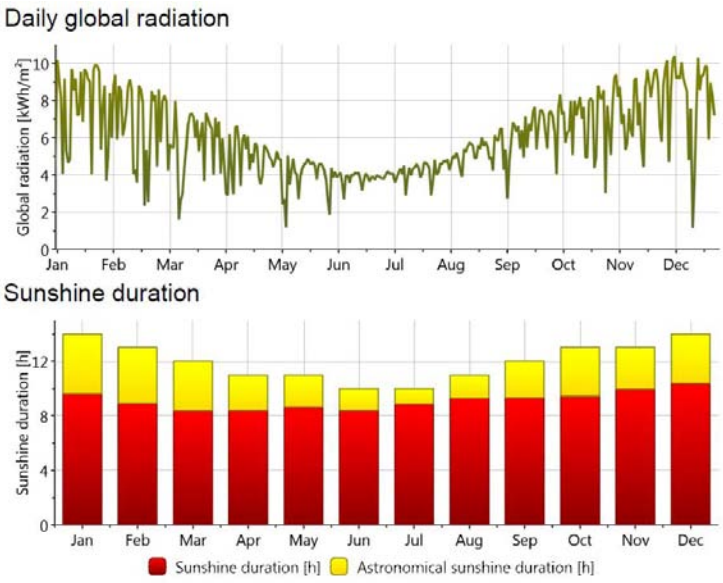

Figure 38: Daily global radiation and Sunshine duration for Letsatsi (Meteonorm V7.0, 2013)

Lastly, the two factors described above are further compounded by another phenomenon. Performance of solar PV modules is highly sensitive to module temperature. Module temperature in turn is sensitive to ambient temperature, irradiation levels and mounting method. The method used to describe the effect of module temperature on efficiency is the commonly used "*NOCT*" method (as described in the methodology: Solar Data and PV yield). This brings about an interesting correlation between yield, ambient temperature and irradiation as can be seen in Figure 39 below.

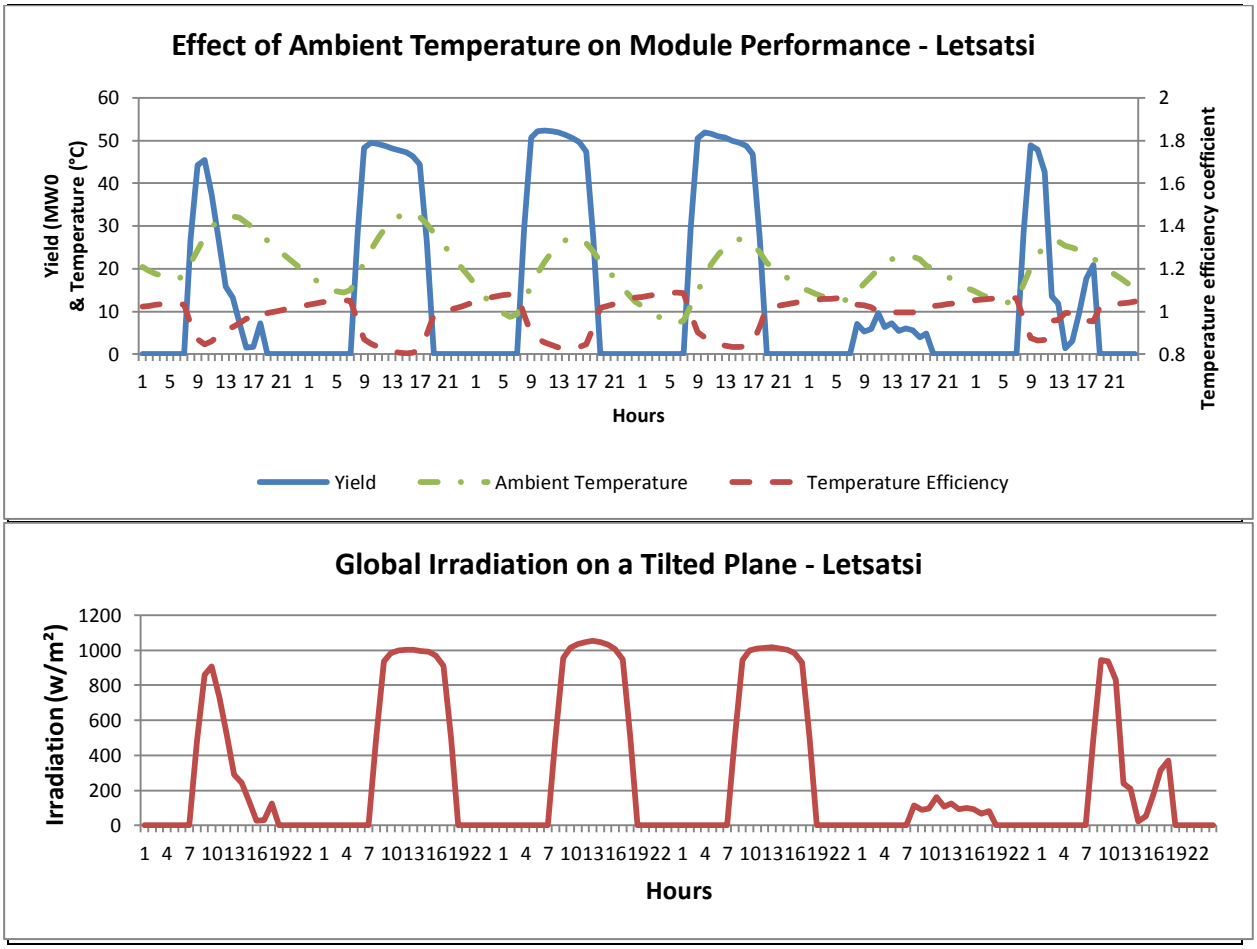

Figure 39: Effect of Ambient Temperature and Irradiation on Module Performance - Letsatsi

The graphs above describe yield, ambient temperature and efficiency due to temperature and global irradiation for 6 typical days for the month of March for the Letsatsi site. From Figure 37 above, we can draw the conclusion that March is a month of high temperature and irradiance, but with a high incidence of rainy days. This mix of conditions is succinctly portrayed above with 3 days of clear sunlight and high temperatures, signified by the smooth symmetrical curves, and three days of variable conditions, signified by the erratic curves. Looking at the top graph, it can be seen that on the days of high irradiation, the yield closely matches the sudden increase in irradiation for the morning period, before peaking at 10h00. Ambient temperature, on the other hand, is still dependent on irradiation levels, but lags behind, peaking only in the afternoon. During this rapid increase of temperature across midday, a critical point is reached where irradiation levels are at maximum, but no longer increasing and the temperature efficiency coefficient starts to gain significance. Looking at the curves above, this happens approximately between just before midday and 16h00 for March, causing the yield to taper off slowly in the afternoon.

From the findings for individual plants above, we can expect that the overall yield for the whole system will closely follow the trends above, particularly those of the plants in and around the Northern Cape. As a result the expected trends for the overall system yield are:

- High levels of yield across the whole year
- Summer peaks from 10h00 – 12h00 with yields tapering off in the afternoon
- High 'plateauing' peaks during the winter months
- Longer yield duration in the low demand season
- Shorter yield duration in the high demand season

6.1.2. Overall yield trends

The overall yield for the base case can be seen in Figure 40 below.

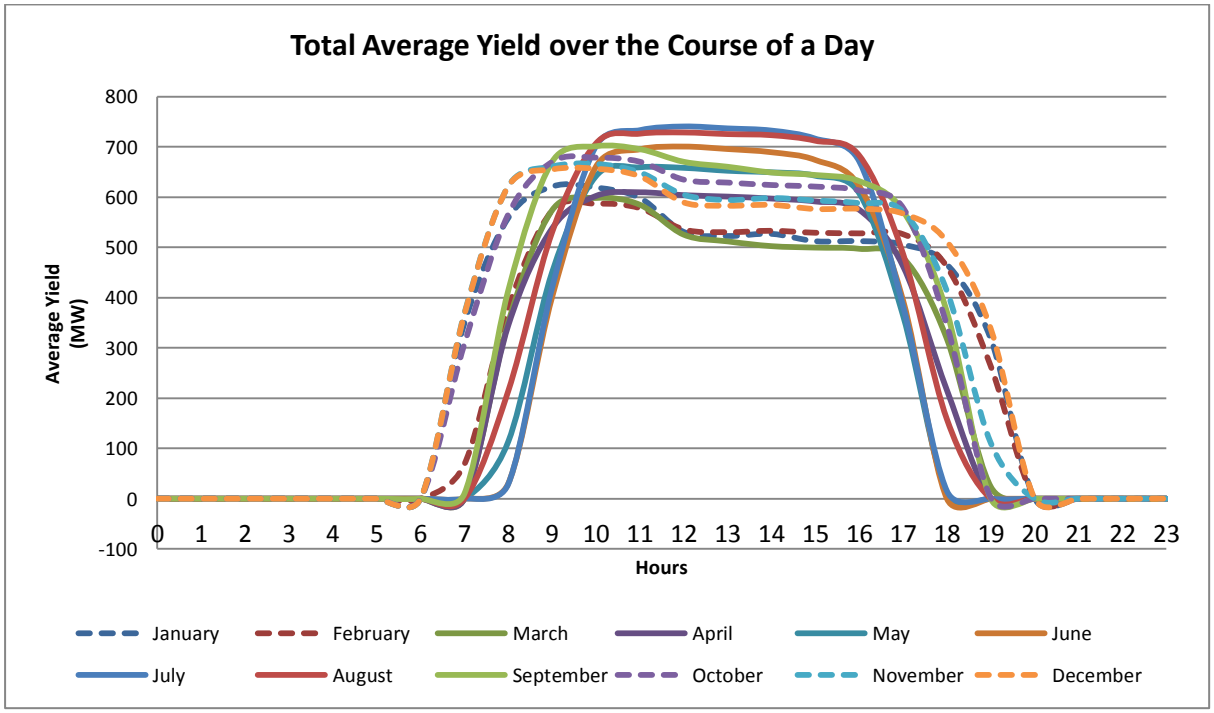

Figure 40: Average daily PV yield for base case

As predicted from behaviour of individual plants the following trends where found:

- Summer peak from 09h00 – 11h00
- Summer yield then reducing slightly at 12h00, but with high yields continuing until approximately between 17h00 and 18h00 before dropping off sharply
- Higher flatter yields during the winter months from 10h00 – 16h00

Furthermore, it was found that output from the PV plants in summer was over a significantly longer period of the day than the winter months. Output occurs from as early as 06h00 till 20h00 in summer. In contrast, in the middle of winter yield is only experience from 08h00 to 18h00. Even with this difference however, the base case shows on average a fairly stable and predictable output over the entire year. This is in agreement with Ummel's (2013) results shown in Figure 12. He found that

there were no significant seasonal differences in peak efficiency over the course of the day, with peak values occurring around 10h00, and summer efficiency remaining high into the evening.

The above trends are reflected in Figure 41 below, which describes the daily overall yield over a year.

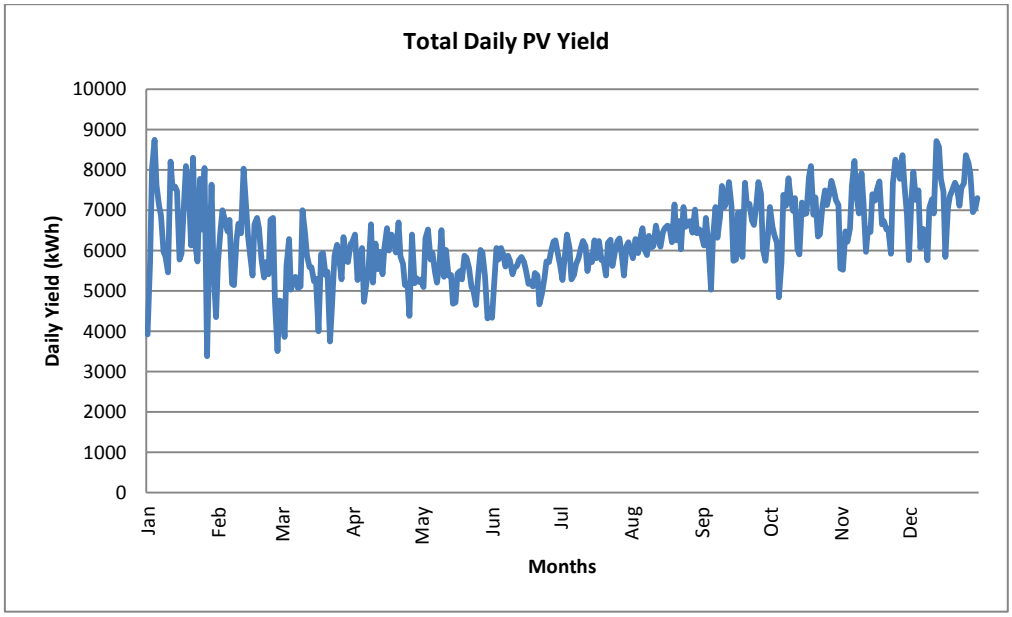

Figure 41: Daily PV yield over a year

Significant peaks in yield are experienced in January, February, March, November and December. However, the yield during this period is significantly more variable, with significant lows also experienced, particularly during the first three months of the year. Additionally the yields experienced during the winter months are still very respectable, with a condensed predictable output.

For the base case this allows us to draw the conclusion that favourable C_r values will be found over the whole year, particularly during the hours across midday. These hours will differ from winter to summer:

- Summer – approximately 09h00 – 14h00
- Winter – approximately 10h30 – 16h30

Of course, factors in the scenario analysis could significantly alter these expectations, especially when one considers Figure 42 below.

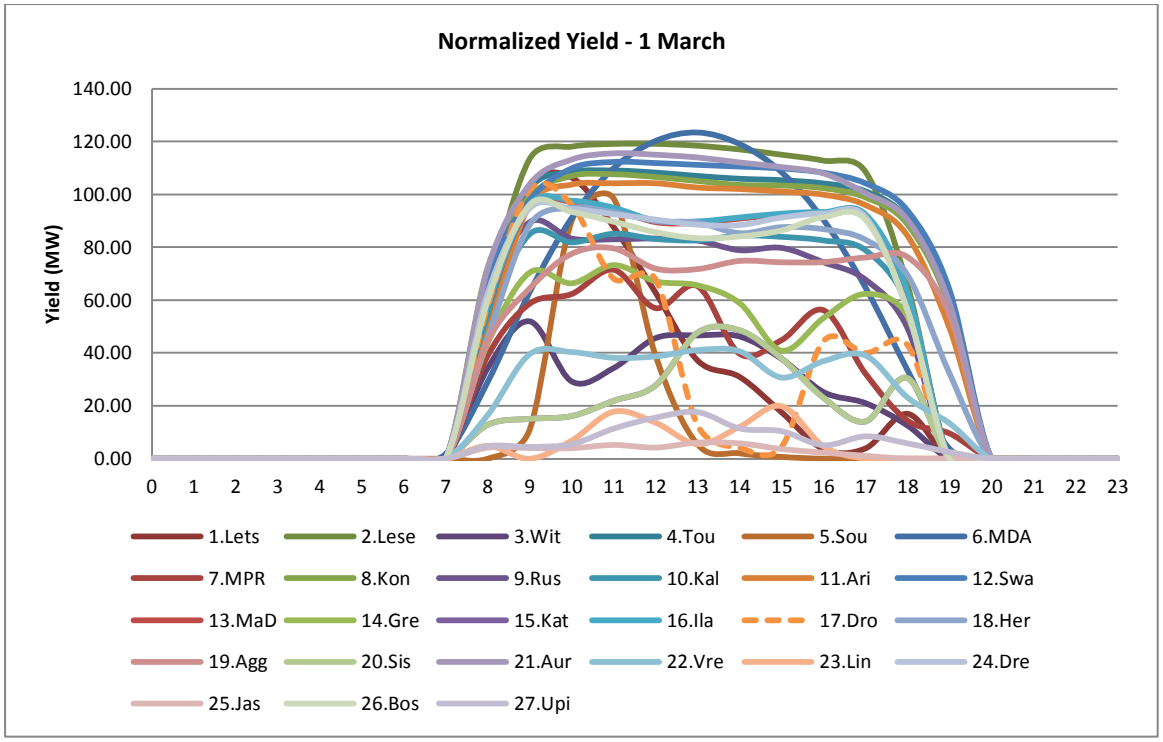

Figure 42: Normalized PV Yield for 1 March – Base case

Above is a representation of base case yield on 1 March, except that the installed capacities of all the plants have been altered so that they are all the same. This allows for a direct comparison of yield on a day to day basis. Above is a particularly volatile day, with plant outputs ranging from constant to highly variable. This highlights the effect of geographic dispersion on yield.

Say for example that all PV capacity in SA was installed at *Droogfontein* (Dashed). This would result in a greatly variable yield, in turn greatly reducing the reliability of PVG. This amongst other effects will be explored further in the scenario analyses below.

6.1.3. Conclusion

For the overall PV system the following was found:

- For the base case scenario, on average 2287.4 GWh/yr of energy will be produced from PV at an average performance ratio of 75%
- Average yearly yield was within a worst case scenario of 3.9% of results from industry standard simulation packages SAM and PVSyst

Looking at individual trends the following was found:

- A definite peak in supply in the months of low demand between 10h00 and 12h00 before tapering off into the afternoon
- High constant yields in the winter months, which apart from the Western Cape is generally higher than summer months

This then feeds into the overall yield trend:

- Summer peak from 09h00 – 11h00
- Summer yield then reducing slightly at 12h00, but with high yields continuing until approximately between 17h00 and 18h00 before dropping off sharply
- Higher flatter yields during the winter months from 10h00 – 16h00
- Considerably longer periods of yield in the summer, from 06h00 – 20h00
- Shorter periods of yield in the winter, from 08h00 – 18h00

6.2. C_r results – Base Case

The C_r of PV in SA was explored using the equivalent-load-carrying-capability (ELCC) metric. In order to do this the firm capacity, and hence the LCC ratio for the existing thermal system was initially calculated. This allowed for calculation of PV's C_r, by finding the change in firm capacity that results from adding PV capacity to the system, and comparing it to the change in firm capacity from the addition of an equivalent thermal unit.

Below are the main C_r results (see appendix D for more detailed results).

6.2.1. LCC of thermal system

The LCC of the thermal system was evaluated at a 98% level of reliability. Table 12 below describes the total installed capacity of the system, the resultant firm capacity at 98% confidence and the resultant LCC.

Table 12: LCC of Thermal system at 98% Reliability

LCC - Thermal	
Total Installed Capacity	43468 MW
Reliability Target	98%
Firm Capacity	37918MW
LCC %	87.2%
Inflation on demand	13%

Thus at a confidence level of 98% the firm capacity of the thermal system is 37 918MW. This means that out of the total capacity (43 468MW), 87.2% of it can be relied upon at 98% confidence level. The LCC of the system changes with a change in confidence level and can be used to generate a curve similar to that described by Garver (1966) (see Figure 20). This is done in Figure 43 below, and additionally shows the effect of the additional PV capacity for the base case at different confidence levels.

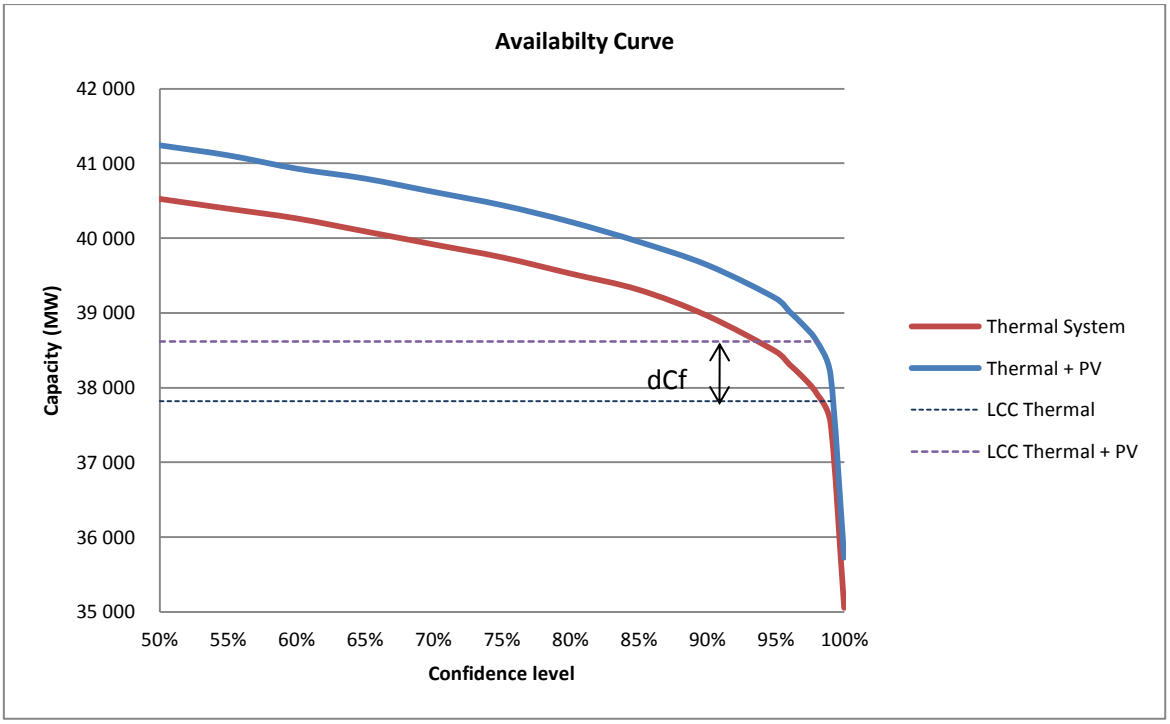

Figure 43: LCC of Thermal System at various reliability targets

Figure 43 above shows the cumulative probability curve of the firm capacity at different reliabilities for the original system (Red) and for a system including PV (Blue). The PV curve corresponds to an annual period at 12h00, and results in a capacity credit of 0.75.

6.2.2. PV C_r – Base Case

Based on the analysis of yield trends for PV, the LCC for PV was calculated for different 'subsets' i.e. for different parts of the day and year that PV yield could add value to the system.

For the base case the diurnal trend of C_r was evaluated for the following periods:

- Annual
- Summer, Autumn, Winter and Spring
- High Demand Period
- Low Demand Period

Below are the main results for the Base Case:

Table 13: Diurnal trend of Annual LCC and Capacity Credit - Base Case

Base Case				PV Cap	1054.6	MW
Annual Capacity Credit - Diurnal Trend						
Time	**LCC PV**	**LCC Sys**	**FC – Sys[1]**	**dCf[2]**	**Equivalent Thermal**	**Capacity Credit**
			MW	**MW**	**MW**	

Reliabilty level: 98%						
06h00	0.0%	85.3%	37945	27	26.4	0.025
08h00	0.4%	86.1%	38305	387	440.2	0.417
10h00	45.6%	86.8%	38626	708	809.2	0.767
10h00	37.5%	86.8%	38608	690	788.5	0.748
14h00	37.8%	86.7%	38572	654	747.1	0.708
16h00	34.6%	86.7%	38554	636	726.4	0.689
18h00	0.3%	85.9%	38239	321	364.3	0.345
20h00	0.0%	85.3%	37929	11	8.0	0.008

1 – FC: Firm Capacity

2 – dCf: Change in Firm Capacity

Table 14: Diurnal Trends of annual, high demand and low demand periods – Base Case

Base Case - Capacity Credits			
	Annual	**High Demand Period**	**Low Demand Period**
06h00	0.025	0.000	0.020
08h00	0.417	0.166	0.524
10h00	0.767	0.777	0.718
10h00	0.748	0.835	0.708
14h00	0.708	0.835	0.689
16h00	0.689	0.767	0.680
18h00	0.345	0.132	0.423
20h00	0.008	0.000	0.000

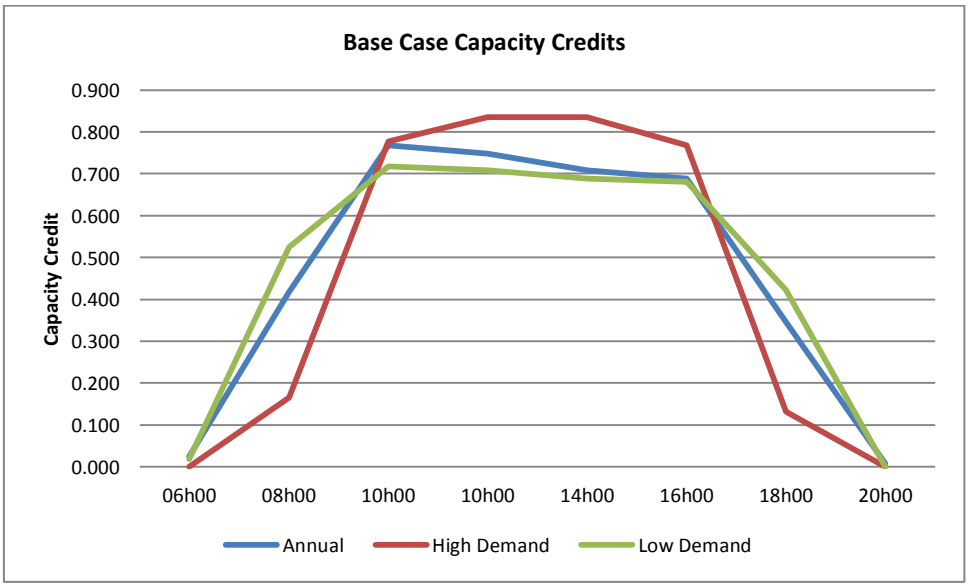

Figure 44: Diurnal trends of capacity credits for Annual, Low and High demand periods – Base Case

At the chosen reliability level of 98% we can see in Figure 44 that the annual C_r closely mimics the diurnal trend found from the yield analysis discussed above. A peak C_r of 0.77 is found at 10h00

before reducing slightly across the afternoon to 0.69 at 16h00 and then dropping off in the evening. The way that the C_r is calculated has the potential to produce some misleading results, particularly during the morning and evening periods. As discussed in 5.3.2, a cumulative distribution is used to calculate the likely yield that will be received at that time. While for wind this is satisfactory, because it relies on the probability of wind occurring, which could happen at any time. PV on the other hand relies on the position of the sun in the sky and this varies with season and time of day. Thus when considering a prolonged period such as a year, at 08h00 for example, there might be large percentage of reasonable yields in summer, autumn and spring but in winter will not be. Even so, the annual C_r at 08h00 is fairly high at 0.42, whereas during high demand it is 0.17. Thus the annual C_r at these times can misrepresent the likely PV generation. Therefore it is likely that C_r at higher intervals would yield more accurate results. It is however a fair representation of the C_r over the midday hours, hours that we are more concerned about in any case.

From a system operator's point of view the diurnal trend for the year is a good indication of what can be relied on over the middle of the day. They would however, be most likely to consider the period from 10h00 – 16h00 to be the peak generation hours for PV. Furthermore, they would also most likely err on the side of caution and take the lowest C_r during that time as the C_r for the day.

Following this logic we find the following C_r's for the midday period:

- Annual – 0.69
- High Demand – 0.77
- Low Demand – 0.68

Looking at Figure 44 above, we see that while the period of high demand has high midday C_r's in the range of 0.77 – 0.84, indicative of the large number of winter peaking plants discussed in 6.1.2 above, these high C_r's are in a narrow timeframe (10h00 – 16h00), when compared to that of the low demand period. Low demand still adds significant value to the system at 08h00 and 18h00.

This allows us to draw the following conclusions:

- The trends in C_r on a seasonal basis follow that of the seasonal yield patterns
- High capacity credits in the range of 0.69 to 0.84can be expected between 10h00 and 16h00 throughout the year
- During the low demand period the C_r values are still significant at 8h00 and 18h00 in the range of 0.42 to 0.53

Even so, the Low demand period covers approximately 75% of the year. Values from a period of this length are sure to include a change in season, thus producing some misleading results, particularly in the morning and the evening. Further insight is gained when looking at seasonal variation of C_r, as shown in Table 15 and Figure 45 below.

Table 15: Seasonal Variation in capacity credits – Base Case

Base Case - Seasonal Variation				
	Summer	**Autumn**	**Winter**	**Spring**
06h00	0.078	0.000	0.000	0.029
08h00	0.611	0.320	0.166	0.611

10h00	0.708	0.708	0.777	0.758
10h00	0.660	0.660	0.835	0.758
14h00	0.660	0.660	0.835	0.708
16h00	0.611	0.660	0.767	0.708
18h00	0.563	0.275	0.132	0.466
20h00	0.078	0.000	0.000	0.000

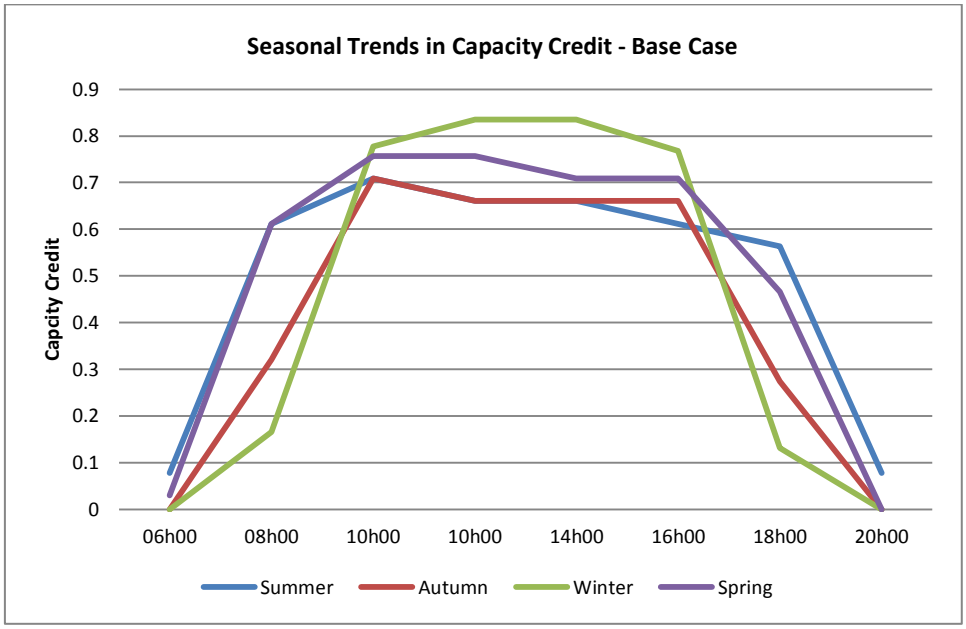

Figure 45: Seasonal Variation in capacity credits – Base Case

From the yield analysis we saw that there are minor changes from season to season (see Figure 40). These include extended hours of energy production toward the summer months, with significant peaks around 10h00. Additionally, in winter we saw higher yields during the middle of the day, but over a shorter period. As can be seen this has translated into the C_r results in Figure 45 above.

It is particularly interesting to compare the diurnal trend between C_r in winter and summer. It was found that between 08h00 and 18h00 in summer has a relatively low C_r between 0.61 and 0.56. This is much lower than winters C_r which is between 0.76 and 0.83. However, the latter is only approximately found between 10h00 and 16h00. Spring is a favourable combination of the two with C_r values around 0.76 during the middle of the day, while still maintaining reasonable amounts of capacity credit in the morning and evening. Autumn on the other hand, has a definite peak in C_r around 10h00 of 0.71, before stabilising between 12h00 and 16h00 at 0.66.

From this we can deduce that the reason for high winter C_r's is the large number of PV plants located in winter-favourable climates, and the condensed nature of yield over this period (shown in Figure 41). Furthermore, the high variation in yield over the summer months causes the C_r to be lower, but over an extended portion of the day. However, a certain granularity to the results, due to them being recorded every two hours, is a bit of shortfall when trying to delve deeper into changes in C_r over the course of a day. Furthermore this granularity is increased by the use of a cumulative distribution used to sample PV yields, which is made up of ten increments of 10% each. This causes a reduction in sensitivity that can be remedied through use of a bigger distribution.

Maximum demand for the year is experienced in July at approximately 19h00. A preliminary investigation showed that PV adds nothing to the generation capacity at this time, thus not adding any value. During the low demand months however, the morning peak between 09h00 and 12h00 is only marginally lower than the evening peak at 20h00. This morning peak in demand coincides with a peak in supply from the PV, thus in this context adding significant value to the system

6.2.3. Conclusion

For the base case C_r values have been explored for different subsets, from which points of interest have been discussed. From this we can draw the following conclusions:

- LCC of the thermal system is 87.2%
- Annual C_r trends follow trends found in the yield analysis discussed in 6.1.2
- C_r results considered over a long period can be misleading for the early morning and late evening
- From a system operator's point of view significant value is added to the system by PV between 10h00 and 16h00 throughout the year. Taking the worst case from this period can be considered the C_r for the day. These values were found to be:
    - Annual - 0.69
    - High Demand - 0.77
    - Low Demand - 0.68
- During the low demand period significant C_r value is still found around 08h00 and 18h00 in the range of 0.42 – 0.54
- Seasonal variations provide a greater insight into C_r during the year
- High instances of winter C_r's between 0.77 and 0.84 are found due to the high concentration of plants in good winter production areas. They are however, found over a short period of the day (10h00 - 16h00)
- Summer has the lowest C_r's at 0.56 – 0.61 but produce reasonable C_r's values from 08h00 - 18h00
- Spring is a favourable combination of both winter and summer with a C_r of 0.76 over midday, while still having prolonged periods of daily yield

6.3. Scenario analysis A: Effect of Geographic Dispersion on C_r

The effect of geographic dispersion on C_r has been evaluated for four scenarios:

- **Scenario A** – Base case; Total spread
- **Scenario B** – Only plants located in the Northern cape
- **Scenario C** – Total capacity concentrated in De Aar
- **Scenario D –** Total capacity concentrated in Soutpan

The following results were found for annual, low demand and high demand periods.

Table 16: Effect of geographic dispersion on annual capacity credits

Annual Capacity Credits				
Scenario	A	B	C	D
06h00	0.025	0.029	0.029	0.000
08h00	0.417	0.408	0.233	0.417
10h00	0.767	0.758	0.680	0.611
10h00	0.748	0.758	0.873	0.563
14h00	0.708	0.738	0.855	0.514
16h00	0.689	0.738	0.641	0.514
18h00	0.345	0.340	0.214	0.078
20h00	0.008	0.011	0.011	0.000

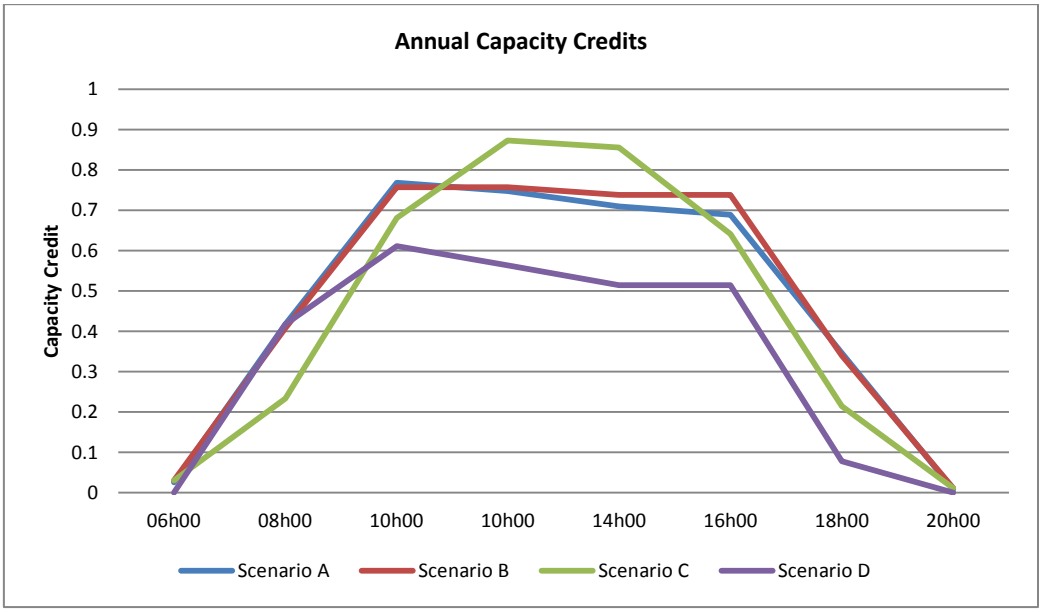

Figure 46: Effect of geographic dispersion on annual capacity credits

One of the main goals of this thesis is to show that C_r decreases as geographic dispersion decreases. At first glance of Figure 46, scenarios A through C seem to show the opposite to be true with the highest C_r's experienced in scenario C. However, upon closer inspection, we can see that this is not the case. Annually, scenarios A and B show very similar results of 10h00 peak between 0.7 and 0.8, remaining constant until 16h00. Furthermore reasonable C_r values of above 0.4 are experience at 08h00 and 18h00. The similarities between these two are to be expected, because the majority of the plants considered in scenario A are also considered in Scenario B (16 out of 27).

Contrastingly, when looking at scenario C (all PV focussed at De Aar), we see remarkably high values (peaking at 0.87) over the middle of the day. However when one looks between 08h00 and 10h00 one can see that the values for A and B are approximately 0.2 and 0.1 higher respectively. Similarly for 16h00 and 18h00, the inverse is true. Additionally, when considering the system operator logic

of before (Taking the lowest value over the midday period as the significant value for the day) we can draw the following C_r results over the midday period:

- A – 0.69
- B – 0.74
- C – 0.64
- D – 0.51

Even so scenario C has remarkably high results. As the C_r must follow the yield performance of the location, this points toward a number of reasons for this behaviour. Firstly this tells us that SA has a particularly conducive climate to PV generation and the site chosen has a particularly stable and high yield across the year. Secondly, that the C_r calculation method and the hourly time series data possibly failed to accurately capture the effect of cloud cover on a PV plant. These points were tested by introducing another singular location (Soutpan) in the form of Scenario D. In line with what was initially expected, scenario D has lower diurnal C_r's, with midday values in the range of 0.51 to 0.61. This is in line with the hypothesis that C_r decreases with a decrease in geographic dispersion. This becomes more apparent when considering high vs. low demand below.

Table 17: Effect of geographic dispersion on high demand capacity credits

High Demand Capacity Credits				
Scenario	**A**	**B**	**C**	**D**
06h00	0.000	0.000	0.000	0.000
08h00	0.166	0.146	0.151	0.611
10h00	0.777	0.805	0.660	0.902
10h00	0.835	0.829	0.902	0.902
14h00	0.835	0.839	0.879	0.902
16h00	0.767	0.781	0.621	0.805
18h00	0.132	0.136	0.102	0.000
20h00	0.000	0.000	0.000	0.000

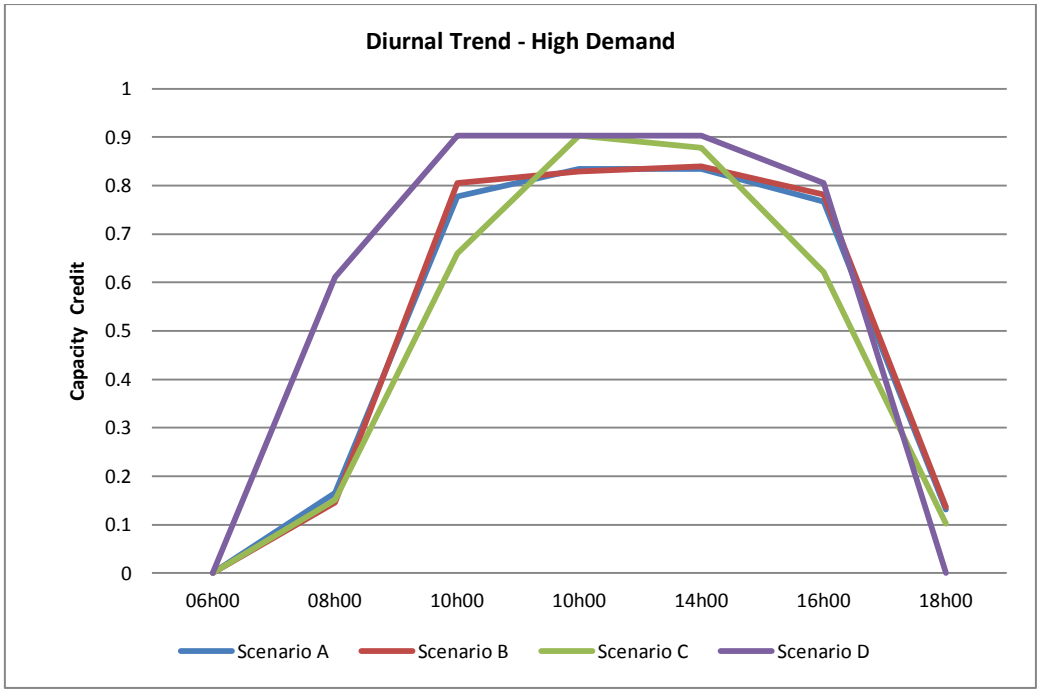

Figure 47: Effect of geographic dispersion on high demand capacity credits

High demand values show that now Scenario D has the highest C_r values at 0.90 over midday, whereas A and B are fairly consistent with the annual trend being only slightly higher at 0.77 to 0.84. Scenario C has a much narrower curve, peaking between 12h00 and 14h00 before tapering off sharply. Being located in the north east of SA, Scenario D still peaks at 10h00, but has a significant C_r at 08h00 of 0.61.

A different trend is found during the low demand period however, shown in Figure 48 below.

Table 18: Effect of geographic dispersion on low demand capacity credits

Low Demand Capacity Credits				
Scenario	**A**	**B**	**C**	**D**
06h00	0.020	0.029	0.039	0.000
08h00	0.524	0.505	0.272	0.762
10h00	0.718	0.767	0.708	0.514
10h00	0.708	0.738	0.708	0.466
14h00	0.689	0.708	0.855	0.417
16h00	0.680	0.694	0.631	0.417
18h00	0.423	0.423	0.233	0.126
20h00	0.000	0.000	0.000	0.000

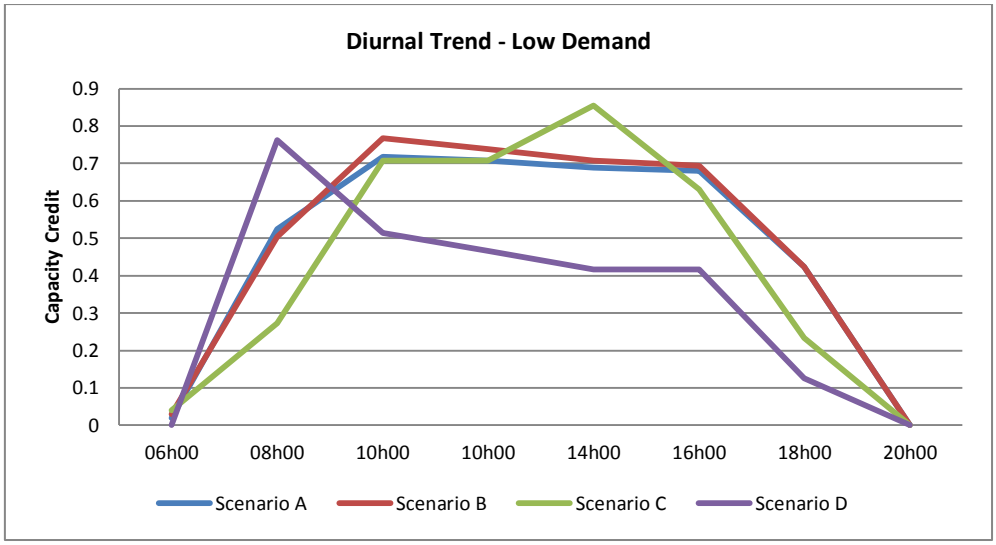

Figure 48: Effect of geographic dispersion on low demand capacity credits

Scenarios A and B again are consistent with values between 0.68 and 0.77 over midday. C and D on the other hand show drastically different results from high demand. D peaks at 08h00 at 0.77, before dropping off sharply over midday to the low value of 0.42 at 16h00. This extreme peak at 08h00 is surprising, but shows the difference in solar time between itself and the plants located west of its location and is reflective of the high variation in yields experienced in the afternoon of this period. Furthermore, it suggests that cloud builds up in distinct pattern during this period. Scenario C again has a narrower curve, only having significant C_r's between 10h00 and 16h00. This allows us to draw the following conclusion; while focussing all the PV in one area doesn't necessarily cause lower C_r over midday, the results become much more variable when compared to the more geographically dispersed scenarios from hour to hour and season to season. This is because the yield values are now dependant on a singular weather and season pattern. Thus while D might produce favourable results during high demand, the low demand results are much poorer. Conversely C produces favourable results in the low period. Therefore if the PV was split between these two locations the average C_r would go up, proving that sustained C_r over daylight hours increases with geographic dispersion.

6.3.1. Conclusion

One of the main goals of this thesis is to prove that C_r decreases with a decrease in geographic dispersion. From the above findings the following conclusions were drawn:

Annual:

- Whilst the highest C_r values were experienced from scenario C (0.87), they only occurred between 12h00 and 14h00. From a system operator's point of view the following C_r's were found for the annual period:
    - A – 0.69
    - B – 0.74
    - C – 0.64
    - D – 0.51

- Scenarios A and B have similar results throughout the day, which is to be expected as the majority of A is made up of B (16 out 27 plant locations)
- Annually Scenario D is in line with expectations

High demand vs. Low demand:

- Seasonal variation was found to be the greatest for scenarios C and D (scenarios of least geographic dispersion), whereas scenarios A and B remained fairly constant throughout the year
- Scenarios C and D complement each other across the seasons, thus if the total PV capacity was spread between the two their daily average C_r would increase

Therefore, we can say that as geographic dispersion decreases, the seasonal variability increases, and as a result the C_r decreases.

6.4. Scenario Analysis: Effect of Penetration Levels on C_r

It was hypothesised that the C_r of PV would decrease with level of penetration increase. The results of the simulation are shown below.

Table 19: Level of Penetration vs. capacity credit

Level of Penetration vs Capacity Credit						
% Pen	**PV Capacity**	**LCC System**	**FC[1] - System**	**dCf[2]**	**% of PV Cap**	**Capacity Credit**
	MW		MW	MW		
2.4%	1054.6	87.0%	38688	770	73%	0.83
4.6%	2000	86.2%	39165	1247	62%	0.72
9.2%	4000	85.1%	40367	2449	61%	0.68
13.8%	6000	83.9%	41476	3558	59%	0.67
18.4%	8000	82.7%	42536	4618	58%	0.66
23.0%	10000	81.4%	43496	5578	56%	0.65

1 – FC: Firm Capacity
2 – dCf: Change in Firm Capacity

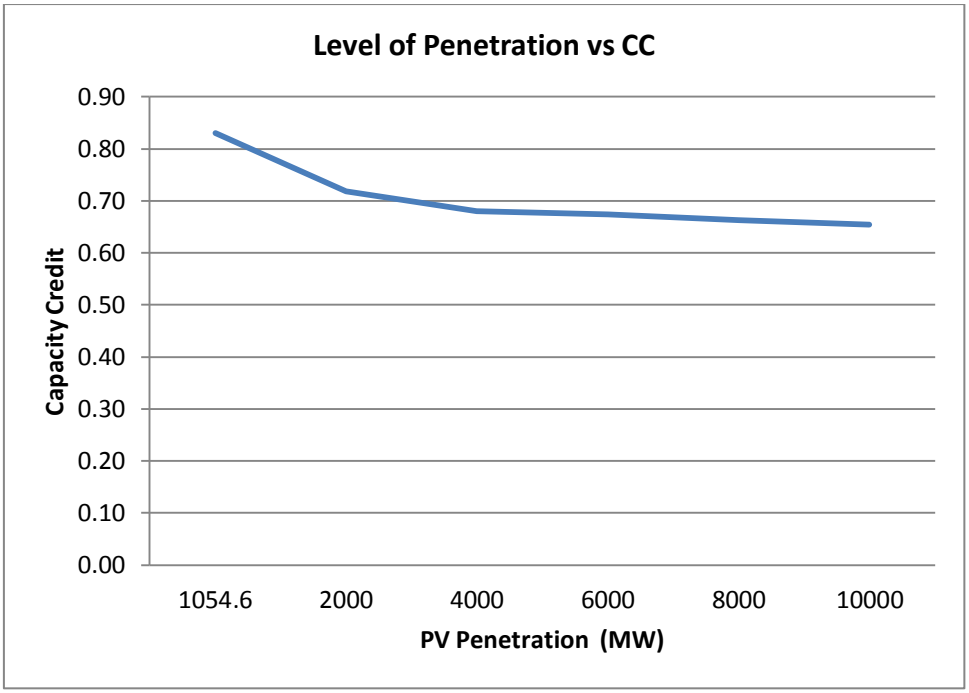

Figure 49: Level of penetration vs. capacity credit

Figure 49 above proves the hypothesis true on a yearly basis. Looking at Table 1, this makes sense, as the capacity of PV added to the system increases the relative change in firm capacity (dC_f) decreases. While PV is still at a low penetration level, the systems LCC and hence the firm capacity is still governed predominantly by thermal units, which have a low LOLP. As PV capacity is increased the system LCC becomes more dependent on the variable PV's LOLP decreasing accordingly. Thus the resultant dC_f becomes smaller, requiring a lower capacity of equivalent thermal unit to provide the same dC_f, and hence lowering the C_r.

Initially the C_r is high at 0.83, but drops of quickly to 0.72 and 0.68 for 4.6% and 9.2% penetration respectively. From there the curve flattens out, decreasing in a linear manner, with a 0.66 C_r at 23% penetration.

6.5. Dispatch model outputs

A dispatch model has been used to simulate real time operation of the South African power system. Monte Carlo simulation was used to generate annual values from average monthly values.

Figure 50 below shows a typical real time dispatch for each season (See Appendix E from greater detail).

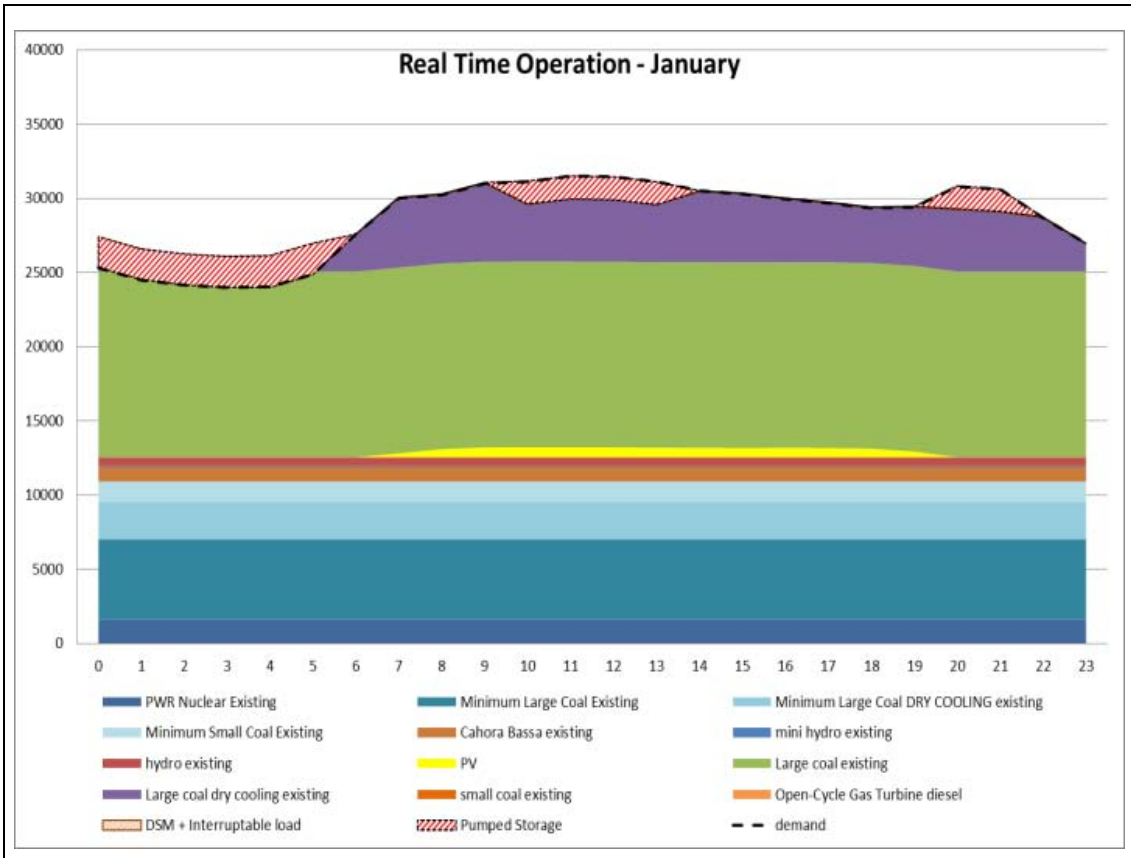
Real Time Operation - January
40000
35000
30000
25000
20000
15000
10000
5000
0
0 1 2 3 4 5 6 7 8 9 10 11 12 13 14 15 16 17 18 19 20 21 22 23
PWR Nuclear Existing
Minimum Large Coal Existing
Minimum Large Coal DRY COOLING existing
Minimum Small Coal Existing
Cahora Bassa existing
mini hydro existing
hydro existing
PV
Large coal existing
Large coal dry cooling existing
small coal existing
Open-Cycle Gas Turbine diesel
DSM + Interruptable load
Pumped Storage
demand

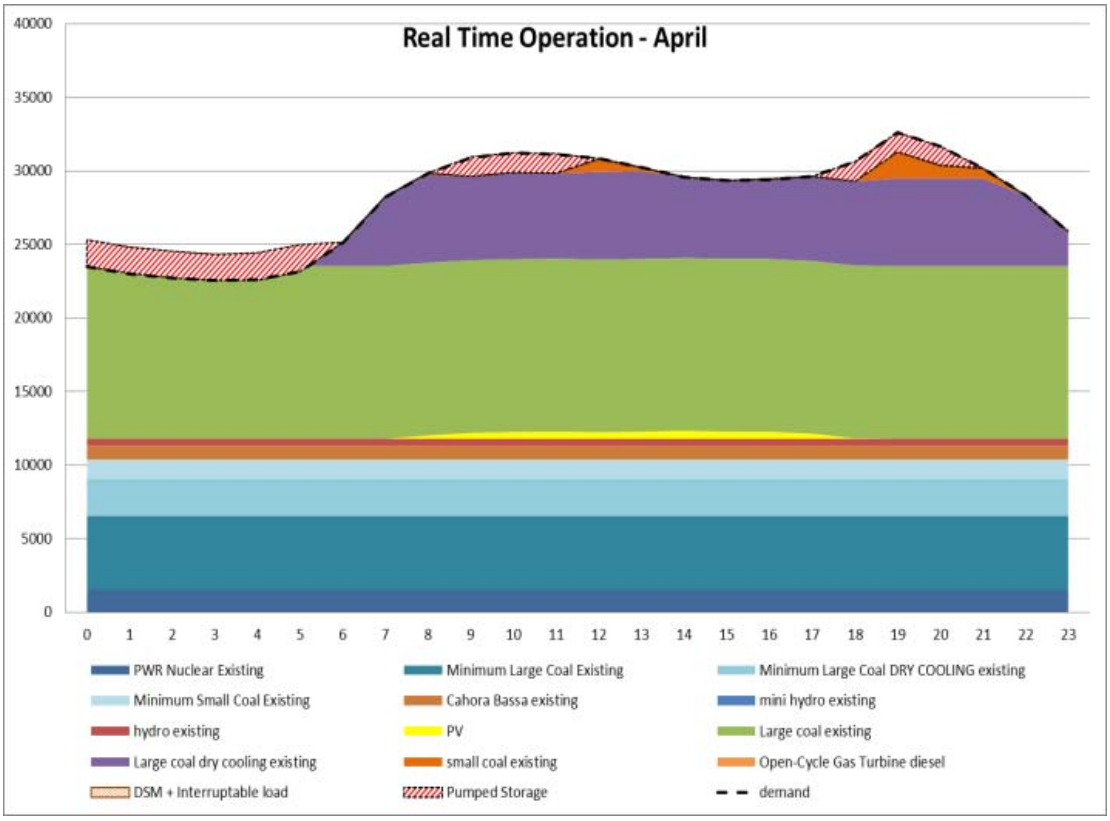
Real Time Operation - April
40000
35000
30000
25000
20000
15000
10000
5000
0
0 1 2 3 4 5 6 7 8 9 10 11 12 13 14 15 16 17 18 19 20 21 22 23
PWR Nuclear Existing
Minimum Large Coal Existing
Minimum Large Coal DRY COOLING existing
Minimum Small Coal Existing
Cahora Bassa existing
mini hydro existing
hydro existing
PV
Large coal existing
Large coal dry cooling existing
small coal existing
Open-Cycle Gas Turbine diesel
DSM + Interruptable load
Pumped Storage
demand

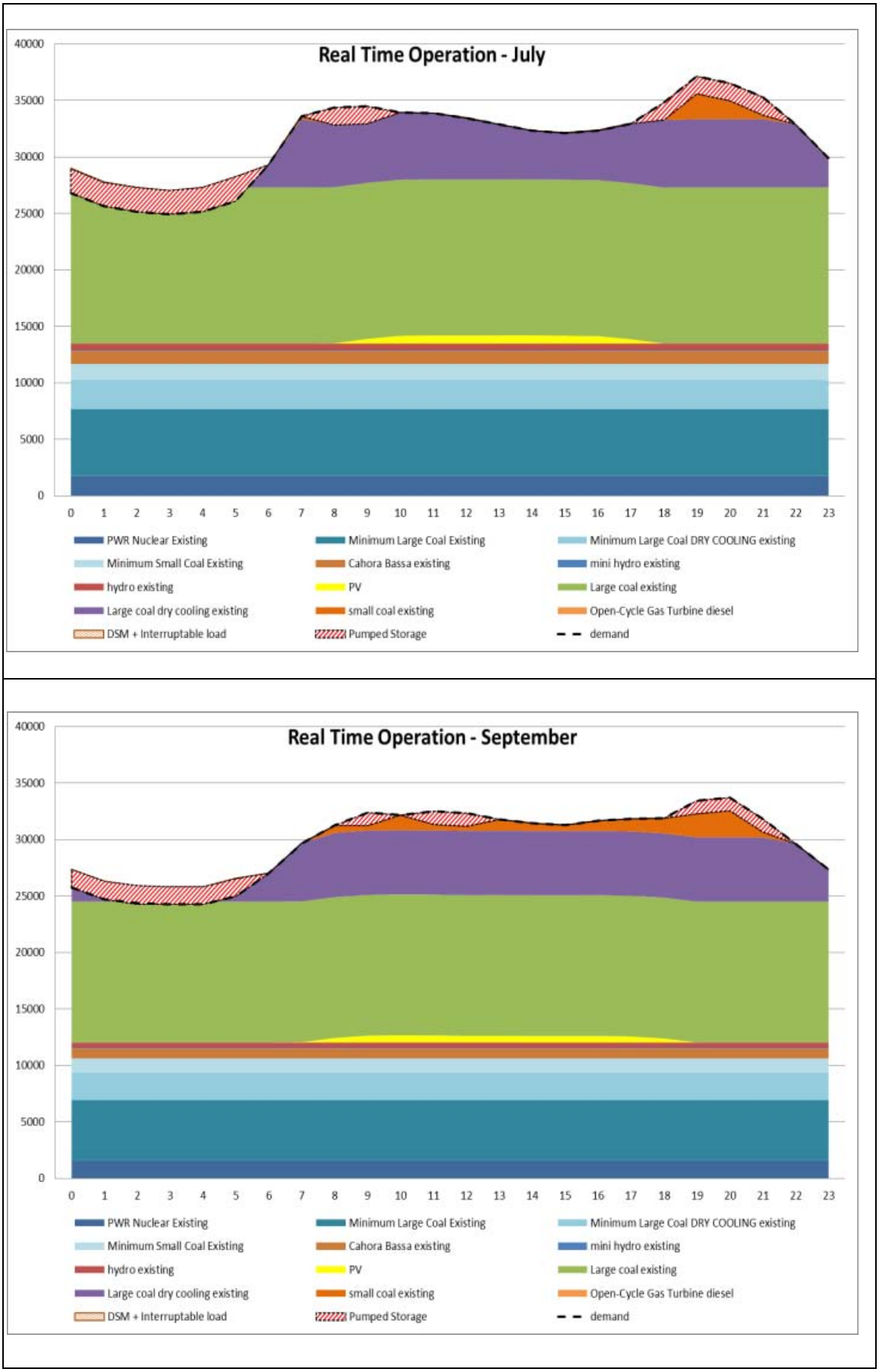

Figure 50: Typical Real time dispatch for summer, autumn, winter and spring (See Appendix E for more details)

The seasonal variation in supply and demand is clearly displayed above. A distinct peak can be seen in the winter month of July, with the additional demand being met by small coal and OCGT during the peak. Summer (January) conversely displays no distinct peak, with midday demand mimicking the supply from PV (in yellow). Spring and autumn are a mixture of winter and summer with both a midday and evening peak.

Annual values were calculated for 5 basic scenarios similar to those above with the aim of testing the effect of geographic dispersion on the Power system:

- No PV - Existing system with no PV
- Scenario A - Base Case: fully dispersed plants based on REIPPP round 1 & 2
- Scenario B – PV plants located only in the Northern Cape
- Scenario C – All capacity focussed in De Aar
- Scenario D – All capacity focussed in Soutpan

Additionally the consequence of employing various reliability levels was explored for the base case. Below are main results of these tests.

Table 20: Dispatch outputs for the Base Case with forecast load inflated at different reliability levels

Scenario	Test Parameter	TWh dispatched	EENS[1]	LOLE[2]	Energy value of fuel	Cost of Fuel	CO2	LOLP[3]
		TWh	GWh	Hours	PJ	Mill R	MTonnes	
Base Case	Load not inflated	254.978	1 018.38	1 056	2 355.9	40 296.212	225.917	12.0%
Base Case	Reliability 90%	256.528	9.07	25	2 370.7	35 849.395	228.133	0.29%
Base Case	Reliability 98%	256.269	9.65	25	2 366.7	35 720.602	227.755	0.29%

1 – EENS: Expected energy not served
2 – LOLE: Loss of load expected
3 – LOLP: Loss of load probability

Inflation of load was heavily debated during construction of the dispatch model. The more conservative the stipulated reliability level of the system is, the greater the forecast load is in the day-ahead model. This is because it is inflated by firm capacity (see chapter 6.2.1) which is directly related to reliability. Theoretically, through the inflation of demand this choice should affect day-ahead commitment of thermal units and as a result energy produced, fuel consumed and loss of load (LOL) occurrences. This in turn will affect CO_2 production and cost incurred.

The results for three variations on the base case are displayed above in Table 20. Cases of load not inflated, 90% reliability (Eskom's lower band currently), and 98% reliability were tested. It was found that:

1) As expected in all three cases dispatch similar amounts of energy
2) The first case (load not inflated) has used the least amount of fuel in energy terms, but has been the most expensive in doing so due to high gas consumption, costing approximately R4.5 Billion more than the other two cases.
3) Similar results are observed at 90% and 98% reliability except that, contrary to expectation 90% reliability uses more fuel and produces a greater amount of CO_2 for a similar amount of MWh dispatched

4) The first case (load not inflated) has the most amount of LOL occurrences resulting in a LOLP of 12%
5) The vast majority of outages were experienced in the last two months of the year, where interestingly the highest amount of maintenance was allocated (see appendix E for full tables).

While seemingly contradictory the 2nd finding above is easily understood. Less thermal capacity has been committed a day ahead of time due to a reduced net load. From this one would think that with less capacity being committed, less fuel would be have been used resulting in a lower cost. However, as a result of the reduced commitment more supply is struggling to meet load on an hourly basis once random forced outages have been taken into consideration. This effectively causes OCGT (normally a peaking plant) to try make up this gap in supply, and run throughout most of the day. Economically OCGT plants only make sense as peaking plants due to their high cost of fuel (almost 10 times the price of coal - see Table 9). This has resulted in a high cost and high rate of outages, as seen in result 4, without any significant changes in CO_2 production. This illustrates the benefits of employing day ahead forecasting and load inflation.

The cases at 90% and 98% reliability on the other hand have very similar results to each other. This was to be expected as the load is inflated by similar LCC values (89.18% and 87.2% respectively). Even so, one would expect that LOL occurrences would be slightly more in the system with a lower reliability level. However, both systems have LOLP of approximately 0.2%. 25 hours of outages is equal to 0.29% of a year and is thus the LOLP over this period. However, when describing the resultant reliability of the system it is cleaner to only compare it against the peak hours. Therefore if we make the assumption that there is an average of 1 - 3 peak hours every day over a year, we are left with a reliability of the system in the range of 93.2% to 97.7%, which agrees with our inferences made in chapter 5.3.1 of 90-98% reliability. This lack of difference in LOL, while a significant finding in itself, might suggest that in future iterations the MC simulation needs to be run until convergence occurs. A more likely explanation is that the changes in variability from the relatively low levels of penetration being tested above in conjunction with a conservative mean absolute error (MAE) used in the forecast is not great enough to have a marked difference on the reliability of the system.

It is also noted that at 90% reliability more fuel is consumed and more CO_2 is produced than at 98% reliability. This again is counterintuitive, but noting that while 0.1% more MWh of energy is dispatched at 90%, 0.17% more fuel and CO_2 is produced at 0.36% more cost. This suggests that instead of causing more outages, less committed capacity a day-ahead has result in more thermal plants running at lower efficiencies, or a greater amount of OCGT being employed.

Result 5 is interesting, in that there seems to be a direct correlation between maintenance and number of outages. In conjunction, the summer load profile (see real time dispatch for January Figure 50) has no distinct peak, resulting in multiple hours of peak load across the day. Thus if an outage occurs more hours of LOL will be experienced then compared to that of a day in July with a distinct peak hour for example. This result is not an empirical observation from raw data, but rather an output directly from the model and could be due to a problem with the unit outage scheduling algorithm. It seems more likely however that this result is a consequence of the approach in simulating outages as follows. If a unit outage occurs it is simulated as unavailable for the whole 24 hour period, thus for a period with a relatively flat profile (such as November and December) if a LOL occurs it will affect multiple hours of the day.

A chosen reliability of 98% was then used to test the different scenarios, the results of which are shown in Table 21 below:

Table 21 Dispatch model outputs for different scenarios

Scenario	Test Parameter	TWh dispatched	EENS[1]	LOLE[2]	Energy value of fuel	Cost of Fuel	CO2	LOLP[3]
		TWh	GWh	Hours	PJ	Mill R	MTonnes	
No PV	No PV	257.070	1.97	8	2 399.2	36 248.90	230.884	0.09%
Base Case	Full Spread	256.269	9.65	25	2 366.7	35 720.60	227.755	0.29%
Scenario B	Northern Cape	256.211	10.56	19	2 365.7	35 699.71	227.660	0.22%
Scenario C	De Aar	255.863	2.66	8	2 363.7	35 637.53	227.430	0.09%
Scenario D	Soutpan	256.456	3.45	11	2 371.9	35 798.03	228.258	0.13%

1 – EENS: Expected energy not served
2 – LOLE: Loss of load expected
3 – LOLP: Loss of load probability

Again, due to the same load profile very similar amounts of energy are dispatched. The lowest LOLP of 0.09% is found for the "No PV", or existing system and as can be expected it has the highest fuel consumption, cost of fuel and CO_2 produced. Significantly, a saving of R528.3 million on fuel costs and 3.13 million tonnes of CO_2 is achieved by introducing PV into system as described in the base case.

Surprisingly, LOL decreases with geographic dispersion with Scenario C (least dispersed) having the same amount of outages as the original system. Scenario D, the other least dispersed option, also shows low amounts of outages. Similar trends are seen in fuel use and CO_2 produced for the 4 scenarios. These differences are largely minimal, but suggest that the reliability of the system is increased by moving all PV to the De Aar area. This is correlated by the fact that the highest C_r values where achieved by Scenario C particularly during the high demand period (Figure 47) and during the late afternoon for the low demand period (Figure 48).

In the previous chapters it was noted that the C_r values strongly followed the patterns found in the yield analysis. As yield is directly related to capacity factor (CF – being actual yield over theoretical yield), we can expect that there will additionally be a relationship between C_r and CF of PV. Average capacity factors (CF) were calculated using the dispatch model for the base case scenario and compared against the relevant C_r. This was done for annual, low demand and high demand periods with the following results:

Annual C_r and CF	Low Demand C_r and CF	High Demand C_r and CF

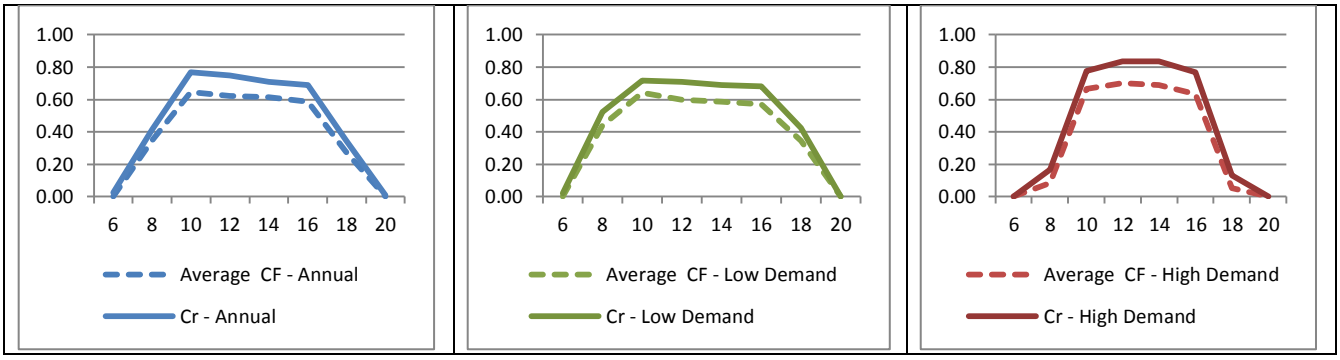

Figure 51: Correlation between Capacity Credits and average Capacity Factors

Looking at Figure 51 it was found that there is a direct relationship between C_r and CF of PV in all cases. As a result all C_r and CF values for annual, low and high demand periods were plotted against each other, shown in Figure 52 below.

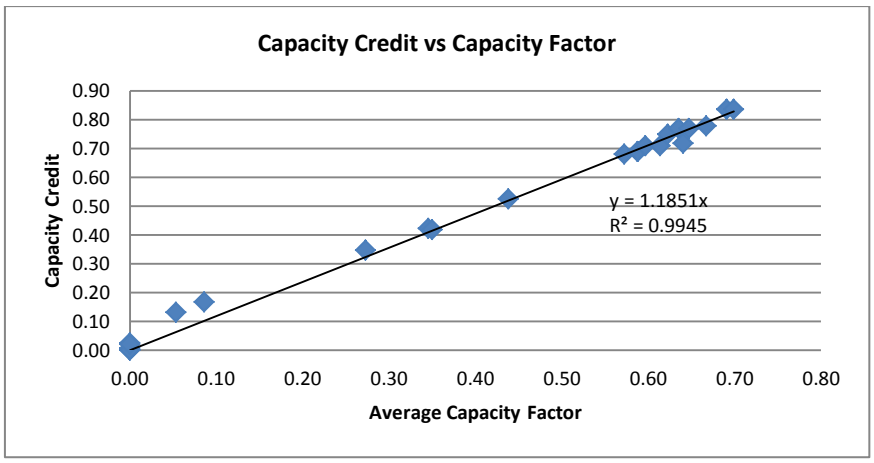

Figure 52: Capacity Credit vs. Average Capacity Factor of PV

The is a large grouping of high CF data points on the graph, due to the majority of measured points being over midday, but additionally there is enough lower CF points to make it statistically significant. This is confirmed by an R^2 value close to 1. Thus it was found that there was a direct relationship between CF and C_r particularly for CF's above 0.1. For this particular system the relationship was found to be:

$$Cr = 1.1851CF \qquad (37)$$

This is an important result in that it can be used to further estimate C_r values for this particular system using the dispatch model in a simple and easy manner.

6.5.1. Conclusion

Results from annual dispatch simulations have been discussed above. Below are the main findings.

Initially the base case was run at different reliability levels, causing a variation in day ahead commitment of thermal plants it was found that:

- While not inflating the load might result in the least amount of fuel being used, it also results in a large number of outages and high costs. This is due to OCGT plants running throughout the day trying to make up the deficit in supply.
- 90% reliability results in relatively higher CO_2 produced and greater amounts of fuel consumed suggesting the system runs less efficiently at 90% then 98% reliability.
- The majority of LOL occurrences were found to have occurred in November and December, coinciding with months of maximum allotted maintenance. This suggests a direct relationship between outages and maintenance, which is further exacerbated by multiple peak hours found particularly in these months.
- At both 90% and 98% imposed reliability levels, outages of 25 hours were experienced. Assuming that on average there are between 1 – 3 hours of outages per day, this suggests that the systems resultant reliability is between 93.2% and 97.7%.
- This lack of difference in LOL between 90% and 98% suggests that the variability experienced from the relatively low levels of penetration being tested above in conjunction with a conservative mean absolute error (MAE) used in the forecast is not great enough to have a marked difference on the reliability of the system.

The dispatch model was then run for four basic scenarios of geographic dispersion, and it was found that:

- The lowest LOLE was understandably found for the existing system without PV at 8 hours/year, but surprisingly this value was matched by scenario C (all PV capacity in De Aar)
- Savings of R4.45 billion/year (1.5%) and 2.22 million tonnes of CO_2 produced/year (1.4%) were realised by introducing PV to the system.
- LOL decreases with geographic dispersion suggesting that having all PV in the Northern Cape is not detrimental to the variability of supply. This however, could be related to high performances of the geographically focussed scenarios between critical LOL hours (particularly in November and December) causing less outages to occur.

Average CF was then compared to C_r and it was found that:

- There is a direct relationship between C_r and average CF of PV which can easily be used to quickly estimate C_r values from the dispatch model. For this system this relationship can be shown through

$$Cr = 1.1851CF \qquad (38)$$

7. CONCLUSIONS AND RECOMMENDATIONS

The utilisation of energy from renewable sources such as solar PV for generating electric power is being given serious consideration around the world. This is due to global concerns of climate change, pollution, greenhouse gasses, increases in conventional fuel costs and potential energy shortages arising from rising demand.

Many consider solar PV to be a promising alternative source of energy due to its apparent environmental, social and economic benefits. This together with government incentives and IPP programmes such as REIPPPP has allowed for investment in PV in South Africa (SA).

Solar irradiation is a variable energy source and thus serious consideration needs to be given to the effect that PV might have on the reliability of the system. As a result traditional methods of evaluating power system reliability cannot be used when utility-scale PV is introduced to the system. Thus probabilistic methods are employed to evaluate reliability.

In this thesis time series data was used to simulate the yield from 27 PV plants, as defined by the preferred bidders in round 1 and round 2 of the REIPPP process, through a yield model developed for this investigation. The resultant yield data was then input into a dispatch model including conventional generators. Loss-of-load-probability (LOLP) and Monte Carlo Simulation (MCS) were used to assess the capacity credit (C_r), or value that PV adds to the system. The C_r was evaluated using effective load carrying capability (ELCC) method, which describes how much the additional PV capacity contributes to the firm capacity of the system when compared to an equivalent thermal unit.

A dispatch model was then created to evaluate the effect that introducing PV has on other aspects of the SA power system, such as:

- GJ of fuel used and CO_2 produced by the system with and without PV
- Loss-of-load expectancy (LOLE) and expected energy not supplied (EENS) reliability indices
- Associated costs

Along with the C_r these were evaluated for a number of scenarios with several main goals in mind. These were to show that: PV can add to the firm capacity system; the C_r can be effectively described using the ELCC metric; and that the C_r and hence the reliability of the system is negatively affected by a decrease in geographic dispersion and an increase in PV penetration level.

7.1. Summary of findings

The results can be split up into three parts:

1. PV yield
2. C_r evaluation
3. Dispatch model outputs

Individual yields from each PV plant were evaluated, and it was found that:

- For the base case scenario, on average 2287.4 GWh/yr of energy will be produced from PV at an average performance ratio of 75%
- Yields in summer peak from 09h00 – 11h00, and cover a large portion of the day, while higher flatter yields are experienced in winter between 10h00 and 16h00

The results of the yield analysis then allowed for evaluation of the C_r, with the main result displayed in Figure 53 below.

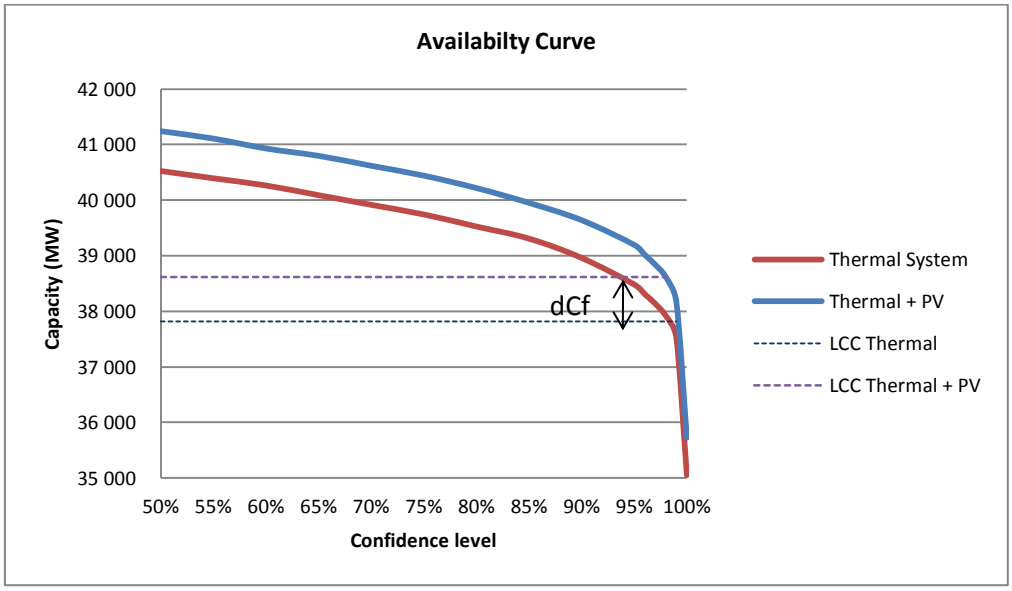

Figure 53: LCC of Thermal System at various reliability targets

Shown above is a cumulative probability curve of the firm capacity at different reliabilities for the original system (Red) and for a system including PV (Blue). The PV curve corresponds to an annual period at 12h00, and has a resultant capacity credit of 0.75.

Other main findings include

- The LCC of the existing predominantly thermal system at a 98% reliability is 87.2% and has a firm capacity of 37 918 MW
- From a system operator's point of view, significant value is added to the system by PV between 10h00 and 16h00 throughout the year. Taking the worst case from this period can be considered the C_r for the day. These values were found to be:
    - Annual - 0.69
    - High Demand - 0.77
    - Low Demand - 0.68

The effect of geographic dispersion on C_r values was then tested, with Figure 54 showing the annual diurnal trend for 4 different scenarios.

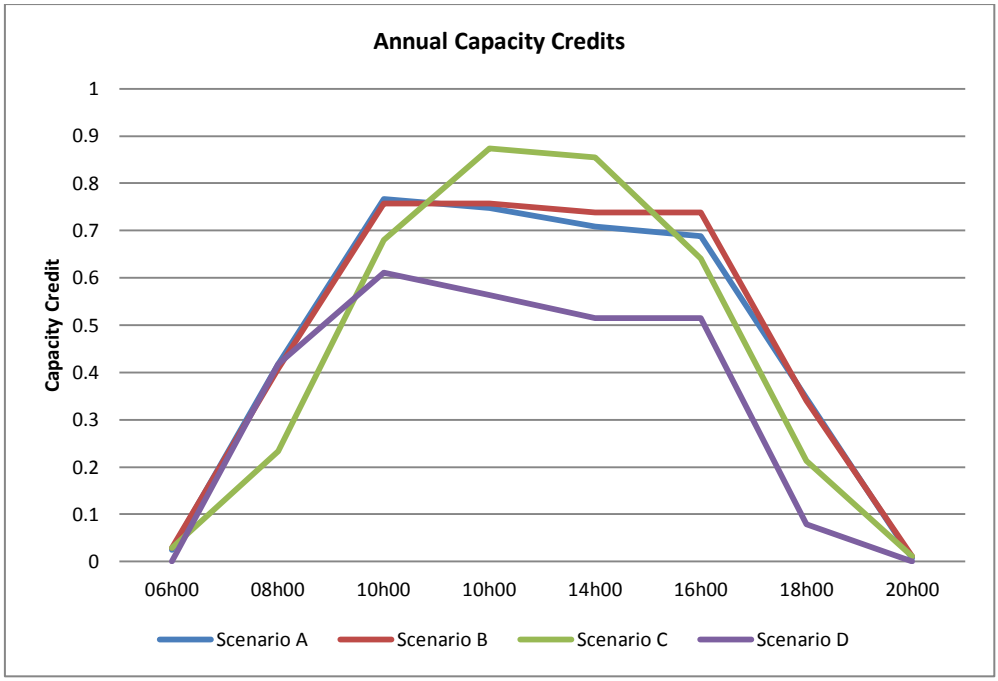

Figure 54: Effect of geographic dispersion on annual capacity credits

- Whilst the highest C_r values were experienced from scenario C (0.87), they only occurred between 12h00 and 14h00. From a system operator's point of view the following C_r's were found:
    - A – 0.69
    - B – 0.74
    - C – 0.64
    - D – 0.51

Therefore, we can say that as geographic dispersion decreases, the seasonal variability increases, and as a result the C_r decreases.

The effect of penetration level on C_r values was then evaluated for an annual period for 12h00. Initially a high C_r of 0.83 is found, but this drops of quickly to 0.72 and 0.68 as penetration levels increase to 4.6% and 9.2%. The rate of decrease in C_r then reduces until a value 0.66 C_r is found at 23% penetration

Optimal dispatch of SA's power system including PV was then simulated and it was found that:

- At both 90% and 98% imposed reliability levels, LOLE equalled 25 hours/year. Assuming that on average there are between 1 – 3 hours of outages per day, this suggests that the systems resultant reliability is between 93.2% and 97.7%.
- Savings of R4.45 billion/year (1.5%) and 2.22 million tonnes of CO_2 produced/year (1.4%) were realised by introducing PV to the system.
- LOL decreases with geographic dispersion suggesting that having all PV in the Northern Cape is not detrimental to the variability of supply.

Average CF was then compared to C_r and it was found that:

- There is a direct relationship between C_r and average CF of PV which can easily be used to quickly estimate C_r values from the dispatch model. For this system this relationship can be shown through

$$Cr = 1.1851CF \qquad (39)$$

7.2. Conclusion

The results show that the yield of the plants considered was accurately simulated with annual values within 2.9% and 3.9% of yearly simulations carried out in industry recognised packages, PVSyst and SAM respectively. It was found that along with consistently high yearly yields during the day throughout the year, the yields followed particular seasonal trends with the highest yields experienced in winter, reflecting that the majority of plants are located within the Northern Cape, which has a winter conducive to PV generation. The total system PV generation would not therefore be particularly reduced by moving all PV capacity to the Northern Cape. However, the current spread of plants complement each other both in terms of seasonal generation and diurnal generation trends. Furthermore, from the results we can postulate that if this spread were to be increased higher yields would be experienced over an increased length of the day, which is currently contained to between 10h00 and 16h00 with a definite peak in yield over 10h00.

Probability and cumulative distributions were derived from the yield results and used to calculate the ELCC metric which was used as a proxy for Cr. Over long periods, however, this method might be misleading for extreme results, such as early morning or late evening, due to an averaging effect of the probability distributions. This drawback is unique to solar applications, in that the yield follows seasonal trends, and, unlike wind, there is not always a chance that the sun might be shining. This drawback can be effectively mitigated through evaluation of shorter periods, and in our case is not really a concern because we focussed more on values over midday.

High C_r values were experienced in winter of between 0.77 and 0.84 due to the high concentration of plants in good winter production areas. They are, however, found over a short period of the day (10h00 - 16h00). During the low demand period significant C_r value is still found around 08h00 and 18h00 in the range of 0.42 – 0.54. From this we can conclude that year round high C_r values are experienced between 10h00 and 16h00, but that significant value can still be seen on either side of this for large portions of the year.

At first glance, C_r values are not reduced by a decrease in geographic dispersion, and it seems that part of the hypothesis of this work has been proven false. However, while scenario C has the highest daily C_r's, they are over the relatively short period of 12h00 to 14h00. When we look at the critical hours of 10h00 and 16h00 the results show that the C_r's are lower than that of the two more dispersed scenarios. Thus, when applying the system operators logic, and taking the lowest C_r value over 10h00 to 16h00 as the C_r for the period, we can draw the conclusion C_r does indeed decrease with a decrease in geographic dispersion.

Furthermore the effect of geographic dispersion was further tested by moving total PV capacity to a more variable site in the Limpopo province and the results show that this scenario behaved more predictably with lower annual C_r's over the day. Additionally, upon delving deeper, it was found that seasonal variation was the greatest for scenarios C and D, whereas scenarios A and B remained fairly constant throughout the year. In fact, scenarios C and D complement each other across the seasons, thus if the total PV capacity was spread between the two, we can postulate that their daily average C_r would increase. This allows us to draw the conclusion that the seasonal variability decreases with an increase in geographic dispersion, and hence C_r values would increase with increased geographic dispersion.

Similarly, a simple analysis of C_r at 12h00 for the year was evaluated for different levels of penetration. Predictably, the results show that indeed, the C_r does decrease with an increase level of penetration. This makes sense, because while PV is still at a low penetration level, the systems LCC and hence the firm capacity is still governed predominantly by thermal units, which have a low LOLP. As PV capacity is increased the system LCC becomes more dependent on the variable PV's LOLP decreasing accordingly. Thus the resultant change in firm capacity becomes smaller, requiring a lower capacity of equivalent thermal unit to provide the same dC_f, hence lowering the C_r. Thus along with the conclusion above, we can say that the hypothesis of this dissertation has been proven to be true, even if some surprising results were encountered along the way.

In the simulation of the dispatch model, surprising results were once again encountered. The lowest LOLE was understandably found for the existing system without PV at 8 hours/year, but surprisingly this value was matched by scenario C (all PV capacity in De Aar). Furthermore, the majority of outages simulated in the model were found to have occurred in November and December (months of low demand), coinciding with months of maximum allotted maintenance. This suggested a direct relationship between outages and maintenance, which is further exacerbated by multiple peak hours found particularly in these months and the nature of outage simulation in the model. This allows us to draw the conclusion that it is possible that the low outages experienced by scenario C could be related to high yield performances during critical LOL hours, particularly in November and December. Furthermore, this highlights one of the drawbacks in using MCS and LOLP in this type of analysis, in that it assumes that level of load and outages are not related, where in reality they are. If this relationship were to be taken into consideration, more outages would be experienced in periods of high demand, such as mid-winter.

From all of the above we can conclude that the current mix of PV plants in the SA power system will provide good all year round yields, particularly adding value to the system between 10h00 and 16h00. These values will not be particularly hampered if all plants were to be moved to the Northern Cape, where high constant yields are experienced year round, with particularly high values generated during the winter period. If, however, the combine PV capacity is moved to a more singular location; seasonal variability becomes more of a consideration, even if surprisingly high C_r's are seen for two hours over midday. Thus the study confirms that indeed, C_r does decrease with an increase in penetration and a decrease in geographic dispersion. Furthermore, the results of the dispatch model show, that there is significant value attached to including PV in a power system. With savings of R4.45 billion/year and 2.22 million tonnes of CO_2 produced/year it is easy to conclude that this is the case.

This study has provided an estimate of the C_r of solar PV, which can now be used as an exogenous input into further research, optimisation models and arguments for the benefits of electricity generated from solar power. Furthermore, it has provided an algorithm that can be used to estimate the C_r from measured PV capacity factors for the South African power system. Additionally, it has introduced into the public domain a simple working dispatch model that will hopefully influence and stimulate future research in renewables and the South African power system.

The concepts presented and examples illustrated in this thesis have the potential to help system planners and utility managers to assess the reliability and value that PV can add to the system for different spatiotemporal scenarios and provide useful input into the decision making process.

7.3. Future work

The purpose of academic work is to not only add to the body of knowledge of the area researched, but to additionally spark interest and debate around the topic, thereby aiding further research.

In this dissertation a model has been built that has produced useful results, but perhaps more importantly, can be used and adapted for further research. Below are suggestions that will add to the research completed in this work, and enhance further research in this area.

- In this work historical times series data has been used to model demand without taking uncertainty into consideration. In reality demand can be forecasted reasonably accurately in the short term, but is still subject to uncertainty particularly as the range of forecast is extended. Thus it is suggested that future work incorporate a probability distribution of demand, therefore increasing the stochastic nature of the analysis.
- The dispatch model built was developed in Microsoft Excel, which limited the Monte Carlo simulation to 100 runs (not enough for convergence). It is suggested that this model be transferred into a programme such as Matlab to avoid these computing constraints and allow for convergence to occur. This will open further analysis opportunities, such as considering multiple years of data and reducing the granularity of the simulation.
- It is suggested that extreme events be imposed on the model to test how the system reacts.
- Simulation of solar PV variations, such as tracking arrays and optimal tilt angles should become features of the model.
- The effect of geographic dispersion on the reliability of the system at higher penetration levels should be tested.

The integration of these proposed improvements to future models could greatly enhance our knowledge of the impact of utility scale PV in SA and inform the future long term energy planning process.

Bibliography:

Amelin, M., 2009. Comparison of Capacity Credit Evaluation Methods for Conventional Power Plants and Wind Power. *IEEE Transactions on Power Systems,* 24(1), pp. 685-691.

Bagen, 2005. *Reliability and Cost/Worth Evaluation of Generating Systems Utilizing Wind and Solar Energy,* Saskatoon: University of Saskatchewan.

Baker, E., Fowlie, M., Lemoine, D. & Reynolds, S., 2013. *The Economics of Solar Electricity,* s.l.: Annual Review of Resource Economics 5.

Bekker, B., 2007. Irradiation and PV array energy output, cost, and optimal positioning estimation for South Africa. *Journal of Energy in Southern Africa,* 18(2), pp. 15 - 25.

Billinton, R. & Allan, R., 1996. *Reliability evaluation of power systems.* 2nd ed. New York: Plenum Press.

Billinton, R. & Bollinger, K. E., 1968. Transmission system Reliability Evaluation Using Markov Processes,. *IEEE Trans. Power Apparatus Syst.,* PAS-87(2), pp. 538-547.

Brosz, C., Maddox, R. & Forwood, G., 2012. *ARUP's Internal White Paper on Solar Energy,* London: ARUP.

CEP, 2013. *SoDa: Overview of the SoDa service.* [Online]
Available at: http://www.soda-is.com/eng/about/
[Accessed 19 November 2013].

Conti, S. & Raiti, S., 2007. Probabilistic load flow using Monte Carlo techniques for distribution networks with photovoltaic generators. *Solar Energy,* Volume 81, pp. 1473-1481.

Denholm, P. & Hummon, M., 2012. *Simulating the value of concentrating solar power with thermal energy storage in a production cost model,* Denver: NREL.

DGS, 2009. *Planning and Installing Photovoltaic Systems.* Second ed. Berlin: Earthscan.

DOE, 2011. *Intergrated Resource Plan for Electricity 2010 to 2030 - Revision 2 - Final Report.* Pretoria: Government Gazette.

DOE, 2012. *Announcement of Preferred Bidders of the IPP Procurement Programme.* [Online]
Available at: http://www.ipprenewables.co.za/#page/1209
[Accessed 25 April 2013].

DoE, 2012. *Request for qualification and proposals for new generation capacity under the IPP procurement programme: Part B - Qualifiation criteria,* Pretoria: SA department of Energy.

Dragoon , K. & Shumaker, A., 2010. *Solar Variability and Grid intergration,* s.l.: Sandia: Renewable North West Project.

Edkins, M., Marquad, A. & Winkler, H., 2010. *South Africa's renewable energy policy roadmaps ,* Cape Town: Energy Research Centre.

EPRI, 2010. *Addressing Solar Photovoltaic Operations and Maintenance Challenges,* Palo Alto: Electric Power Research Institute.

ERC, 2010. *Sustainable National Accessible Power Planning Model v3.0 2010-2040 beta 10.* Cape Town: Energy Research Centre (UCT).

Eskom, 2006. *Integrated Strategic Energy plan 10,* Pretoria: Eskom.

Eskom, 2010. *Load data used for analysis supporting the MYPD2 application,* Pretoria: Eskom.

Eskom, 2012. *The strategic 2040 transmission network study: Presentation to GPTRC.* s.l.:s.n.

Eskom, 2013. *Tariffs and Charge Booklet 2013/14.* [Online]
Available at: www.eskom.co.za/tariffs
[Accessed 29 11 2013].

Eskom, 2014. *Eskom: South African Power Utility - Supply Status.* [Online]
Available at: http://www.eskom.co.za/Whatweredoing/SupplyStatus/Pages/Supply_Status2.aspx
[Accessed 12 1 2014].

Feldman, D. et al., 2012. *Photovoltaic Pricing Trends: HIstorical, Recent and Near Term Projections,* Denver: NREL.

Garver, L., 1966. Effective Load Carrying Capabilty of Generating Units. *IEEE Transactions on Power Apparatus and Systems ,* 85(8), pp. 8-18.

Gaver, D., Montmeat, F. & Patton, A., 1964. Power system reliability I: Measures of reliability and methods of calculation. *IEEE Trans. Power Apparatus Syst,* July, Volume 83, pp. 727-737.

GIZ, 2011. *Capacity Credit of Wind Generation in South Africa,* Pretoria: Deutsche Gesellschaft für Internationale.

Gowrisankaran, G., Reynolds, S. & Samano, M., 2013. *Intermittency and the value of renewable energy,* s.l.: National Bureau of Economic Research.

Hart, E. K. & Jacobson, M. Z., 2010. *Supplementary information to: A Monte Carlo Approach to Generator Portfolio Planning and Carbon Emissions Assessments of Systems with Large Penetrations of Variable Renewables: Supplemental Information,* Stanford: Stanford university.

Hart, E. K. & Jacobson, M. Z., 2011. A Monte Carlo approach to generator portfolio planning and carbon emissions assessments of systems with large penetrations of variable renewables. *Renewable Energy,* Volume 36, pp. 2278-2286.

Helioclim, 2009. *Helioclim: Providing information on Solar Radiation.* [Online]
Available at: http://www.helioclim.org/
[Accessed 19 November 2013].

Holttinen, H. et al., 2006. *Design and operation of power systems with large amounts of wind power, first results of IEA collaboration..* Adelaide, Austrailia, Global Wind Power Conference.

Huber , N., 2011. *Intergrating Renewables into the Grid: An Energy Dispatch Model,* Cambrige: University of Cambridge.

IEA, 2010. *Power Generation from coal: Measuring and reporting Efficiency performance and CO2 emissions,* Paris: Coal Industry Advisory Board.

Jones, A. D. & Underwood, C. P., 2000. *A Thermal Model for Photovoltaic Systems,* Newcaslte upon Tyne: Unversity of Northumbria.

JRC, 2012. *Photovoltaic Geographical Information System (PVGIS) - Database help,* Ispra, Italy: Institute for Energy and Transport - European Commission.

Karlsson, M., Palm, J. & Widen, J., 2009. *Interdisciplinary Energy System Methodology,* s.l.: Arbetsnotat.

King, D. L., Boyson, W. E. & Kratochvill, J. A., 2004. *Photovoltaic Array Performance Model,* Albuquerque, New Mexico: Sandia National Laboratories.

Kou, Q., Klein, S. & Beckman, W. A., 1998. *A Method For Estimating the Long Term Performance of Direct-Coupled PV Pumping Systems,* Wisconsin: University of Wisconsin Solar Energy Laboratory .

Lacey, M., 1998. *Statistical Topics for Yale stats 101.* [Online]
Available at: http://www.stat.yale.edu/Courses/1997-98/101/binom.htm
[Accessed 03 12 2013].

Lamont, A., 2008. Assessing the long-term system value of intermittent electric generation technologies. *Energy Economics,* Issue 30, pp. 1208-1231.

Lew, D. & Milligan, M., 2011. *The Value of Wind power forecasting,* Washington, DC: NREL.

Luque, A. & Hegedus, S., 2011. *Handbook of Photovoltaic Science and Engineering.* 1st ed. Winchester: John Wiley & Sons.

Madaeni, S., Sioshansi, R. & Denholm , P., 2012. *Comparing capacity value estimation techniques for photovoltaic solar power,* s.l.: IEEE Journal of Photovoltaics.

Masters, G., 2004. *Renewable and efficient electric power systems.* Hoboken, NJ: John Wiley and Sons.

Matshoge, T. & Sebitosi, A. B., 2010. The mapping of maximum annual energy yield azimuth and tilt angles for PV installe at all locations in SA. *Journal of Energy in SA,* 21(4), pp. 2-6.

Mermoud, A., 2013. *PVSyst V6.10.* Geneva: Group of Energy - Unversity of Geneva.

Meteonorm V7.0, 2013. *Meteonorm site data report,* Letsatsi: meteonorm V7.0.20.22267.

Meteotest, 2013. *Meteonorm Global Meteorological Database V7: Handbook Part 1,* Bern: Meteotest.

Miller, A. & Lumby, B., 2012. *Utility Scale Solar Power Plants: A Guide for Developers and Investors,* New Delhi: International Finance Corporation.

Milligan, M. & Parsons, B., 1997. *A Comparison and Case Study of Capacity Credit Algorithms for Intermittent Generators.* Washington, NREL.

NASA, 2013. *Surface meteorology and Solar Energy: A renewable energy resource web site (release 6.0).* [Online]
Available at: https://eosweb.larc.nasa.gov/cgi-bin/sse/sse.cgi
[Accessed 19 November 2013].

NERC, n.d.. *Understanding the Grid: Reliability Terminology.* [Online]
Available at: http://www.nerc.com/
[Accessed 20 05 2014].

Norris, B. L. & Dise, J. H., 2013. *High Resolution PV modelling for Distribution Circuit Analysis,* Napa: NREL.

NREL, 2013. *NREL: National Centre for Photovoltaics.* [Online]
Available at: http://www.nrel.gov/ncpv/images/efficiency_chart.jpg
[Accessed 19 12 2013].

NREL, 2013. *System Advisor Model 2013.* s.l.:NREL.

Perez, R., Taylor, M., Hoff, T. & Ross, J., 2008. Reaching Consensus in the Definition of Photovoltaics Capacity Credit in the USA: A Practical Application of Satellite-Derived Solar Resource Data. *IEEE JOURNAL OF SELECTED TOPICS IN APPLIED EARTH OBSERVATIONS AND REMOTE SENSING,* 1(1), pp. 28-34.

Pudaruth, G. & Li, F., 2008. Capacity Credit Evaluation: A literature review. *DRPT2008,* pp. 2719-2724.

PVSyst SA, 2012. *PVSyst contextual Help,* Bern: PVSyst.

PVsyst, 2012. *PVsyst 6.0 - Photvoltaics System Study,* Geneva: PVsyst SA.

REN21, 2011. *REN21: Renewables 2011 Global Status ,* Paris: Ren21.

Sharma, B. D., 2011. *Performance of Solar Plants in India,* New Delhi: Central Electricity Regulatory Commission New Delhi.

SMA, 2013. *SMA.* [Online]
Available at: http://www.sma.de/en/company/about-sma/company-profile.html
[Accessed 14 12 2013].

SMA, n.d. *Performance Ratio - Quality factor for the PV plant,* s.l.: SMA - Technical information.

SolarGIS, 2013. *Comparison of SolarGIS with other solar data sources.* [Online]
Available at: http://solargis.info/doc/119
[Accessed 20 12 2013].

Solarplaza, 2011. *Solarplaza - Top 10 World's Most Efficient Solar PV Modules (Poly-Crystalline).* [Online]

Available at: http://www.solarplaza.com/top10-polycrystalline-module-efficiency/
[Accessed 24 May 2013].

Solmetric, 2011. *Guide to interpreting I-V curve Measurments of PV arrays,* s.l.: Sometric.

Stats SA, 2012. *Electricity generated and available for distribution,* Pretoria: Stats SA.

Suntech-Power, 2013. *Suntech.* [Online]
Available at: http://www.suntech-power.com/en/about/about-suntech
[Accessed 14 12 2013].

The Energy Blog, 2013. *The Energy Blog.* [Online]
Available at: http://energy.org.za/knowledge-resources/renewable-energy-projects-south-africa/utility-scale-project-map?resetfilters=0&clearordering=0&clearfilters=0
[Accessed 29 11 2013].

Ummel, K., 2013. *Planning for large-scale wind and solar power in South Africa: Identifying cost-effective deployment strategies through spatiotemporal modeling (Draft),* Cape Town: Center for Global Development.

USC, 2005. *Energy Policy of 2005,* Washington: Public Law.

Van Wijk, A., 1990. *Wind energy and electricity production. Doctoral thesis,* s.l.: Utrecht University.

Van Zyl, D., 2012. *Modelling of South African Wind farm's electricity production,* Cape Town: University of Stellenbosch.

Voorspools , K. R. & D'haeseleer, W. D., 2005. *An analytical formula for the capacity credit of wind power,* Leuven: University of Leuven.

Watsun Simulation Laboratory, 1992. *WATGEN's Users Manual and program documentation,* Ontario: University of Waterloo.

APPENDIX A – PV TECHNOLOGY

There are two main types of c-Si cells: monocrystalline-silicon (mono –Si) and polycrystalline-silicon (poly – Si). Mono-Si is generally more efficient, but more difficult to manufacture than poly-Si and as a result is also more expensive to produce (Brosz, et al., 2012).

Below in table Table 22 and Table 23 are the top 5 most efficient, commercially available mono-Si and Poly-Si modules respectively in 2012. Additionally, below the tables are images of a typical panel for each variation.

Table 22: Top 5 Most Efficient Commercially Available Mono-Si 2012 (Solarplaza, 2011)

Manufacturer	Module Efficiency	Cell Efficiency	Module Type
SunPower	20.40%	22.80%	E20 / 333 SOLAR PANEL
AUO	19.50%	n/a	PM318B00
Sanyo	19.00%	21.60%	HIT-N240SE10
Jiawei	18.30%	21.01%	JW-S100
Crown RE	18.30%	n/a	Summit 100LM
Industry Average	15-16%	n/a	Varies

Figure 55: SunPower E20/333 Mono-Si Module (Solarplaza, 2011)

Table 23: Top 5 Most Efficient Commercially Available Poly-Si 2012 (Solarplaza, 2011)

Manufacturer	Module Efficiency	Cell Efficiency	Module Type
Solland Solar	16.00%	n/a	Sunweb
Siliken	15.70%	n/a	SLK72P6L-305
LDK Solar	15.67%	18.33%	LDK-200P-24(s)
Vikram	15.63%	n/a	Eldora 280 (300)
Wiosun	15.54%	17.12%	E300P
Industry Average	13-15%	n/a	Varies

Figure 56: NewEdge CS6P Poly-Si Module (Solarplaza, 2011)

Silicon is a universally abundant element and is the 2nd most abundant element in the earth's crust (Brosz, et al., 2012). Even so, solar grade purity for silicon is extremely high (99.9999%) and as a result is an expensive component of the solar PV module costs (Brosz, et al., 2012). This has led industry to develop less expensive materials, thin film (using less silicon or other materials) being one. The market share for this technology is being led by cadmium telluride (CdTe), followed by amorphous silicon and the other polycrystalline materials: copper indium (gallium) and diselenide (CIS or CIGS) (Brosz, et al., 2012).

There is large array of technological choice when considering a PV design. Figure 57 below describes the efficiencies of the different options.

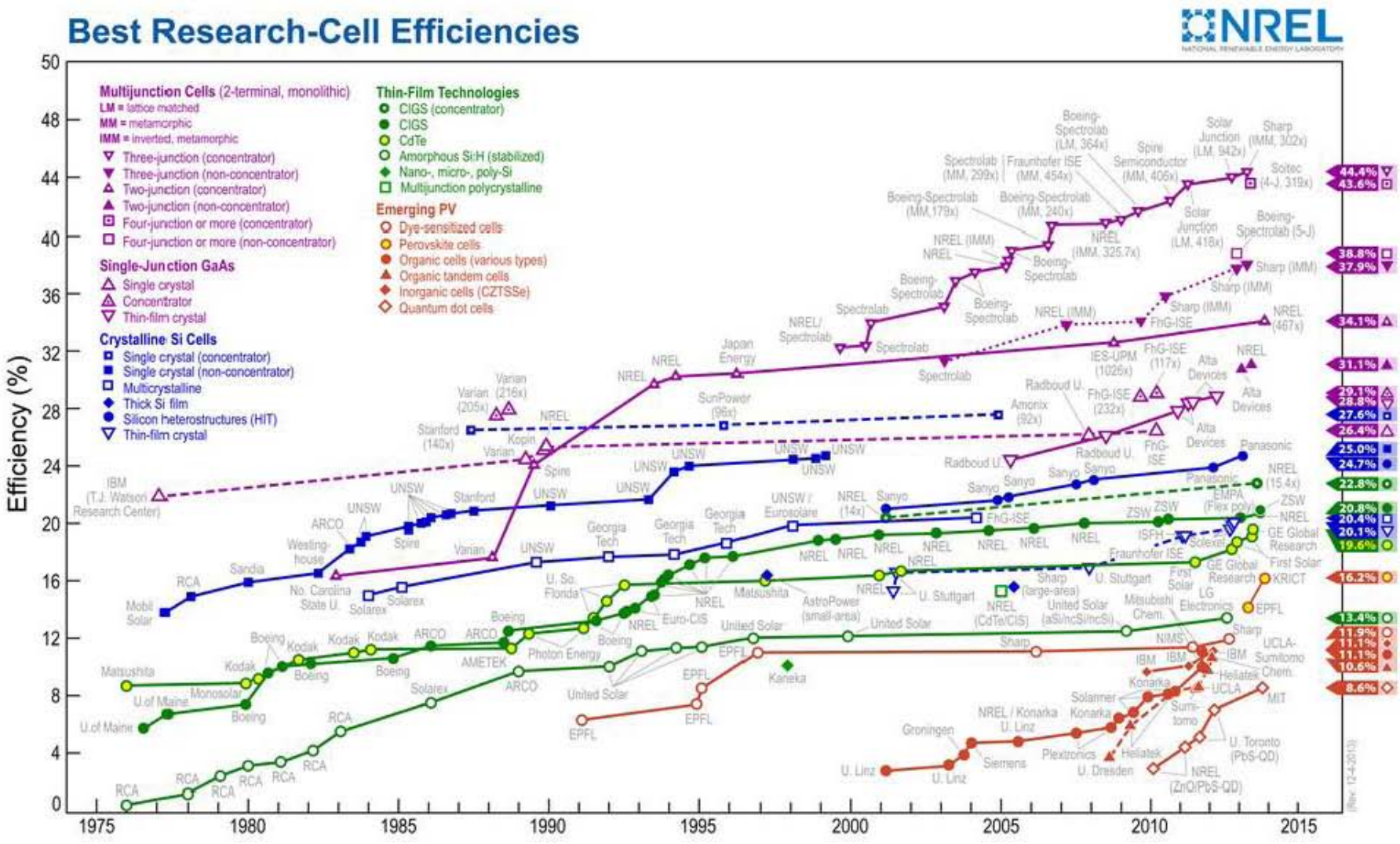

Figure 57: Relative Efficiencies for different PV Technologies (NREL, 2013)

APPENDIX B – SYSTEM DESIGN

Basic layout

The basic layout for a utility scale PV plant is shown in Figure 58 below.

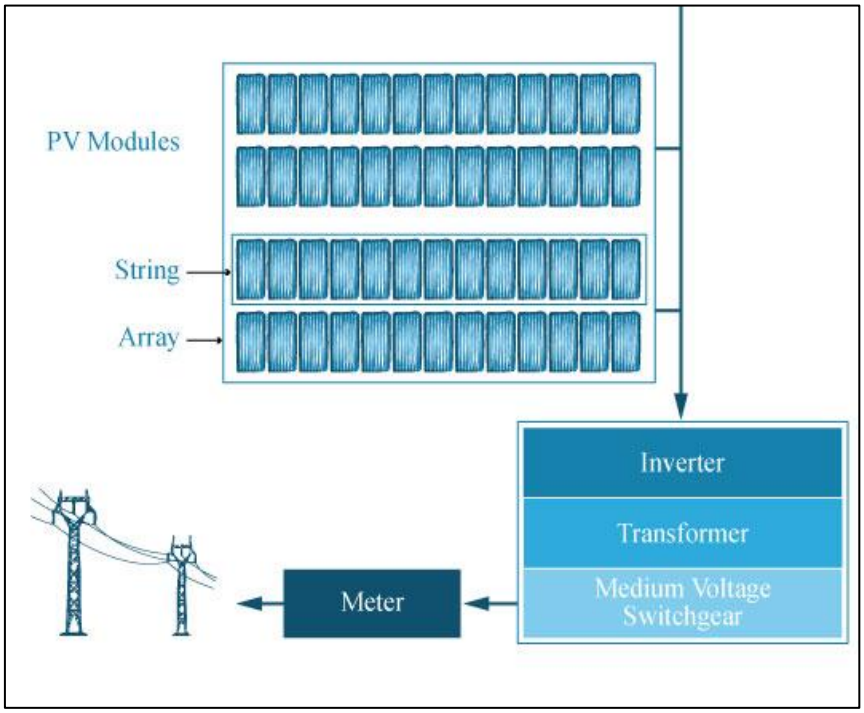

Figure 58: PV plant basic layout

In simple terms energy is collected from the sun by the panels and sent to the inverters. The inverters then convert the energy supplied from direct current to alternating current power, from which it's stepped-up in the transformer, metered and evacuated to the grid. Through this process losses are incurred as shown in Figure 59 below.

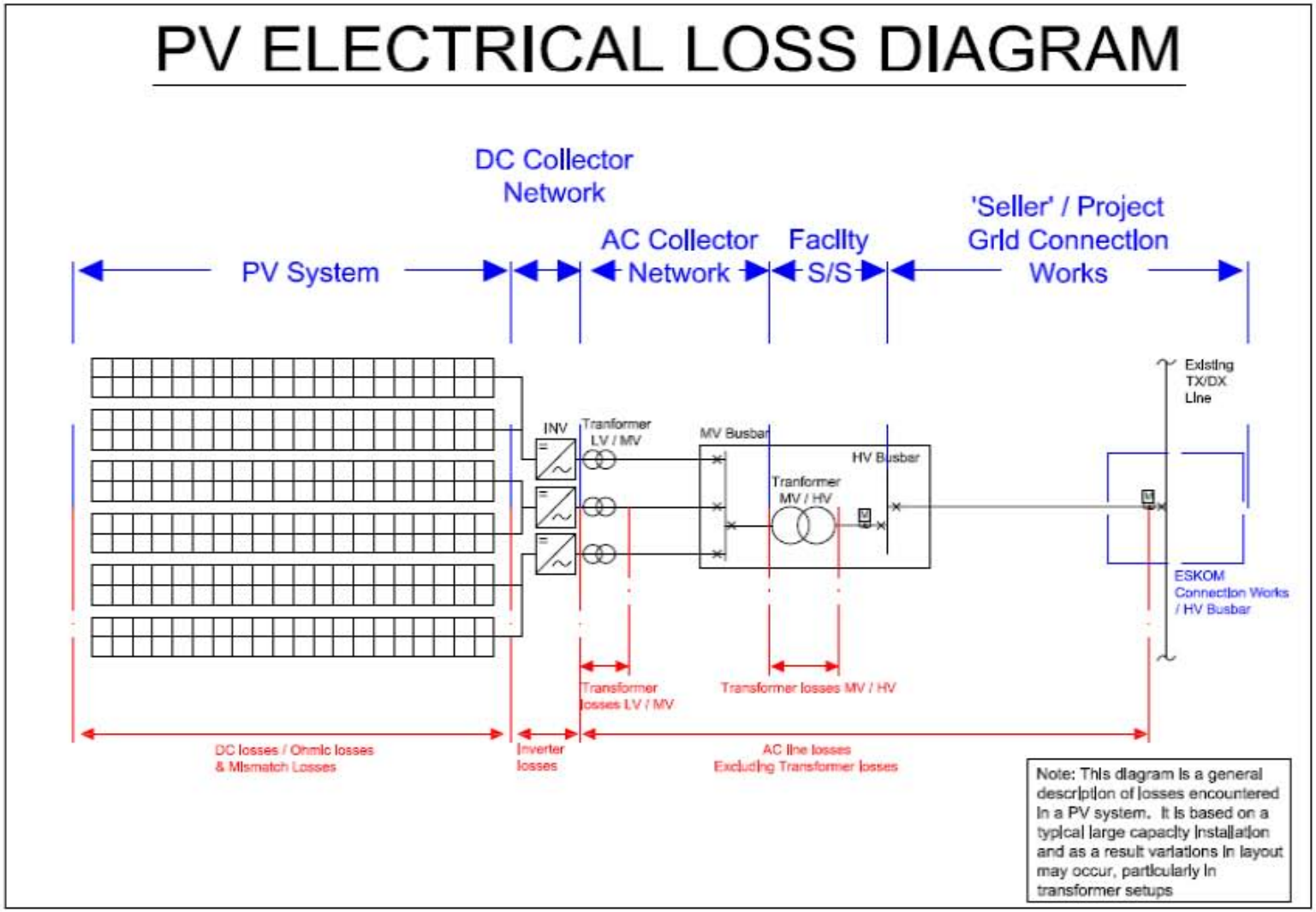

Figure 59: Electrical loss diagram

System Losses

In this design, losses up until the grid connection point have been considered. These are the losses experienced by the system that cause the power to actually be delivered to the grid to be lower than that produced by the modules. There are several reason for these losses from cable loss to dirt on the modules. Figure 59 above describes a typical large scale PV plant, and the different parts that make up the whole. System losses considered are spread across these different parts, and can be further separated into 3 groups, as shown in Table 24 below.

Table 24: System losses

Category	Loss Description
Shading and Spectral	Near side shading losses
	Reflection losses (IAM factor)
PV Modules	PV loss due to irradiance level
	Quality loss
	Array soiling loss
	Module array mismatch loss
	DC Ohmic wiring loss
AC electrical components	Inverter efficiency loss
	AC Ohmic wiring loss
	Transformer loss

Near Side shading

For multi-row utility scale PV systems near side shading or row-to-row shading is inevitable at certain times of the day. This is dependent on the inter row spacing, tilt angle and module orientation of the plant (Luque & Hegedus, 2011). All these factors are in the hands on the designer, and providing that the plant is not constrained by available area a benchmark of 2-4% losses is generally aimed for (Luque & Hegedus, 2011).

New software provides the option to sophisticatedly model both near and horizons shading losses, but older packages tend to treat shading as a constant loss factor. The approach taken in this research follows this method with a constant loss factor of 2.5%.

Reflection losses (IAM Factor)

The ratings on a PV module data sheet have been determined at standard test conditions (STC). This requires perpendicular light, whereas in reality large angles of incident angles occur (Sharma, 2011). This results in higher reflection losses than accounted for under STC. Sharma (2011) suggest that a loss of 1% is sufficient for plants facing the equator at a tilt angle equal to that of sight latitude.

Losses taken from sites modelled in PVSyst however, are approximately 2.5% based on a bo parameter (a parameter outline by the ASHRAE standards) of 0.05 (PVSyst SA, 2012). Thus the more conservative value of 2.5% has been used in our calculations.

PV loss due to Irradiance level

The vast majority of all modules experience a reduction in efficiency under low light intensity (Sharma, 2011). This is dependent on module selection and irradiation intensity of the site considered thus can vary greatly. On average the PVSyst modelling results showed losses of 0.6% was experienced across SA. This shows a good quality of light intensity for SA. How taking note that this can vary from site to site, a safety factor of 2 was used resulting in a loss of 1.2%

Quality loss

The quality loss is used to show the discrepancy between modules in real life and that of the manufacturer specifications. The manufacturer specification generally comes with a tolerance, and the default is to use half the modules lower tolerance (Mermoud, 2013). Thus 0.8% has been used.

It can additionally be used to take long term degradation into consideration.

Soiling loss

This loss parameter allows for specification dirt, bird excrement and other accumulation on the panels that inhibits irradiation from reaching the cells. Losses in the range of 1% are generally acceptable (Sharma, 2011), but in our case many of the sites are in dusty areas of low rainfall and water shortages. Additionally if we conservatively assume that the panels will only be washed once a year and loss of 2.5% is more likely.

Module array mismatch loss

In a solar array, multiple modules are connected in series and parallel. These modules are not identical, and thus the whole chain of modules is constrained to perform at the level of the worst case module (Sharma, 2011). These days manufacturers offer modules sorted with only positive tolerances. Thus a low loss of 1% is used.

DC Ohmic wiring loss

Losses experienced through the DC wiring network from module array to invertor. Standard loss of 1.25% is used.

Inverter efficiency loss

An inverter changes DC electricity to AC electricity for use on the grid. The efficiency of the inverter is how well it changes DC to AC electricity. Modern inverters are very efficient, with SMA central invertor chosen showing losses of only 1.9%. Typically invertors of this type are in the range of 96 – 98.5% efficient (Sharma, 2011).

AC Ohmic wiring loss

Losses experienced through the AC wiring network from invertor to transformer. Dependant on length and width of cable specified. A conservative value of 0.5% is used.

Transformer losses

An external transformer is used to step up the system from a low voltage (LV) network to a medium of high voltage (MW/HV) network. This allows for energy transport through the grid with minimum losses. The losses experienced in a transformer can be split into iron loss and resistive loss. A standard loss of 1.2% has been assumed (PVSyst SA, 2012).

APPENDIX C – TECHICAL DATA

APPENDIX D – CAPACITY CREDIT DETAILED RESULTS

Availability of Existing System and Base Case:

Table 25: Availability of Existing System and Base Case

Availability Curves	Thermal System		Thermal + PV	
Total Installed Capacity	43468 MW			
Reliability Target	LCC (MW)	LCC (%)	LCC (MW)	LCC (%)
50%	40 525	93.3%	41 242	92.6%
55%	40 394	93.0%	41 108	92.3%
60%	40 264	92.7%	40 930	91.9%
65%	40 090	92.3%	40 797	91.6%
70%	39 916	91.9%	40 619	91.2%
75%	39 743	91.5%	40 441	90.8%
80%	39 526	91.0%	40 218	90.3%
85%	39 308	90.5%	39 951	89.7%
90%	38 961	89.7%	39 640	89.0%
95%	38 483	88.6%	39 195	88.0%
96%	38 309	88.2%	39 017	87.6%
97%	38 136	87.8%	38 839	87.2%
98%	37 918	87.3%	38 617	86.7%
99%	37 528	86.4%	38 172	85.7%
100%	35 052	80.7%	35 725	80.2%

Annual Capacity Credits:

Table 26: Annual Capacity Credits – Scenario A

Scenario A				PV Cap	1054.6	MW
Yearly Capacity Credit - Diurnal Trend						
Time	LCC PV	LCC Sys	FC - Sys	dCf	Equivalent Thermal	Capacity Credit
			MW	MW	MW	
Reliability level: 98%						
06h00	0.0%	85.3%	37945	27	26.4	0.025
08h00	0.4%	86.1%	38305	387	440.2	0.417
10h00	45.6%	86.8%	38626	708	809.2	0.767
12h00	37.5%	86.8%	38608	690	788.5	0.748
14h00	37.8%	86.7%	38572	654	747.1	0.708
16h00	34.6%	86.7%	38554	636	726.4	0.689
18h00	0.3%	85.9%	38239	321	364.3	0.345

20h00	0.0%	85.3%	37929	11	8.0	0.008

Table 27: Annual Capacity Credits – Scenario B

Scenario B				PV Cap	1054.6	MW
Yearly Capacity Credit - Diurnal Trend						
Time	**LCC PV**	**LCC Sys**	**FC - Sys**	**dCf**	**Equivalent Thermal**	**Capacity Credit**
			MW	**MW**	**MW**	
Reliability level: 98%						
06h00	0.0%	85.3%	37949	31	31.0	0.029
8am	0.3%	86.1%	38296	378	429.9	0.408
10h00	43.1%	86.8%	38617	699	798.9	0.758
12h00	36.1%	86.8%	38617	699	798.9	0.758
14h00	37.4%	86.8%	38599	681	778.2	0.738
16h00	32.7%	86.8%	38599	681	778.2	0.738
18h00	0.3%	85.9%	38234	316	358.6	0.340
20h00	0.0%	85.3%	37932	14	11.4	0.011

Table 28: Annual Capacity Credits – Scenario C

Scenario C				PV Cap	1054.6	MW
Yearly Capacity Credit - Diurnal Trend						
Time	**LCC PV**	**LCC Sys**	**FC - Sys**	**dCf**	**Equivalent Thermal**	**Capacity Credit**
			MW	**MW**	**MW**	
Reliabilty level: 98%						
06h00	0	0.853	37949	31	31.0	0.029
08h00	0.002	0.8572	38136	218	245.9	0.233
10h00	0.207	0.8664	38546	628	717.2	0.680
12h00	0.369	0.8704	38723	805	920.7	0.873
14h00	0.404	0.87	38706	788	901.2	0.855
16h00	0.274	0.8656	38510	592	675.9	0.641
18h00	0.001	0.8568	38118	200	225.2	0.214
20h00	0.000	0.853	37932	14	11.4	0.011

Table 29: Annual Capacity Credits – Scenario D

Scenario D				PV Cap	1054.6	MW
Yearly Capacity Credit - Diurnal Trend						
Time	**LCC PV**	**LCC Sys**	**FC - Sys**	**dCf**	**Equivalent Thermal**	**Capacity Credit**
			MW	**MW**	**MW**	
Reliabilty level: 98%						

06h00		0.853	37918	0	0.0	0.000
08h00		0.861	38305	387	440.2	0.417
10h00		0.864	38483	565	644.8	0.611
12h00		0.864	38439	521	594.2	0.563
14h00		0.863	38394	476	542.5	0.514
16h00		0.863	38394	476	542.5	0.514
18h00		0.854	37994	76	82.7	0.078
20h00		0.853	37918	0	0.0	0.000

Seasonal Variation in Capacity Credits:

Table 30: Summer Capacity Credits – Scenario A

Summer				PV Cap	1054.6	MW
Yearly Capacity Credit - Diurnal Trend						
Time	**LCC PV**	**LCC Sys**	**FC - Sys**	**dCf**	**Equivalent Thermal**	**Capacity Credit**
			MW	**MW**	**MW**	**EFC**
Reliability level: 98%						
06h00	0.0%	85.4%	37994	76	82.7	0.078
08h00	24.8%	86.5%	38483	565	644.8	0.611
10h00	29.0%	86.7%	38572	654	747.1	0.708
12h00	28.8%	86.6%	38528	610	696.6	0.660
14h00	25.1%	86.6%	38528	610	696.6	0.660
16h00	27.7%	86.5%	38483	565	644.8	0.611
18h00	20.0%	86.5%	38439	521	594.2	0.563
20h00	0.0%	86.5%	37994	76	82.7	0.078

Table 31: Autumn Capacity Credits – Scenario A

Autumn				PV Cap	1054.6	MW
Yearly Capacity Credit - Diurnal Trend						
Time	**LCC PV**	**LCC Sys**	**FC - Sys**	**dCf**	**Equivalent Thermal**	**Capacity Credit**
			MW	**MW**	**MW**	**EFC**
Reliability level: 98%						
06h00	0.0%	0.0%	37918	0	0.0	0.000
08h00	2.5%	85.9%	38216	298	337.9	0.320
10h00	49.2%	86.7%	38572	654	747.1	0.708
12h00	34.9%	86.6%	38528	610	696.6	0.660
14h00	30.7%	86.6%	38528	610	696.6	0.660
16h00	28.6%	86.6%	38528	610	696.6	0.660
18h00	0.2%	85.8%	38174	256	289.6	0.275
20h00	0.0%	0.0%	37918	0	0.0	0.000

Table 32: Winter Capacity Credits – Scenario A

Winter				PV Cap	1054.6	MW
Yearly Capacity Credit - Diurnal Trend						
Time	**LCC PV**	**LCC Sys**	**FC - Sys**	**dCf**	**Equivalent Thermal**	**Capacity Credit**
			MW	**MW**	**MW**	**EFC**
Reliability level: 98%						
06h00	0.0%	0.0%	37918	0	0.0	0.000
08h00	1.0%	85.6%	38074	156	174.7	0.166
10h00	57.6%	86.9%	38635	717	819.6	0.777
12h00	59.0%	87.0%	38688	770	880.5	0.835
14h00	59.8%	87.0%	38688	770	880.5	0.835
16h00	51.5%	86.8%	38626	708	809.2	0.767
18h00	0.1%	85.5%	38043	125	139.0	0.132
20h00	0.0%	0.0%	37918	0	0.0	0.000

Table 33: Spring Capacity Credits – Scenario A

Spring				PV Cap	1054.6	MW
Yearly Capacity Credit - Diurnal Trend						
Time	**LCC PV**	**LCC Sys**	**FC - Sys**	**dCf**	**Equivalent Thermal**	**Capacity Credit**
			MW	**MW**	**MW**	**EFC**
Reliability level: 98%						
06h00	0.0%	85.3%	37949	31	31.0	0.029
08h00	31.6%	86.5%	38483	565	644.8	0.611
10h00	47.3%	86.8%	38617	699	798.9	0.758
12h00	46.2%	86.8%	38617	699	798.9	0.758
14h00	46.9%	86.7%	38572	654	747.1	0.708
16h00	45.4%	86.7%	38572	654	747.1	0.708
18h00	25.9%	86.2%	38350	432	491.9	0.466
20h00	0.0%	0.0%	37918	0	0.0	0.000

<u>High Demand Variation in Capacity Credits:</u>

Including Test of Equation 18

Table 34: High Demand Capacity Credits – Scenario A

Scenario A							PV Cap		1054.6 MW		
High Demand Capacity Credit - Diurnal Trend							TEST				
Time	**LCC PV**	**LCC Sys**	**FC - Sys**	**dCf**	**Equivalent Thermal**	**CC**	**%diff**	**No. Eq.Thermal units**	**Eq TH cap**	**Res PV Cap**	**CC**

			MW	MW	MW				MW	MW	
Reliabilty level: 98%											
06h00	0.0%	0.0%	37918	0	0.0	**0.000**	0.0%	0	0	0	**0.000**
08h00	1.0%	85.6%	38074	156	174.7	**0.166**	-1.9%	1	154.9	1055	**0.147**
10h00	57.6%	86.9%	38635	717	819.6	**0.777**	0.5%	5	774.5	990	**0.782**
12h00	59.0%	87.0%	38688	770	880.5	**0.835**	-0.5%	6	929.4	1120	**0.830**
14h00	59.8%	87.0%	38688	770	880.5	**0.835**	-0.5%	6	929.4	1120	**0.830**
16h00	51.5%	86.8%	38626	708	809.2	**0.767**	2.3%	5	774.5	980	**0.790**
18h00	0.1%	85.5%	38043	125	139.0	**0.132**	-13.2%	0	0	0	**0.000**

Table 35: High Demand Capacity Credits – Scenario B

Scenario B						PV Cap 1054.6 MW					
High Demand Capacity Credit - Diurnal Trend							TEST				
Time	**LCC PV**	**LCC Sys**	**FC - Sys**	**dCf**	**Equivalent Thermal**	**CC**	**%diff**	**No. Eq Thermal units**	**Eq TH cap**	**Res PV Cap**	**CC**
			MW	**MW**	**MW**				**MW**	**MW**	
Reliabilty level: 98%											
06h00	0.0%	0.0%	37918	0	0.0	0.000	0.0%	0	0	0	0.000
08h00	0.1%	85.5%	38056	138	154.0	0.146	0.2%	1	155	1045	0.148
10h00	55.4%	86.9%	38661	743	849.4	0.805	1.0%	6	929	1140	0.815
12h00	59.7%	87.0%	38683	765	874.7	0.829	2.3%	6	929	1090	0.853
14h00	60.7%	87.0%	38692	774	885.1	0.839	1.3%	6	929	1090	0.853
16h00	51.9%	86.9%	38639	721	824.2	0.781	0.1%	5	775	990	0.782
18h00	0.1%	85.5%	38047	129	143.6	0.136	0.5%	1	155	1095	0.141

Table 36: High Demand Capacity Credits – Scenario C

Scenario C				PV Cap	1054.6	MW
High Demand Capacity Credit - Diurnal Trend						
Time	**LCC PV**	**LCC Sys**	**FC - Sys**	**dCf**	**Equivalent Thermal**	**Capacity Credit**
			MW	**MW**	**MW**	
Reliabilty level: 98%						
06h00	0.0%	0.0%	37918	0	0	0.000
08h00	0.0%	85.6%	38061	143	160	0.151
10h00	42.2%	86.6%	38528	610	697	0.660
12h00	65.0%	87.1%	38750	832	952	0.902
14h00	63.8%	87.1%	38728	810	926	0.879
16h00	42.8%	86.5%	38492	574	655	0.621
18h00	0.0%	84.5%	38016	98	108	0.102

Table 37: High Demand Capacity Credits – Scenario D

Scenario D			PV Cap	1054.6	MW
High Demand Capacity Credit - Diurnal Trend					
Time	**LCC Sys**	**FC - Sys**	**dCf**	**Equivalent Thermal**	**Capacity Credit**
		MW	**MW**	**MW**	
Reliabilty level: 98%					
06h00	0.0%	37918	0	0.0	0.000
08h00	86.5%	38483	565	644.8	0.611
10h00	87.1%	38750	832	951.8	0.902
12h00	87.1%	38750	832	951.8	0.902
14h00	87.1%	38750	832	951.8	0.902
16h00	86.9%	38661	743	849.4	0.805
18h00	0.0%	37918	0	0.0	0.000

Low Demand Variation in Capacity Credits:

Table 38: Low Demand Capacity Credits – Scenario A

Scenario A				PV Cap	1054.6	MW
Low Demand Capacity Credit - Diurnal Trend						
Time	**LCC PV**	**LCC Sys**	**FC - Sys**	**dCf**	**Equivalent Thermal**	**Capacity Credit**
			MW	**MW**	**MW**	
Reliability level: 98%						
06h00	0.0%	85.3%	37940	22	21	0.020
08h00	2.3%	86.3%	38403	485	553	0.524
10h00	44.1%	86.7%	38581	663	757	0.718
12h00	33.5%	86.7%	38572	654	747	0.708
14h00	35.5%	86.7%	38554	636	726	0.689
16h00	32.5%	86.6%	38546	628	717	0.680
18h00	0.7%	86.1%	38310	392	446	0.423
20h00	0.0%	85.2%	37918	0	0	0.000

Table 39: Low Demand Capacity Credits – Scenario B

Scenario B				PV Cap	1054.6	MW
Low Demand Capacity Credit - Diurnal Trend						
Time	**LCC PV**	**LCC Sys**	**FC - Sys**	**dCf**	**Equivalent Thermal**	**Capacity Credit**
			MW	**MW**	**MW**	
Reliability level: 98%						
06h00	0.0%	84.3%	37949	31	31	0.029

08h00	1.0%	86.3%	38385	467	532	0.505
10h00	41.0%	86.8%	38626	708	809	0.767
12h00	35.0%	86.8%	38599	681	778	0.738
14h00	33.0%	86.7%	38572	654	747	0.708
16h00	31.0%	86.7%	38559	641	732	0.694
18h00	1.0%	86.1%	38310	392	446	0.423
20h00	0.0%	85.2%	37918	0	0	0.000

Table 40: Low Demand Capacity Credits – Scenario C

Scenario C				PV Cap	1054.6	MW
Low Demand Capacity Credit - Diurnal Trend						
Time	**LCC PV**	**LCC Sys**	**FC - Sys**	**dCf**	**Equivalent Thermal**	**Capacity Credit**
			MW	**MW**	**MW**	
Reliability level: 98%						
06h00	0.0%	85.32%	37958	40	41	0.039
08h00	1.0%	85.80%	38172	254	287	0.272
10h00	20.0%	86.70%	38572	654	747	0.708
12h00	36.0%	86.70%	38572	654	747	0.708
14h00	38.0%	86.96%	38706	788	901	0.855
16h00	25.0%	86.54%	38501	583	666	0.631
18h00	0.0%	85.72%	38136	218	246	0.233
20h00	0.0%	85.20%	37918	0	0	0.000

Table 41: Low Demand Capacity Credits – Scenario D

Scenario D			PV Cap	1054.6	MW
Low Demand Capacity Credit - Diurnal Trend					
Time	**LCC Sys**	**FC - Sys**	**dCf**	**Equivalent Thermal**	**Capacity Credit**
		MW	**MW**	**MW**	
Reliability level: 98%					
06h00	85.2%	37918	0	0.0	0.000
08h00	86.0%	38621	703	803.5	0.762
10h00	86.3%	38394	476	542.5	0.514
12h00	86.2%	38350	432	491.9	0.466
14h00	86.1%	38305	387	440.2	0.417
16h00	86.1%	38305	387	440.2	0.417
18h00	85.4%	38038	120	133.3	0.126
20h00	85.2%	37918	0	0	0.000

Level of Penetration vs. Capacity Credit:

Table 42: Level of penetration vs. capacity credit - detailed

Level of Penetration vs Capacity Credit								
PV Capacity	**LCC System**	**FC - System**	**dCf**	**% of PV Cap**	**Equiv. Therm - No. of Units**	**Equivalent Thermal - Cap**	**Resultant PV Cap**	**Capacity Credit**
1054.6	87.0%	38688	770	73%	6	929.4	1120.0	0.83
2000	86.2%	39165	1247	62%	9	1394.1	1940	0.72
4000	85.1%	40367	2449	61%	17	2633.3	3870	0.68
6000	83.9%	41476	3558	59%	25	3872.5	5750	0.67
8000	82.7%	42536	4618	58%	34	5266.6	7950	0.66
10000	81.4%	43496	5578	56%	41	6350.9	9700	0.65

APPENDIX E – DISPATCH MODEL DETAILED RESULTS

Testing Dispatch at different levels of reliability:

Table 43: Dispatch model results: Base case – 90% reliability

Base Case	Yearly	Reliability 90%				
	MWh dispatched	EENS	LOLE	Energy value of fuel	Cost of Fuel	CO2
	MWh	MWh	Hours	GJ	R	Tonnes
January	20 308 036	0	0	186 184 570	2 795 141 691	17 919 862
February	21 113 820	283	1	197 045 542	2 977 351 977	18 961 954
March	21 243 079	538	1	198 457 223	3 000 774 836	19 097 447
April	20 306 939	71	1	188 339 155	2 833 033 620	18 126 295
May	21 375 813	254	1	196 838 121	2 959 246 683	18 944 536
June	22 261 165	0	0	204 470 704	3 075 657 497	19 678 846
July	22 714 265	1450	2	207 993 875	3 129 988 833	20 017 699
August	21 975 711	1357	3	201 083 084	3 031 580 969	19 351 643
September	21 863 746	1205	2	202 311 335	3 052 750 081	19 469 396
October	21 512 196	98	2	199 338 931	3 007 862 110	19 183 354
November	21 530 867	909	4	200 301 399	3 088 715 973	19 264 715
December	20 322 504	2903	8	188 353 490	2 897 290 558	18 116 801
Year	**256 528 143**	**9 068**	**25**	**2 370 717 430**	**35 849 394 828**	**228 132 549**

Table 44: Dispatch model results: Base case – Load not inflated

Base Case	Yearly	Load not inflated				
	MWh dispatched	EENS	LOLE	Energy value of fuel	Cost of Fuel	CO2
	MWh	MWh	Hours	GJ	R	Tonnes
January	20 234 964	23 936	41	185 843 305	3 188 602 562	17 819 345
March	20 513 994	28 687	44	190 365 123	3 117 766 589	18 278 112
April	20 500 940	21 542	28	190 320 545	3 029 073 985	18 288 766
May	21 387 719	17 821	24	196 837 916	3 119 445 638	18 917 317
June	22 425 231	34 432	41	206 021 267	3 343 223 874	19 786 609
July	22 710 411	14 234	20	207 741 312	3 291 184 653	19 965 379
August	22 120 833	32 601	30	203 489 177	3 229 679 740	19 555 724
September	21 611 044	36 004	36	199 704 947	3 216 617 197	19 184 073
October	21 339 607	153 427	157	197 730 135	3 676 924 282	18 910 817
November	21 219 128	252 263	257	197 064 770	3 913 264 369	18 804 956
December	19 761 131	365 675	309	183 727 969	3 807 178 691	17 505 335
Year	**254 977 809**	**1 018 376**	**1 056**	**2 355 929 459**	**40 296 211 754**	**225 916 571**

Table 45: Dispatch model results: Base case – 98% reliability

Base Case	Yearly	Reliability 98%				
	MWh dispatched	EENS	LOLE	Energy value of fuel	Cost of Fuel	CO2
	MWh	MWh	Hours	GJ	R	Tonnes
January	20182590	0	0	184444308	2766664619	17752765
February	21022568	65	1	196201909	2964314335	18880820
March	21097270	1194	4	196701148	2978656126	18927708
April	20638291	52	1	191069953	2871405475	18389574
May	21248473	55	1	195487135	2936319381	18814956
June	22430069	0	0	205874974	3092152918	19814782
July	22849563	2513	2	209263994	3161461862	20137839
August	22007821	190	1	201887978	3036852545	19430269
September	21520459	0	0	198708633	2990675673	19124000
October	21502029	49	1	199206807	2998218392	19171938
November	21506284	3509	7	199745276	3041094879	19217857
December	20263884	2020	7	188079074	2882785824	18092153
Year	**256269300**	**9648**	**25**	**2366671190**	**35720602029**	**227754660**

Testing Dispatch for different scenarios:

Table 46: Dispatch model results: no PV

No PV	Yearly	reliability 98%				
	MWh dispatched	EENS	LOLE	Energy value of fuel	Cost of Fuel	CO2
	MWh	MWh	Hours	GJ	R	Tonnes
January	20 385 992	0	0	188 738 032	2 831 070 478	18 166 036
February	21 092 369	0	0	198 673 515	3 016 639 615	19 116 123
March	21 284 991	147	1	200 617 450	3 046 230 495	19 303 153
April	20 594 848	204	1	192 938 768	2 915 757 732	18 566 676
May	21 441 984	0	0	199 134 721	2 989 848 604	19 166 237
June	22 243 634	464	1	205 934 506	3 104 171 961	19 818 623
July	22 731 406	0	0	209 684 422	3 151 705 740	20 181 032
August	22 060 702	0	0	204 258 274	3 074 637 649	19 658 031
September	21 842 807	1092	3	204 397 083	3 092 972 892	19 668 632
October	21 618 325	55	1	202 663 940	3 066 562 717	19 501 888
November	21 611 576	0	0	203 123 767	3 072 740 236	19 546 268
December	20 161 373	7	1	189 086 293	2 886 557 767	18 191 022
Year	**257 070 008**	**1 970**	**8**	**2 399 250 771**	**36 248 895 888**	**230 883 721**

Table 47: Dispatch model results: Scenario B

Scenario B	Yearly	reliability 98%				
	MWh dispatched	EENS	LOLE	Energy value of fuel	Cost of Fuel	CO2
	MWh	MWh	Hours	GJ	R	Tonnes
January	20 196 758	0	0	184 569 748	2 770 583 646	17 764 492
February	21 098 200	244	1	196 690 777	2 969 421 895	18 928 251
March	21 026 935	57	1	195 982 337	2 957 393 182	18 860 302
April	20 570 972	414	1	190 644 586	2 870 198 776	18 347 754
May	21 470 819	0	0	197 723 182	2 968 528 907	19 030 401
June	22 384 843	0	0	205 346 736	3 083 676 830	19 764 033
July	22 817 954	0	0	209 400 054	3 156 695 453	20 152 091
August	21 941 971	456	1	200 911 127	3 023 649 792	19 336 001
September	21 448 768	0	0	198 231 302	2 978 546 155	19 078 901
October	21 659 863	51	1	200 363 987	3 028 414 587	19 281 136
November	21 313 284	3521	6	198 087 272	3 024 390 581	19 056 888
December	20 280 496	5817	8	187 724 173	2 868 209 489	18 059 564
Year	**256 210 864**	**10 560**	**19**	**2 365 675 280**	**35 699 709 294**	**227 659 815**

Table 48: Dispatch model results: Scenario C

Scenario C	Yearly	Reliability 98%				
	MWh dispatched	EENS	LOLE	Energy value of fuel	Cost of Fuel	CO2
	MWh	MWh	Hours	GJ	R	Tonnes
January	19 768 276	0	0	181 044 756	2 715 671 347	17 425 558
February	21 032 738	0	0	196 180 408	2 960 750 656	18 879 301
March	21 203 488	307	1	197 942 354	3 001 600 237	19 046 440
April	20 557 097	364	1	191 081 842	2 876 222 802	18 389 930
May	21 447 098	0	0	196 781 180	2 952 256 265	18 940 097
June	22 429 046	0	0	205 980 008	3 095 939 553	19 824 516
July	22 794 987	127	1	208 685 736	3 140 543 336	20 084 261
August	22 038 421	0	0	201 956 457	3 032 469 383	19 437 779
September	21 712 505	0	0	200 465 052	3 014 205 736	19 293 534
October	21 542 098	272	1	199 289 290	3 009 954 531	19 178 094
November	21 383 303	0	0	198 865 435	3 002 376 430	19 137 505
December	19 953 870	1589	4	184 967 482	2 835 541 570	17 792 759
Year	**255 862 926**	**2 659**	**8**	**2 363 240 001**	**35 637 531 846**	**227 429 773**

Table 49: Dispatch model results: Scenario D

Scenario D	Yearly	Reliability 98%				
	MWh dispatched	EENS	LOLE	Energy value of fuel	Cost of Fuel	CO2
	MWh	MWh	Hours	GJ	R	Tonnes
January	20 190 122	0	0	185 450 862	2 781 762 936	17 849 646
February	21 013 624	67	1	196 588 237	2 981 061 505	18 916 144
March	21 076 494	42	1	196 640 068	2 966 806 818	18 923 685
April	20 711 783	423	1	192 087 062	2 893 995 672	18 486 225
May	21 448 040	0	0	196 149 580	2 943 618 825	18 879 164
June	22 342 136	384	1	204 536 878	3 079 566 981	19 684 720
July	22 747 304	0	0	208 010 589	3 123 269 788	20 020 491
August	22 080 809	0	0	202 243 691	3 041 295 645	19 464 658
September	21 783 327	0	0	201 849 197	3 043 366 015	19 425 332
October	21 480 468	149	1	199 688 384	3 021 008 640	19 215 647
November	21 542 602	54	1	201 551 268	3 067 918 130	19 391 729
December	20 039 631	2336	5	187 102 288	2 854 359 899	18 000 475
Year	**256 456 340**	**3 455**	**11**	**2 371 898 105**	**35 798 030 854**	**228 257 916**

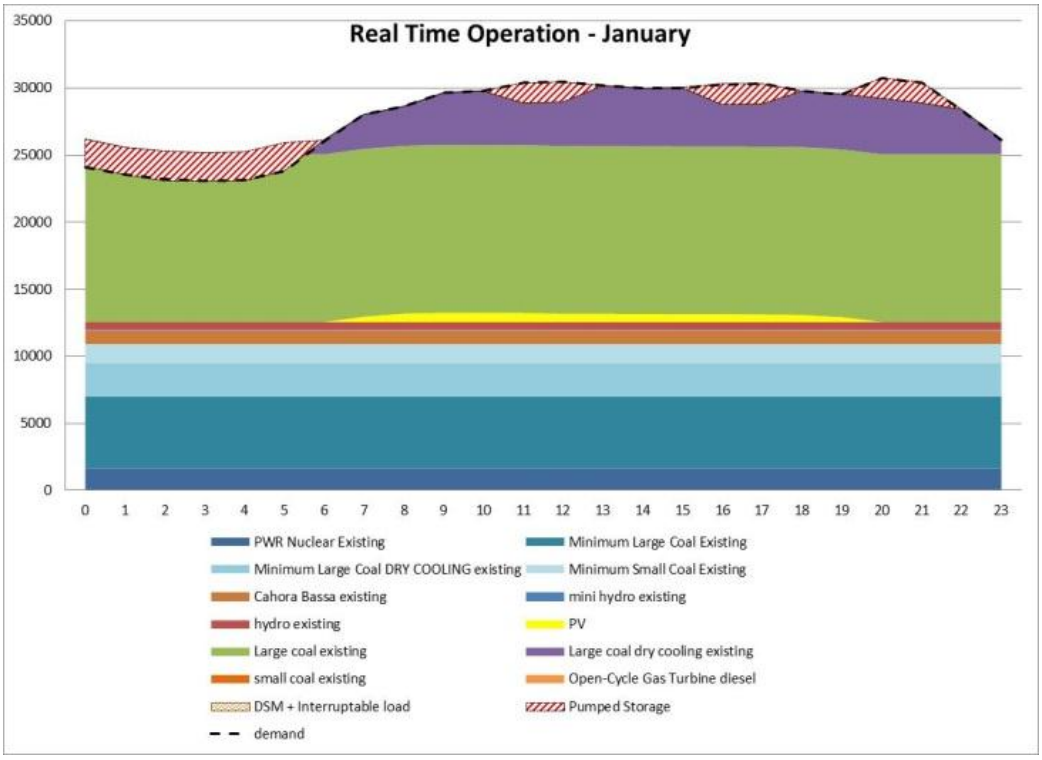

Figure 60: Real time dispatch - summer

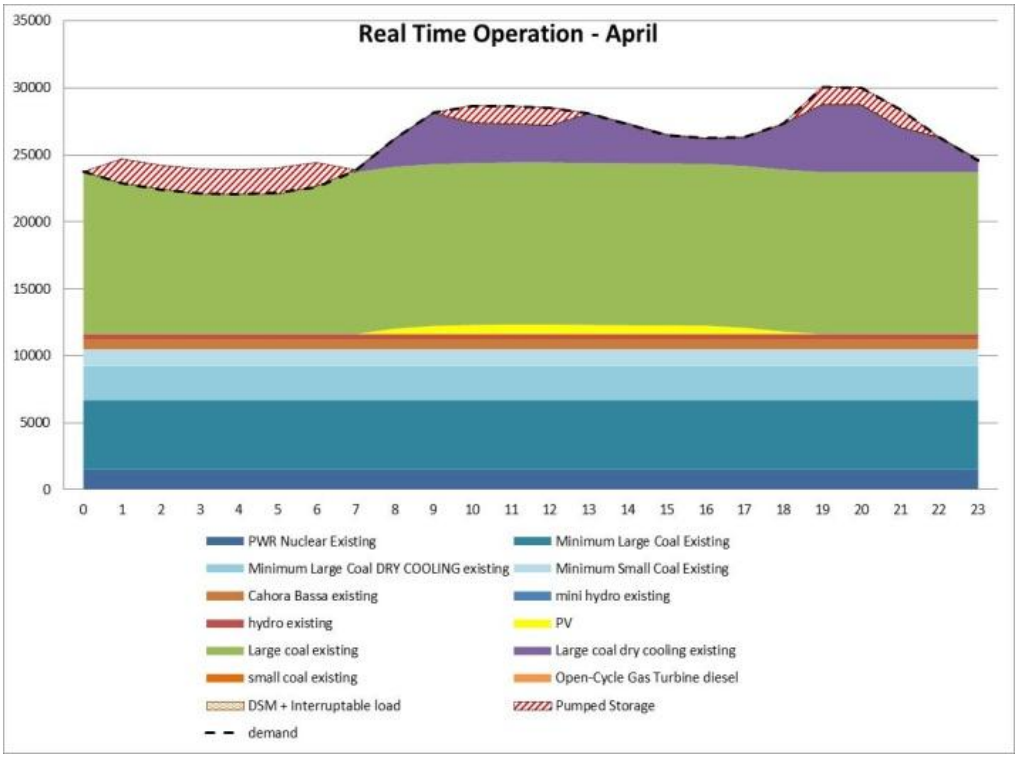

Figure 61: Real time dispatch - autumn

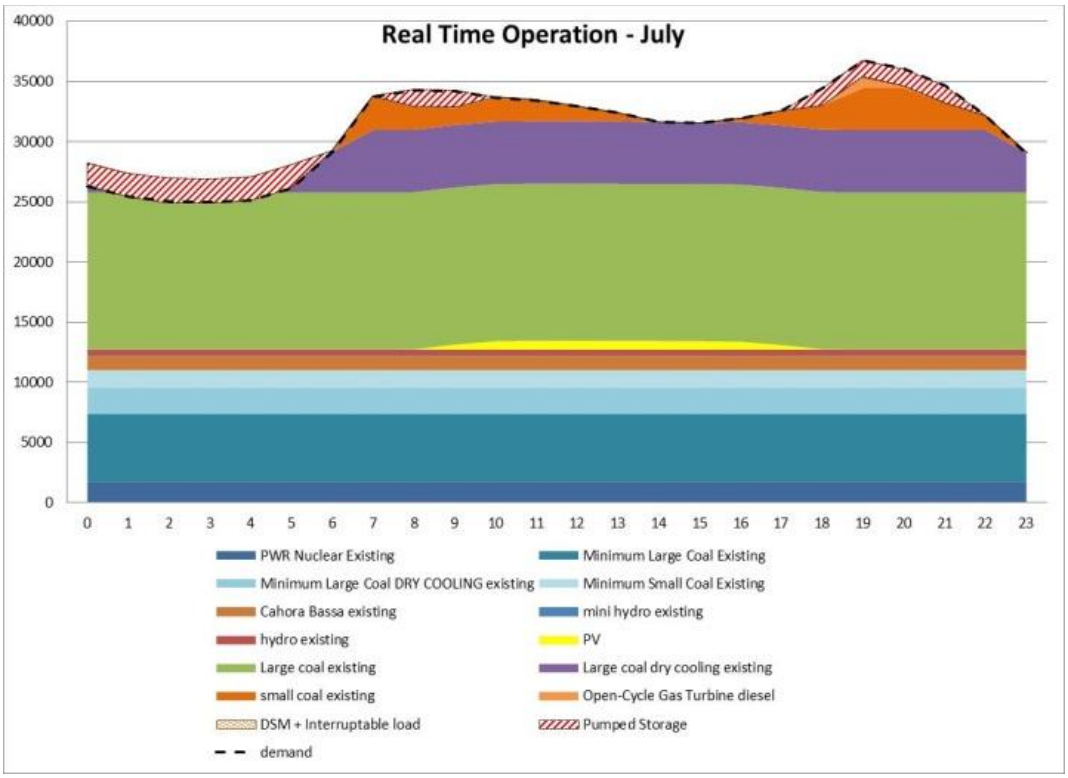

Figure 62: Real time dispatch - winter

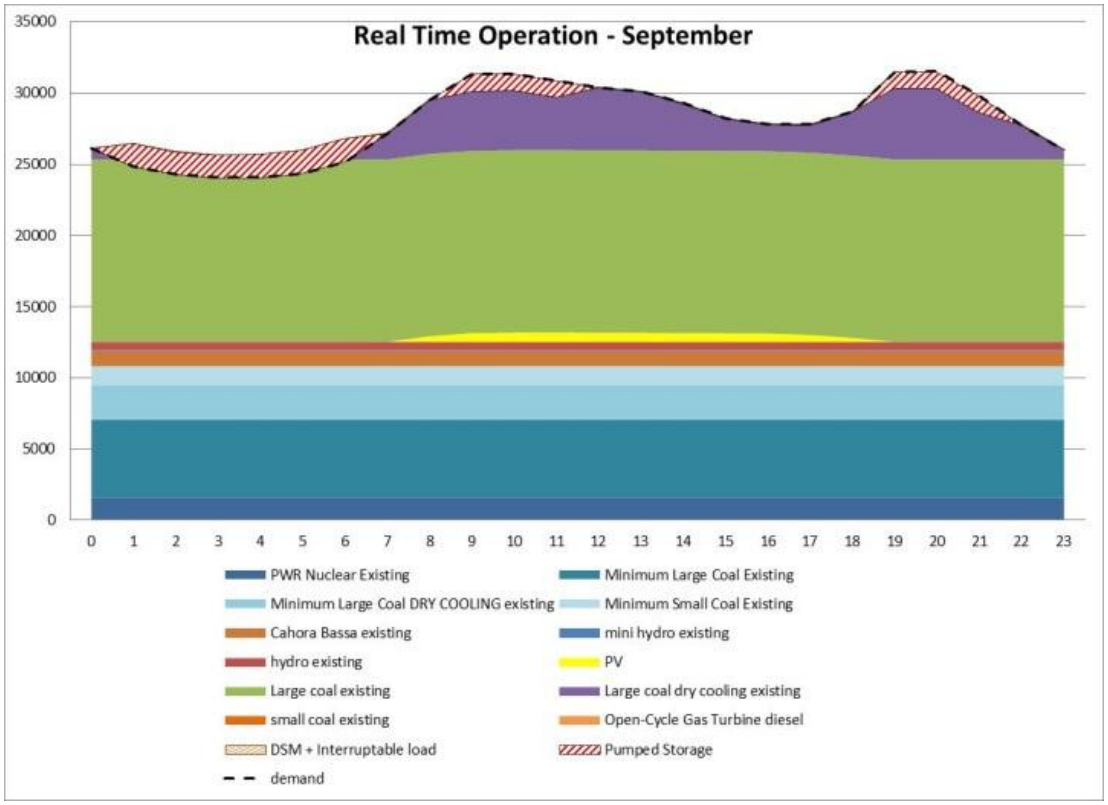

Figure 63: Real time dispatch - spring

APPENDIX F – LOLP CODE AND MCS VBA

LOLP Code:

The LOLP calculator is a publicly available tool written in C++ available through the ERC (ERC, 2010). It is in this form in order to cope with the large number of simulations required for the convergence of results(>50 000).

The nature of the data to be passed from Excel to the App (inputs):

1. Specification of Thermal Units:
   An 'm' by 3 table of numbers, where 'm' is the number of thermal unit types in the system (m<30)
   a. Column 1: number of units for each unit type [ISTNBUN][1],
   b. Column 2: average size of units for each unit type [STUNCP],
   c. Column 3: average probability of outage for each unit type [STUPOR].
2. Specification of wind component:
   An 'M' by 2 table of numbers, where 'M' is the number of columns in the wind output pdf and a number specifying the size of the total wind component (M<30).
   a. Column 1: Output [Pwr],
   b. Column 2: Probability of output [Prob],
   c. Number: Size of total wind component [WNDCP].
3. A few other numbers
   a. 'PEAK' demand,
   b. 'n' the number of simulations.

The nature of the results to be passed back to Excel (outputs):

1. One number being the actual LOLP
2. An 'N' by 2 table of numbers specifying the pdf of available Capacity

Algorithm for calculation of LOLP:

1. For each simulation:
   a. Generate complete unit list
      i. For capacity [UnitCap]: From ISTNBUN and STUNCP
      ii. For Probability of outage [UnitFOR]: from ISTNBUN and STUPOR
   b. Draw a set of uniformly distributed random numbers from 0 to 1 [RndSamples]
   c. Calculate available capacity of thermal unit [TotThermCap]
      TotThermCap = sum((RNDSamples>UnitFOR)*UnitCap)
   d. Calculate available capacity from wind [WindCap] by sampling from the wind pdf then multiplying by WNDCP
   e. If total capacity = WindCap+TotThermCap < PEAK then increment [Failures] counter
2. LOLP = Failures/n

[1] [] used to specify variable name used in Algorithm and Matlab code given in appendix

Matlab Code:

```
% a. Generate complete unit list
for i = 1:m
    UnitCap = [UnitCap repmat(STUNCP(i),1,ISTNBUN(i))];
    UnitFOR = [UnitFOR repmat(STUPOR(i),1,ISTNBUN(i))];
end

UnitCap = repmat(UnitCap,n,1);
UnitFOR = repmat(UnitFOR,n,1);


% b. Draw a set of  uniformly distributed random numbers from 0 to
1
RNDSamples = rand(n,m);

% c. Calculate available capacity of thermal unit
TotThermCap = sum((RNDSamples>UnitFOR).*UnitCap,2);


% d. Calculate available capacity from wind
RndSamples = rand(n,1);

WindCap = windfunc(RndSamples,Pwr,Prob)*WNDCP;


% e. Calculate Total Capacity
TotCap = TotThermCap + WindCap;


% f. Calculate LOLP
LOLP = sum(TotCap<PEAK)/n

% end


function x = windfunc(y,Pwr,Prob)
% inverse function for random sampling for wind component

M = length(Prob);
n = size(y,1);

CumProb = cumsum(Prob); % cumulative probability distribution

bins(:,1) = (y < CumProb(1)) * Pwr(1);

for i = 2:M-1
    bins(:,i) = ((y >= CumProb(i-1)) & (y < CumProb(i))) * Pwr(i);
end

bins(:,M) = (y >= CumProb(M-1)) * Pwr(M);

[d1,d2,x] = find(bins');
```

VBA code for MCS use in the dispatch model:

This VBA was used to record a range of output data upon which the calculation, and day of the month would be refreshed, and the process would be repeated again. The number of simulations used in the dispatch model was 100, but this can easily altered in the code below. It was found however, that when trying to do simulations in the range of n=1000, the computing time became inefficient.

VBA code:

```
Public Sub outputData()

Dim n As Integer
Dim rOutput As Range
Dim wOut As Worksheet
Dim wResult As Range
'Dim dPComplete As Double

UserForm1.Show
Application.ScreenUpdating = False

Set wOut = ThisWorkbook.Worksheets("Sheet1")
Set rOutput = wOut.Range("Output")

For n = 7 To 107

Set wResult = wOut.Range(Cells(n, 1), Cells(n, 6))
wResult.Value = rOutput.Value
   'rOutput.Copy
   'ThisWorkbook.Worksheets("Sheet1").Cells(n, 1).Select

   'Selection.PasteSpecial Paste:=xlPasteValues


   Application.Calculate
   UserForm1.TextBox1.Value = Format((n - 7) / 100, "###.#0%")
   DoEvents

Next n

Application.CutCopyMode = False
Application.ScreenUpdating = True
UserForm1.Hide

End Sub
```